



DIPLOMA THESIS

SATELLITE POWER SYSTEMS

COMMERCIAL PRODUCTS IN SPACE

Performed at:

SUNSPACE

ELECTRONIC SYSTEMS LABORATORY
STELLENBOSCH UNIVERSITY, SOUTH AFRICA

FACHHOCHSCHULE TECHNIKUM WIEN
STUDIENGANG ELEKTRONIK

Performed by:

Marcus EDER

Unterfeldstr. 5; 5101 Bergheim; AUSTRIA

MNr: 9910011021

Mentors:

Company Mentor: M.Eng (e&e), Martin Jacobs, SunSpace

FHS Mentor: Dipl.-Ing. Dr. Felix Himmelstoss

Date: 26.05.2003

Abstract

Power systems, especially the solar array and battery, are often the most expensive components of a satellite system. The recent shift in emphasis towards low cost satellites requires cheaper components, which can be found in commercial products.

The harsh space environment requires special tests before components can be used. Some commercial LiIon cells were analysed and accurate test equipment for battery analysis was developed. Unusual components such as *LEGO* blocks were used to reduce the cost and the time to design the test equipment. A comparison between LiIon and Supercapacitors was made with focus on satellite applications where high power for low duty cycle is required—like Synthetic Aperture Radar (SAR) satellites. Radiation tests on smart power MOSFETs (PROFET[®]) was prepared for use in satellite power systems. No known radiation tests were done on any Infineon PROFET[®].

Some unexpected failures on commercial LiIon cells were found, and the analysis process is discussed.

Key Words

battery; cell selection; satellite; SAR; ultra capacitor; cell balancing; MPP tracking; double layer capacitor; cell matching; solar; lithium ion; Li-Ion; LiIon; cell analysis; radiation test; PROFET

Zusammenfassung

Die Stromversorgung, speziell Solarmodul und Batterie, zählen zu den teuersten Komponenten im Satelliten. Eine immer stärkere Forderung nach kostengünstigen Alternativen ist zu beobachten. Diese Komponenten können in kommerziellen Produkten gefunden werden.

Die rauen Umgebungsbedingungen im Weltall machen Untersuchungen der Bauteile erforderlich, bevor diese verbaut werden können. Einige kommerzielle LiIon Zellen wurden analysiert und Testequipment zur genauen Vermessung der Kenndaten von Batterien und Zellen wurde entwickelt. Unübliche Komponenten wie LEGO wurden in der Konstruktion eingesetzt um Kosten zu minimieren und die Entwicklungszeit zu verkürzen. Ein Vergleich zwischen LiIon Zellen und Supercapacitors wurde durchgeführt im Hinblick auf Satelliten mit extremen Anforderungen in Bezug auf die geforderte Leistung – z. B. SAR¹ - Satelliten. Strahlungstests an smart power MOSFET's von Infineon (PROFET[®]) wurden vorbereitet, da bisher keine derartigen Testergebnisse bekannt sind.

Die Analyse an gebrauchten LiIon Laptop-Packs zeigte unerwartete Fehlerursachen an den Zellen. Der Analyseprozess und die Ergebnisse werden dargestellt.

Schlagwörter

Batterie; Zellauswahl; Satellit; SAR; ultra capacitor; cell balancing; MPP tracking; double layer capacitor; cell matching; solar; lithium ion; Li-Ion; LiIon; cell analysis; radiation test; PROFET

Diese Arbeit wurde mit L^AT_EX gesetzt.

¹Synthetic Aperture Radar

1 Tasks

The purpose of this research was to analyse ways to reduce the costs in satellite power systems.

- The sizing and selecting process for the energy storage of a SAR micro satellite had to be analysed.
- The usability of Commercial Of The Shelf (COTS) LiIon cells had to be analysed.
- Test equipment and test processes to cycle and measure LiIon cells with high accuracy had to be developed. If possible, the test equipment had to be able to cycle and measure other cell types (e.g. NiCd).

During the research for this thesis, smart power switches for the use in satellite power systems (power distribution) were found as alternative to P-channel MOSFET's and a radiation test was required.

Contents

1	Tasks	iv
	List of Figures	ix
	List of Tables	xiii
	Nomenclature	xiv
2	Introduction	1
3	Theoretical Background	2
3.1	The Space Environment	3
3.1.1	The Vacuum Environment	3
3.1.2	The Thermal Environment	4
3.1.3	The Neutral Environment	5
3.1.4	The Plasma Environment	5
3.1.5	The Radiation Environment	6
3.1.5.1	The Van Allen Belts	6
3.1.5.2	Total Dose	7
3.1.5.3	Degradation of Electronics	7
3.1.5.4	Single Event Failure	9
3.1.6	The Micrometeorite Environment	10
3.1.7	Mechanical Shock and Vibration	10
3.2	Orbit Types	11
3.2.1	Low Earth Orbit (LEO)	12
3.2.1.1	Sun-Synchronous	13
3.2.1.2	Sun-Synchronous Dawn - Dusk	13
3.2.1.3	The Polar Orbit	13
3.2.2	Geostationary Earth Orbit (GEO)	14
3.2.3	Other Orbit Types	14
3.2.3.1	The Molniya Orbit	14
3.3	Solar Cell and Module	19
3.3.1	Silicon Cell	20

3.3.2	Other Cell Types	22
3.3.3	The Irradiation Angle	22
3.3.4	Radiation Degradation on Solar Cell	23
3.3.5	Typical Efficiency of Solar Cells	23
3.4	Sizing the Energy Storage	24
3.4.1	For Batteries	24
3.4.1.1	The “C” - Rate	24
3.4.1.2	Battery Charging with known DOD	25
3.4.1.3	Sizing due to Required Energy	26
3.4.1.4	Sizing due to Required Power	26
3.4.2	Sizing Capacitors	26
3.5	Supercapacitors	28
3.6	Lithium-Ion Cells	31
3.6.1	Charging and Discharging of LiIon Cells	31
3.6.2	Buildup of LiIon Cells	33
3.6.3	Safety Mechanism of 18650 Cells	35
3.6.4	Aging Effects on LiIon Cells	35
3.6.5	Classification of Cells	37
3.6.6	Cell and Battery Management	37
3.7	Nickel Cadmium Cells	39
3.8	Nickel Hydrogen Cells	40
3.9	Power System Structures	41
3.10	High Power - Low Duty Cycle Application SAR	42
4	Practical Work	43
4.1	SAR - Analysis of power requirements	44
4.1.1	Power Budget	44
4.1.1.1	Maximum Power	45
4.1.1.2	Average Power and Time	47
4.1.2	Sizing the Solar Array	47
4.1.2.1	Selecting the Solar Cell Type	48
4.1.3	Selecting and Sizing the Energy Storage	48
4.1.4	Conclusion of SAR Power Requirements	48
4.2	Matlab Model for Power Simulation	49
4.2.1	NORAD Two-Line Element	49
4.2.2	Vector System for Matlab Model	50
4.2.3	SunSpace Simulink Model - NORAD	51
4.2.4	MATLAB Model for Simulation	51
4.3	Capacitor Stack - Performance Analysis	54
4.3.1	EOL Simulation with SIMPLORER®	54
4.3.2	Results of the SIMPLORER® Simulation	57
4.4	Lithium-Ion versus Capacitor in High Power Application	58

4.4.1	Discharge Rate	58
4.4.2	Depth of Discharge	59
4.4.3	Specific Energy	60
4.4.4	Specific Power	60
4.4.5	Lifetime of Energy Storage	60
4.4.6	Extra Circuit Requirements	60
4.4.7	Conclusion	61
4.5	MPP vs. Analogue	62
4.6	Analysis of Commercial LiIon Batteries	63
4.6.1	The Analysed Material	63
4.6.1.1	Two IBM Laptop Batteries	63
4.6.1.2	Loose Cells from unknown Source	63
4.6.1.3	Laptop Pack from ASUS (3P3S) and unknown Type (2P4S)	63
4.6.2	Analysis of the Laptop Battery Packs	64
4.6.2.1	The LiIon Cells	64
4.6.2.2	The Cell Protection Electronics	68
4.6.3	The Results	68
4.6.3.1	The Cells	68
4.6.3.2	Protection Circuit	70
4.6.4	Conclusion	70
4.7	Analysis of Space Qualified LiIon Battery from AEA	71
4.8	Lithium-Ion Cell Measurement Process	72
4.8.1	Requirements for Cell Measurement Equipment	72
4.8.1.1	Low Cost	73
4.8.1.2	Measuring of the Charge and Discharge Curve	73
4.8.1.3	Cycling of Cells	73
4.8.1.4	Measuring of Multiple Cells at a Time	73
4.8.1.5	Programmability	75
4.8.1.6	Impedance Measurement	76
4.8.1.7	High Accuracy	76
4.8.1.8	Very High Accuracy Cell - Difference Measurement	76
4.8.1.9	Small Influence due to Measurement	76
4.8.1.10	Modularity, Reusability and Reconfigurability	77
4.8.1.11	Measuring of all Cell Types	77
4.8.1.12	Charging and Discharging at High Rates	77
4.8.2	The setup	78
4.8.3	The Cell Module	78
4.8.4	The Main Control - Module	81
4.8.5	The possible Configurations	81
4.8.6	The IO-Extension	84
4.8.7	The Software Requirements	84

4.8.7.1	The Test Step	84
4.8.7.2	Hazardous Program Situations	90
4.8.8	The Software—Screenshots	91
4.8.9	The Integration	94
4.8.10	The first Test	94
4.8.11	Problems and Solutions	94
4.8.12	Conclusion	94
4.9	Radiation Testing of Components	101
4.9.1	Radiation Test on PROFET [®]	101
4.9.1.1	PROFET [®] - Input Signals	104
4.9.1.2	The Test Circuit	104
4.9.1.3	Radiation Test Description	106
4.9.1.4	The Results for PROFET [®]	106
4.9.1.5	Note To Test Results	106
5	Conclusion	107
	Bibliography	108
A	Appendix	113
A.1	Appendix to Satellite Orbits	114
A.2	MATLAB Simulation Outputs	117
A.3	Analysis of Commercial LiIon Cells	120
A.4	AEA Battery Measurement	121
A.5	Cell Measurement	123
A.6	Radiation Test	126
A.7	Some Ideas for Satellite Systems	130
A.7.1	PC/104-plus	130
A.7.2	Spectrally Sensitive Concentrators for Solar Energy	130
A.7.3	Pressurized Module Battery	130
A.8	Interesting Sources	131
A.8.1	RØMER Mission Technical Description	131
A.8.2	BaSyTec - Battery Testing Equipment	131
A.8.3	Sixth European Space Power Conference	131
B	Acknowledgements	132

List of Figures

3.1	Heat Pipe. (a) Principle of operation. (b) Temperature operating range. [40, p.612]	4
3.2	Electron Belts of the Inner and Outer Zones. The Numbers on the contours represent the \log_{10} of the integral omni directional flux in units of particles per cm^2 and second. The horizontal axis is the magnetic equator marked in units of Earth radii. Only electrons with energies above 0.5 MeV are included. [34, p.200]	7
3.3	Annual dose behind 4mm spherical shielding on circular equatorial orbits in the radiation belts, as function of orbit height [28, p.117] .	8
3.4	Radiation effect on Si solar cell characteristic to show the voltage and current degradation relations (total dose not mentioned, but degradation is worst case). [51, p.154]	9
3.5	Sun-Synchronous Inclination vs. Circular Orbit Altitude [22, p.284]	16
3.6	Geosynchronous Orbit Geometry [22, p.282]: a) vernal equinox shadow; b) summer solistic shadow (summer in the northern hemisphere)	17
3.7	MOLNIYA 3-45 Ground Track from 2003/04/12. Created with WinOrbit using two line elements, downloaded from Celestrak [30], [21].	18
3.8	Two Diode Solar Cell Equivalent Circuit [54]	20
3.9	Equivalent Circuit Diagram for Effective Solar Cell - Characteristic [54]	20
3.10	Structure of a Solar Cell (not to scale)	21
3.11	Triple Junction Solar Cell with an open cell voltage of 2.545V [47] .	22
3.12	The Supercapacitor: (a) storing energy by applying a potential; (b) equivalent circuit and (c) comparison between double-layer capacitor, battery and Al-Elco (electrolytic capacitor). Pictures from [39]	29
3.13	Comparison Between Different Capacitors [53, p.485]	30
3.14	Charge and Discharge Mechanism of LiIon Cells. Negative electrode: Carbon (Graphite, Hard&Soft carbons, etc). Positive electrode: $LiMO_2$ ($M = Co, Ni, Mn$)	32

3.15	Charge Curve of a LiIon Cell. Taken from [20]	32
3.16	Structure of a LiIon Cell taken from [35].	33
3.17	Stylized Depiction of the Assembly Process for Cylindrical LiIon Cells taken from [53, p.280].	34
3.18	The Top Cap of a Panasonic 18650 Cell. (a) The top cap from top side; (b) the top cap from bottom side, rest from metal can removed; (c) top side, top of cap removed with grinder, pressure valve visible, plastic removed; (d) metal of top seal plate (figure 3.17 on page 34) weakened; (e) parts of the top cap, bottom the plastic removed in <i>c</i> , top the isolation between valve disc and circuit breaker, left to right: outer metal part of top cap – visible in <i>a</i> , PTC, valve disc, circuit breaker, inner metal part of top cap – visible in <i>b</i> ; (f) pressure valve left and circuit breaker right.	36
3.19	S-8233A - Battery Protection Circuit [45]	37
3.20	Techniques for Power Regulation. The two basic approaches for the power structure of satellites, taken from [34, p.408]. SA refers to Solar Array and SR relates to Shunt Regulator	41
4.1	Power requirements of different modules	44
4.2	Specification of the different modes	45
4.3	Resulting power budget	46
4.4	Spacecraft Coordinate System	51
4.5	Complete MATLAB Model for Solar Simulation	52
4.6	Circuit in Simplorer to analyse a Capacitor Stack	54
4.7	Simulation of the load behaviour for 2645W constant power discharge. Different scale factors were used to fit all graphs in the same figure. For example, the Output Power stays nearly constant at 2600W (26 from y-axis multiplied with 100W). The Load Resistance drops from around 900mΩ to above 100mΩ (90 from y-axis multiplied by 10mE)	55
4.8	Simulation of thermal losses, and the efficiency of a capacitor stack as a means for energy storage	56
4.9	LiIon and Capacitor Comparison Tool. Price for +/- 0.5% matched Montena BCAP0010A03 capacitors. Power bus voltage is used to size the capacity.	59
4.10	Picture of: (a) the ASUS - Pack and Partly Opened Cells (b) Normal Operation, (c) an Open-Circuit Cell and (d) a Reactivated Cell.; The difference between (b), (c) and (d) is the pressure disk in the middle of the top cap. (b) is domed to the outside (open circuit), while (c) is flat (normal operation) and (d) is pressed in to reconnect the circuit breaker	65

4.11	Circuit a) shows a 3P3S configuration; b) shows a 2P4S configuration; c) shows a 4S2P configuration (structure used by AEA - Technology)	66
4.12	Opening the Cell Fully.	67
4.13	Cell Protection Electronics - Test. (a) the setup with 4 independent adjustable voltage sources and 22E to simulate the behaviour of a LiIon cell and the 220E as load resistor; (b) picture of the test setup; (c) the cell protection electronics	69
4.14	The test setup for the cell measurement electronics.	74
4.15	The scematic of the circuit, required by each cell.	79
4.16	PCB with 3 times the same layout, slightly modified to save wiring effort.	80
4.17	The Main Control Schematic	82
4.18	The IO - extension with Open Collector (OC) output. /OE is Output Enable (low active), CLK is CLoCK signal (rising edge) to store the data, LE is Latch Enable. For pinouts of the connector see table 4.3 on page 87	85
4.19	The IO - Extension - Board	86
4.20	Specification of the used Equipment and General Settings.	91
4.21	Setup Window for Test Procedure.	92
4.22	Data can be Seen during the Test to Check for Correct Operation.	93
4.23	The Complete Setup is shown in (a). The IO-extension next to relays, screw terminal blocks, shunt resistor and the container for 8 LiIon cells is shown in (b).	95
4.24	The Integration at the ESL. (a) is the setup at the ESL, (b) is the capacitor required to decouple the DC voltage from the AC source, (c) is the FLUKE 5100B calibrator used to measure the shunt resistor, (d) are reference resistors to prove the series resistance measurement of the test equipment and (e) is the setup with a solar2000 lamp which is described in section 4.8.10 on page 94	96
4.25	The Test Program for the SOLAR2000 - Lamp.	97
4.26	Output Data, generated during the Test on the SOLAR2000 Lamp.	98
4.27	Terminal Voltage and Accumulated Charge. The voltage on the terminals rises to 10V, if the solar lamp is fully charged—battery is disconnected to protect it from overcharging (10V is the output voltage of the power supply). The Voltage drops to 2V in case that the lamp is completely discharged (over discharge protection disconnects the battery from the terminal; see figure 4.25 on page 97). The short needles down to some hundred millivolt are due to the measurement of the series resistance where only the AC voltage is measured.	99

4.28	Accumulated Energy and Accumulated Charge. It can be seen, that after discharging the same ammount of Charge, the accumulated energy is not zero. This is due to the losses in the battery and the protection electronics.	100
4.29	Radiated circuit (extern) for the room with CO ₆₀ source. Radiated with 2k Rad/h; connected to the Interface and protection - circuit with 5m ribbon cable (CON1) and 5m wire to the power supply (+18V).	103
4.30	Interface and protection - circuit.	105
A.1	Ellipse Geometry. (<i>e</i> is the eccentricity) [22, p.36]	114
A.2	Siderial and Mean Solar Day [40, p.263]	115
A.3	Orbit of the Earth Around the Sun [40, p.258]	115
A.4	Sun-Synchronous Orbits [22, p.285]: a) noon-midnight orbit b) twilight orbit (dawn-dusk)	116
A.5	Azimuth angle over time (Module Azimuth1)	117
A.6	Elevation angle over time (Module Elevation1)	118
A.7	Solar power over time (Module Solar power)	118
A.8	Solar power factor over time (Module Power factor)	119
A.9	Examples of Corrosion Near the Gasket. (a) CGR18650HM; (b) and (c) CGR18650H. (c) Leakage of electrolyte after polishing the rust away	120
A.10	The measured cell voltages on the AEA Battery (electric equivalent with 4S-6P - structure)	122
A.11	Circuit for the relay with options like fuses or resistor and screw terminals.	123
A.12	The LEGO block with the spring forced probe. (a) blue block for negative pole; (b) epoxy glue used to fix the probe in the LEGO block; (c) red lego block used to connect the positive pole of the cell; (d) the negative poles of the setup.	124
A.13	LEGO Building Blocks; higher sticking with more small blocks. (a) best stability, (b) less stability, (c) easy to remove, (d) the power relay mounted on two big blocks, many small blocks would have given a better stability, but not enough small blocks were available.	125
A.14	Radiation Test: (a) radiated electronics; (b) interface and protection electronics; (c) the load (24V/21W bulbs); (d) prepared for the radiation in Stellenbosch; (e) the complete electronics	127

List of Tables

3.1	Total Dose Thresholds of Various Electronic Technologies [51, p.155]	5
3.2	Available Cells from SPECTROLAB; data at 28 °C (End Of Life (EOL): 1 MeV Electron Fluence (1×10^{15} e/cm ²)). Begin Of Life (BOL) and EOL irradiation with the spectrum and energy found at a sun distance of 1AU.	20
3.3	Major Advantages and Disadvantages of LiIon Batteries. Taken from [36, 35.2]	31
3.4	Codes for Rechargeable Li-Systems [1]	38
3.5	Major Advantages and Disadvantages of Sealed Nickel-Cadmium Batteries. Taken from [36, 28.1]	39
3.6	Major Advantages and Disadvantages of the Nickel-Hydrogen Battery. Taken from [36, 32.1]	40
4.1	Results of Battery Analysis (PANASONIC CGR18650H). “high Z” refers to high impedance of the cell (Open Circuit cell). The corrosion with an intensity of one was only visible under the microscope, two was visible on less than half the area near the gasket and three was used to indicate strong corrosion on the cells around the gasket	64
4.2	The Possible Cell Configuration Modes for the two Relays	73
4.3	The Pinning of the Connector to the IO - Card	87
4.4	List of all the Relays. If two abbreviations are combined with a “_”, the first state is the active one (Digital output is H; OC is conducting)	89
A.1	20-pin 2-way Connector (To Load; 24V/21W - bulbs)	126
A.2	26-pin 2-way Connector (Data - Logger & Control)	128
A.3	40-pin 2-way Connector (Circuit Interconnection)	129

Nomenclature

BOL	Begin Of Life
CMOS	Complementary Metal Oxide Semiconductor
COTS	Commercial Of The Shelf
DET	Direct Energy Transfer
DOD	Depth Of Discharge
ECL	Emitter Coupled Logic
EDAC	Error Detection And Correction
EDLC	Electric Double Layer Capacitor
EOL	End Of Life
ESA	European Space Agency
ESD	Electro-Statically Discharge
ESR	Equivalent Series Resistance
GEO	Geostationary Earth Orbit also called GSO Geostationary Satellite Orbit
GPS	Global Positioning System
IEC	International Electrotechnical Commission
LEO	Low Earth Orbit
LiIon	Lithium-Ion
MEO	Medium Earth Orbit
MIS	Metal-Isolator-Semiconductor
MNOS	Metal Nitride Oxide Semiconductor
MPP	Maximum Power Point
NiCd	Nickel Cadmium
NiH ₂	Nickel Hydrogen
NMOS	N-channel Metal Oxide Semiconductor
NORAD	North American Aerospace Defence Command
PCB	Printed Circuit Board
PPT	Peak Power Tracker
PTC	Positive Temperature Coefficient
RTG	Radioisotope Thermo-electric Generator
SAR	Synthetic Aperture Radar
SEB	Single Event Burnout
SEE	Single Event Effects

SEGR	Single Event Gate Rupture
SEL	Single Event Latch-up
SEP	Single Event Phenomena
SEU	Single Event Upset
SGP4	Simplified General Perturbations V.4
SHE	Single Hard Error
SMD	Surface Mounted Device
SOC	State Of Charge
SUNSAT	Stellenbosch University Satellite
TID	Total Ionizing Dose
TTL	Transistor Transistor Logic
USSPACECOM	US Space Command
UT	Universal Time
WDC-A-R&S	World Data Centre-A for Rockets and Satellites

2 Introduction

Since 2001 Students of the Technikum Wien have the possibility to do a practice semester in the ESL¹ at Stellenbosch University. Unfortunately, there was no satellite project at the start of the research for this thesis.

The last satellite (SUNSAT) was a micro satellite with a high-resolution optical camera. In the future a micro satellite may carry Synthetic Aperture Radar (SAR) to take another type of picture of our world and possible types of energy storage should be evaluated.

Components for commercial products are much cheaper than the space-qualified alternative. There is a temptation to use commercially available cells for the energy storage. To be able to work in the satellite power system field, fundamental background knowledge of satellite orbits and the space environment has to be known.

For power systems where solar cells are used, also the basic principles have to be known.

This thesis gives an overview of satellite power systems and the use of commercial products with special focus on commercial LiIon cells.

¹Electronic Systems Laboratory

3 Theoretical Background

The theoretical part should give an overview of factors that influence satellite power systems. An introduction to LiIon, NiCd and double-layer - capacitor as energy storage is made.

3.1 The Space Environment

Most electronic parts are fine for use in space, but for commercial integrated circuits some tests have to be done before these parts are used in space. The space environment is one of the worst environments for mechanical and electronic systems. The following short sections give an overview of some of the problems in space.

3.1.1 The Vacuum Environment

All electronic circuits generate heat due to power losses. In terrestrial applications this thermal energy is mostly removed through convection. An atmosphere (pressurized gas) or fluids are necessary to accomplish this. Other ways to remove the heat from one device are conduction or radiation. Radiation is efficient under high temperature differences between the hot device and its surrounding environment.

Because of the lack of air, thermal contact resistance will increase much if no materials (e.g. epoxy) are used to fill the gap between the two connected materials. On microscopic level the inter-material contact is only 20% to 50% of the actual surface. The thermal resistance in vacuum can go up by a factor of 5 without epoxy, and up to 3 if epoxy filler is used [43]. For electronic parts, which don't need to be specially cooled in terrestrial environment like voltage regulators for low power, power transistors (specially SMD¹) and processors, special design ways have to be considered. For heat distribution, specific heat-pipes [40, p.612], [34, p.412-413], which offer a lower thermal resistance than copper for longer distances, are available (working principle, see figure 3.1 on the following page).

The second big effect of the vacuum is outgassing of devices. In applications with optical devices it is very important, that the optical parts (lenses) stay clean during the mission time. The best way to protect the optics is to avoid outgassing of components, which is done by selecting the right parts. Silicon materials are very likely to outgas. Special care is necessary when selecting cables, gap pads for power devices and adhesives. Non-hermetically sealed components like lead-acid batteries or most aluminium electrolytic capacitors are problematic for use in space. Air filled containers can be used to take advantage of these components. Parts which are designed to withstand a high internal pressure like LiIon batteries or tantalum capacitors are suitable, because the difference is only plus 1 bar.

On the website of the Darnell Group, Inc. [43] one can also find the following information about the quality of the vacuum: "The vacuum 100 miles (161 km) above Earth (considered to be a low orbit) is quite hard—a pressure of less than 10^{-10} Torr². In comparison, the pressure at sea level is about 760 Torr. Note

¹Surface Mounted Device

²Torr is a unit for pressure equal to 133.32 pascal

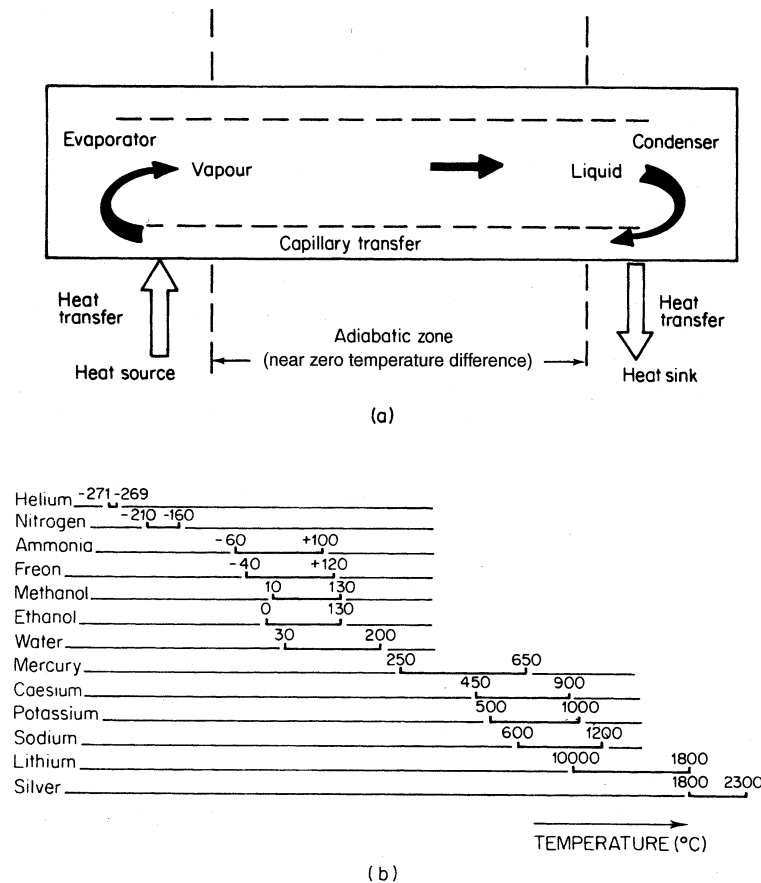


Figure 3.1: Heat Pipe. (a) Principle of operation. (b) Temperature operating range. [40, p.612]

that the best vacuum chambers on the ground can only get to about 10^{-7} Torr, although anything beyond about 10^{-4} Torr has little additional effect. The effects of operating in a vacuum are related to both pressure differential and the absence of air itself.”

3.1.2 The Thermal Environment

Infrared radiation from the Sun—and a small part from the Earth—on the one hand will heat up the satellite, on the other hand the satellite will radiate into space, which is only a few degrees above 0 K. Sun-exposed materials can easily reach temperatures above 400 K. Therefore, thermal stress of satellite materials and satellite structure is high. Fortunately, nearly all satellites have a passive or active temperature management system and most subsystems in the satellite only see a commercial temperature range. Solar arrays are directly exposed to these harsh environments.

Table 3.1: Total Dose Thresholds of Various Electronic Technologies [51, p.155]

Technology	Total Dose Rads (Si)
Complementary Metal Oxide Semiconductor (CMOS)	$10^3 - 10^6$
Metal Nitride Oxide Semiconductor (MNOS)	$10^3 - 10^6$
N-channel Metal Oxide Semiconductor (NMOS)	$10^2 - 10^4$
Emitter Coupled Logic (ECL)	10^7
Transistor Transistor Logic (TTL)	$> 10^6$

3.1.3 The Neutral Environment

“Neutral Environment” refers to the uncharged “rest” of our atmosphere in orbit. At an altitude between 200 km and 600 km, atomic oxygen is the most common constituent (10^{16} to 10^{13} particles per m^3). According to [51, p.92-93] a Spacecraft with a surface of $1 m^2$ at a altitude of 300 km moves at 8 km/s through 10^{15} oxygen atoms per cubic meter. That results in $3 * 10^{22}$ collisions per hour. “As the result of these collisions, the spacecraft (1) will be subjected to drag force (causing orbital decay), (2) may experience material erosion due to sputtering³, (3) may experience material degradation due to atomic oxygen attack, and (4) may generate a significant amount of visible glow.” [51, p.93]

3.1.4 The Plasma Environment

Plasma—the fourth state of matter—refers to ionised gases with thermal energy, which allows the atomic electron to escape from the electrical attraction of the nucleus⁴. The energy of the particles in a plasma is below 100keV and therefore radiation effects can be neglected [29]. In the plasma state, the positive and negative ions can move independently. Over 99% of our universe—Sun, and the stars—are in the plasma state. Plasma reacts with electric and magnetic fields. The highest concentration—value depends on the solar activity—of plasma is found in altitudes around 300km with 6 to 10 times the density of an altitude of 600km [51, p.102]. The high density (10^6 particles cm^{-3}), low energy (0.1 eV) plasma at low altitudes (300km) “acts as a source of neutralizing current” [51, p.126] which is missing in GEO with its low density (<1 particle cm^{-3}) and high energy (5keV to 20keV) plasma [29]. The plasma charges the different materials of the satellite to different voltages. Because of the lack of low energy plasma in GEO, arc discharging is a problem if no prevention is taken. Thus, plasma has positive and

³The impact of a neutral particle with enough energy to free particles of the surface of the satellite (bound energy of the surface atom is less than the impact energy)

⁴positively charged nucleus of an atom

negative effects, depending on the thermal energy. To avoid problems in plasma environment,

- make the surface of *uniform conductivity*—if possible—to avoid arc discharging
- use *common ground, filtering and electromagnetic shielding* to make all modules immune against ESD⁵.
- if necessary, use a *plasma contactor*—if high voltage solar arrays in conjunction with negative structure grounding is used—to keep the potential of the spacecraft close to the plasma.

It should also be mentioned that a small percentage of the outgassed particles of the satellite could be ionized by UV light and then re-attracted to negatively charged surfaces of the satellite (optics). This problem occurs especially in GEO where the Debye length⁶ is much bigger than in LEO [51, p.129].

3.1.5 The Radiation Environment

The Earth is surrounded by a toroid region positioned around the magnetic poles which contains the Van Allen radiation belts.

The Radiation from the Van Allen belt is not the only source of radiation; galactic rays and particles from solar eruptions also exist. These radiations occur in the form of high-energy electrons, protons, neutrons and photons. Fast moving charged particles can produce so-called bremsstrahlung (photon-type) if passing a heavy charged particle in matter decelerates them. Power sources for interplanetary missions use RTG⁷—which are also a source of radiation—to generate the required energy.

Shielding against radiation is done on most satellites with aluminium structures or soft and heavy metal anti-radiation structures.

3.1.5.1 The Van Allen Belts

The Van Allen belts consist of two regions with high-energy electrons, with its maxima at 3000km and 20.000km and a single region of protons with the maximum at 3000km. These regions trap high-energy charged particles (MeV), which degrade material characteristics, produce malfunction or lead to Single Event Effects (SEE) also called Single Event Phenomena (SEP). These regions depend on the Earth's magnetic field, and change with solar activity. The form of the Van

⁵Electro-Staticallly Discharge

⁶length that a ion can travel before it catches an electron

⁷Radioisotope Thermo-electric Generator

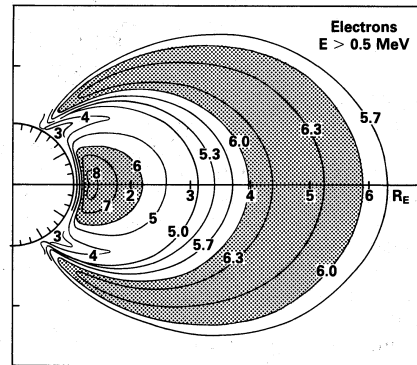


Figure 3.2: Electron Belts of the Inner and Outer Zones. The Numbers on the contours represent the \log_{10} of the integral omnidirectional flux in units of particles per cm^2 and second. The horizontal axis is the magnetic equator marked in units of Earth radii. Only electrons with energies above 0.5 MeV are included. [34, p.200]

Allen belts (figure 3.2) shows a region in the northern and southern hemisphere with a higher flux at lower altitudes because of the magnetic field lines in that region. Radiation in the polar region is therefore significantly higher than at lower inclination⁸ [51], [28] and [40]. The radiation belts are pushed to the Earth on the side of the sun, and in times of high solar activity the radiation belts can reach uncommon low altitudes (LEO). The maxima of the radiation belts can be seen in figure 3.3 on the following page.

3.1.5.2 Total Dose

The Total Ionizing Dose (TID) is the amount of summed radiation that causes malfunction of a device. The total dose threshold for different technologies is shown in table 3.1 on page 5. The radiation dose for equatorial satellites depends much on the altitude as seen in figure 3.3 on the following page. “To calculate TID, contributions by the trapped protons and electrons, secondary bremsstrahlung photons, and solar flare protons must be considered. (The dose due to galactic cosmic ray ions is negligible in the presence of these other sources.)”[33]

3.1.5.3 Degradation of Electronics

Ionization radiation tests are usually done with a Co-60 source. It can be seen that “Many devices are less degraded when they are irradiated without bias, but some types of bipolar structures are more sensitive when they are irradiated in an unbiased condition” [17]. However, other tests on low dropout voltage regulators

⁸Orbit is more an equatorial orbit and not a polar orbit

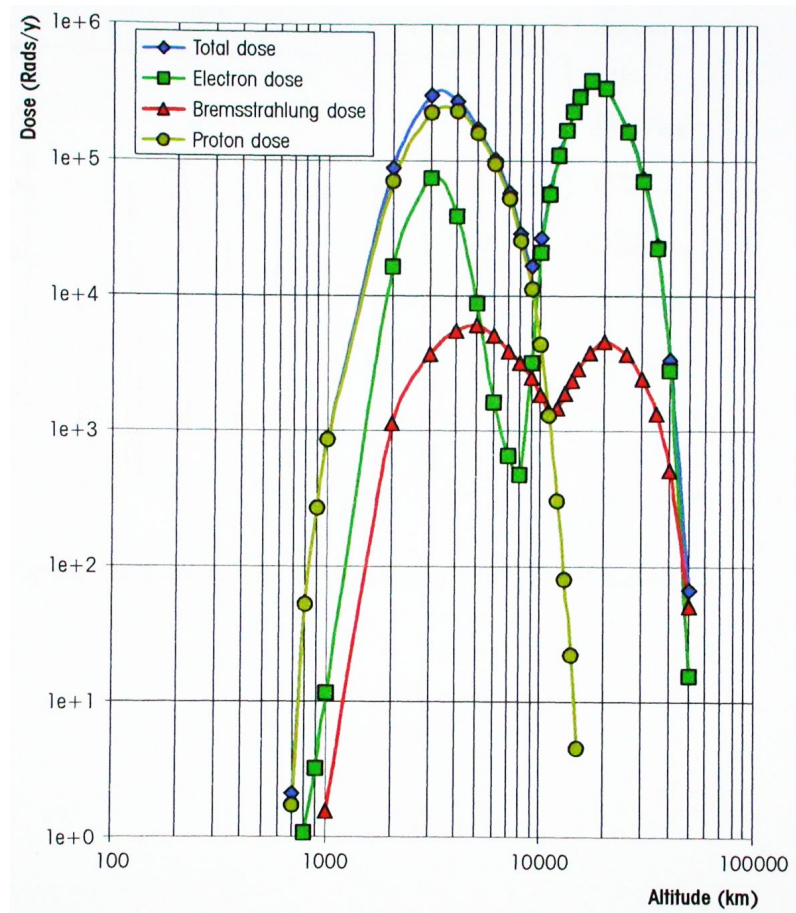


Figure 3.3: Annual dose behind 4mm spherical shielding on circular equatorial orbits in the radiation belts, as function of orbit height [28, p.117]

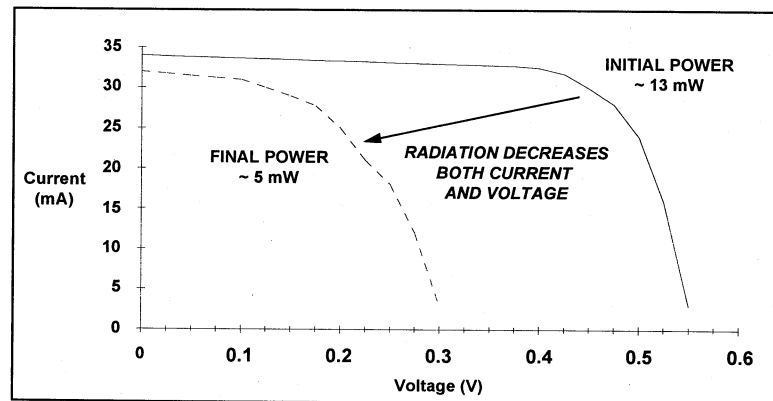


Figure 3.4: Radiation effect on Si solar cell characteristic to show the voltage and current degradation relations (total dose not mentioned, but degradation is worst case). [51, p.154]

showed that some parameters are more influenced during a non-biased irradiation. The dose rate, and not only the total dose, also has a big influence on the test results. A smaller dose rate decreased the value of the total dose [15].

Solar arrays are exposed to the radiation nearly without any protection, which leads to loss of cell-efficiency. As seen in figure 3.4 the voltage degrades more than the current and the EOL⁹ - voltage has to be high enough to power the satellite. Silicon cells are more affected by radiation than GaAs¹⁰.

3.1.5.4 Single Event Failure

Single event failures mostly depend on high-energy particles. High solar activity can compress the Earth's magnetic field—which protects us from parts of the galactic rays—on the sun-facing side that much that GEO - satellites are totally unprotected from galactic rays. Shielding against them is not very effective because these particles can travel through thick material before they lose their energy. The only possibility is to use radiation-hardened devices and design circuits and systems to be safe against SEE. Circuits in power systems must not fail because of a single event. Redundancy for key components is necessary. Single events can cause “hard” or “soft” errors. Where a Single Hard Error (SHE) causes a permanent malfunction, a Single Event Latch-up (SEL) can—if that event doesn't destroy the circuit—be corrected by resetting the device through a power reset. A Single Event Upset (SEU) is a transient pulse or a bit flip in a memory device. To detect bit failure, Error Detection And Correction (EDAC) is necessary. A MOSFET can be affected by a local destructive burnout of drain-source path

⁹End Of Life

¹⁰Gallium Arsenide

(SEB¹¹) or by a destructive burnout of a gate insulator (SEGR¹²). “To calculate the level of SEE hazard, the cosmic ray ions, the trapped protons, and the solar flare protons must be analyzed.” [33]

3.1.6 The Micrometeorite Environment

The chances for a satellite to collide with a micrometeorite, which can cause loss of this satellite, are very small. While particles with a size of less than 0.1 mm (assuming that the speed is 10 km/s and the density is 1 g/cm³) only raise the speed of surface erosion, particles with 1 mm can cause serious damage. A particle with 3 mm diameter moving with the same speed has the same kinetic energy as a bowling ball at 100 km/h. The kinetic energy is:

$$E_K = \frac{mv^2}{2} \quad (3.1)$$

where E_K is the kinetic energy, m is the mass and v is the velocity. The velocity variable has a greater effect on the kinetic energy [51, p.169-184] See also [19].

3.1.7 Mechanical Shock and Vibration

In orbit, the only movement that the on-board systems normally appear mechanically is a correction of the orbit or a turning of the satellite, but these forces are very small. But to get there, a wild ride—due to vibrations on the launch vehicle—with forces of typically 10 to 20 G_(rms) or even more are common. So small parts have to be mounted well. Heavy parts like battery cells should be analysed to make sure that they can withstand these vibrations. [43]

¹¹Single Event Burnout

¹²Single Event Gate Rupture

3.2 Orbit Types

The selected orbit strongly influences the power budget. Some specialized orbits have stable parameters in an energy point of view. As shown in figure A.2 on page 115 the sidereal days¹³ and mean solar days¹⁴ have different lengths.

Most orbits are elliptical and the Earth (or in the case of the Earth orbiting around the sun, the sun) is in one of the focal points (the geometry of an ellipse is shown in figure A.1 on page 114). The area that a spacecraft moves through per time is constant. For satellites the apogee¹⁵ - distance is more influenced by loss of orbital energy (due to drag force; see section 3.1.3 on page 5)—distance becomes less—than the perigee¹⁶, which stays nearly constant over the whole lifetime of the satellite.

Fortunately, the eccentricity for the orbit of the Earth around the sun (figure A.3 on page 115) is very small and therefore we can neglect these changes for a rough sizing of the solar array (see section 4.1.2 on page 47). The change of the sun-to-satellite distance during an Earth orbit is negligible for sizing the solar array—the additional change in distance due to GEO is less than 1 per mill.

But one cannot neglect the eclipse time during the orbit, which strongly depends on the orbit itself. For most orbits the eclipse time changes during the year and only a few orbits (sun-synchronous LEO, see section 3.2.1.1 on page 13) can score with a little change. Eclipse of the sun by the moon was not simulated with the MATLAB tool and is, therefore, not further discussed—information about that can be found in [40, p.299].

The ecliptic plane is the plane in which the Earth moves around the sun. Thus, the sunlight hits the Earth from that direction. The equatorial plane is slanted by 23.5 degrees to the ecliptic plane.

Inclination is the angle of the orbital plane of the spacecraft measured from the equatorial plane. An equatorial orbit has an inclination of 0 deg and a polar orbit an inclination of 90 deg.

One of the most important characteristics for a satellite orbit is the ground track (e.g. MOLNIYA 3-45 see figure 3.7 on page 18), which shows the nadir-pointing path of the satellite on Earth. The ground track has to satisfy the needs of the mission. A special type of ground track is the repeating ground track, in which the satellite always passes the same point on Earth. For inclinations of less than 90 deg and orbit times of less than one day, the satellite will move from west to east and for higher inclinations from east to west. To find the ground track, the Earth's rotation also has to be taken into account.

¹³time for a 360 deg turn of the Earth

¹⁴time from noon to noon at the equator

¹⁵farthest point from Earth

¹⁶closest point to Earth

The higher the inclination, the higher the required energy to reach the orbit. For inclinations higher than 90 deg additional energy (launch vehicle) is needed to overcome the Earth rotation—for inclinations less than 90 deg the Earth donates an extra push to reach the orbit, with the maximum push from the equator for equatorial orbit.

3.2.1 Low Earth Orbit (LEO)

Typical Low Earth Orbit (LEO) spacecrafts have a lifetime of three to eight years. Typical advantages of LEO orbits are:

- Relatively “low” radiation for equatorial orbits.
- True global coverage.
- Lower power requirement for communication.
- Low propagation delay¹⁷ (ca. 5 ms)—important for communication satellites.
- Higher picture resolution with same optics.

Disadvantages are as follows:

- Due to the neutral environment (section 3.1.3 on page 5) reduced lifetime because of loss of orbital energy.
- To get the same coverage/time more satellites are required (especially communication satellites).
- Satellite visibility for only a few minutes per orbit from one ground station (e.g. SUNSAT was visible for 10-12 min typical, 15 min max—for orbit parameters see section 4.2.1 on page 49)
- Range and elevation not constant (intense Doppler effect and varying signal strength).
- Number of eclipses (26000 cycles for a 5 year / 100 min orbit) is very high, so mechanical stress and number of charge/discharge - cycles is high.

The LEO - Orbits (altitude < 1000km) are below the inner Van Allen belt (see section 3.1.5.1 on page 6). For satellites at low inclinations fewer radiation-hardened devices are used than in MEO orbits (see section 3.2.3 on page 14).

3.2.1.1 Sun-Synchronous

Sun-synchronous orbits are orbits in which the satellite always passes the ground at the same local time (12 o' clock orbit a) in figure A.4 on page 116). The inclination for that type of orbit is more than 90 deg and depends on the altitude as shown in figure 3.5 on page 16. The orbital plane of the satellite rotates, because of the oblateness of the Earth, once per year. For more information please refer to orbital mechanics - books e.g. [22, p.283-285], [46, p.275]. In a sun synchronous orbit the angle between the sun and orbit plane is mainly influenced by the angle between the ecliptic and equatorial plane. As a result the generated power stays nearly constant (cf. section 3.3.3 on page 22) over the whole period, except in eclipse.

Sun-synchronous always orbits pass the ground with similar light conditions, except for the seasonal influence. It is easier to compare pictures with the same light conditions (pictures with days or even years in between). Also reflections from lakes, rivers and oceans can be minimized. Orbits for optical Earth - imaging satellites could be selected so that morning fog has time to clear off and early enough not to get the typical clouds of the afternoon. Certain types of imaging applications are not much influenced by clouds. For these applications other orbits (e.g. dawn - dusk, see section 3.2.1.2 have more advantages. So the best parameters for the mission can be selected with the right orbit.

3.2.1.2 Sun-Synchronous Dawn - Dusk

The advantage of a sun-synchronous dawn - dusk orbit is the availability of continuous energy from the sun. Although the satellite is always exposed to the sun, thermal management is easier because of the continuous radiation. SAR - satellites are not influenced much by clouds and light conditions, therefore dawn dusk - orbits are acceptable. The Canadian SAR - satellite "RADARSAT" uses such an orbit.

3.2.1.3 The Polar Orbit

Another special LEO is the polar orbit. Some communication satellites (e.g. the IRIDIUM system) are using this orbit. Total coverage of the Earth is possible. Unfortunately, the population density at high latitudes is not very high, but the highest satellite coverage density is there. [46, p.157], [40, p.649]

3.2.2 Geostationary Earth Orbit (GEO)

GEO¹⁸ can stay—like debris—in orbit for millions of years [19]—much longer than the electronic will last. Typical advantages of GEO orbits are:

- Constant distance and angle with respect to any place on Earth. Transceiver can be fixed. Cheap dishes without any moving parts like television dishes.
- The satellite can be seen from nearly half the globe.
- Continuous sight to the same part of the Earth.
- Only a few discharge cycles during the year figure 3.6 on page 17.

Disadvantages are as follows:

- Energy storage has to be dimensioned to work for ≈ 1 h per day only for a few days a year—not effectively used energy storage.
- During high solar activity—Earth’s magnetic field is pressed to the Earth on the sun-exposed side—the galactic rays are stronger.
- Surface charge is a bigger problem (see section 3.1.4 on page 5).
- Global coverage with one satellite is not possible (3 satellites are needed to reach most of the globe)
- Bad coverage at high latitudes, no coverage at the pole regions.

The GEO altitude is 35786 km and of course the inclination is ≈ 0 . They are used for television (e.g. ASTRA), telecommunication (e.g. INTELSAT) or other purposes where big coverage is necessary.

3.2.3 Other Orbit Types

There are also other orbit types for specific applications. The Global Positioning System (GPS) satellites use a MEO¹⁹ with an orbit time of 12h and a repeating ground track. The inclination is selected with 55 deg [46, p.164]. One very special orbit is the MOLNIYA orbit.

3.2.3.1 The Molniya Orbit

The Molniya orbit is a highly elliptical orbit with the advantage of a big coverage at high latitudes for around 11h per 12h orbit—The coverage of GEO satellites

¹⁷time from Earth to satellite

¹⁸Geostationary Earth Orbit also called GSO Geostationary Satellite Orbit

¹⁹Medium Earth Orbit

is, if ever, very bad at high latitudes. A ground track is shown in figure 3.7 on page 18. The coverage area is above the thin line (for the specific position as indicated through the name of the satellite). The time between the dots (ground track) is 5 min.

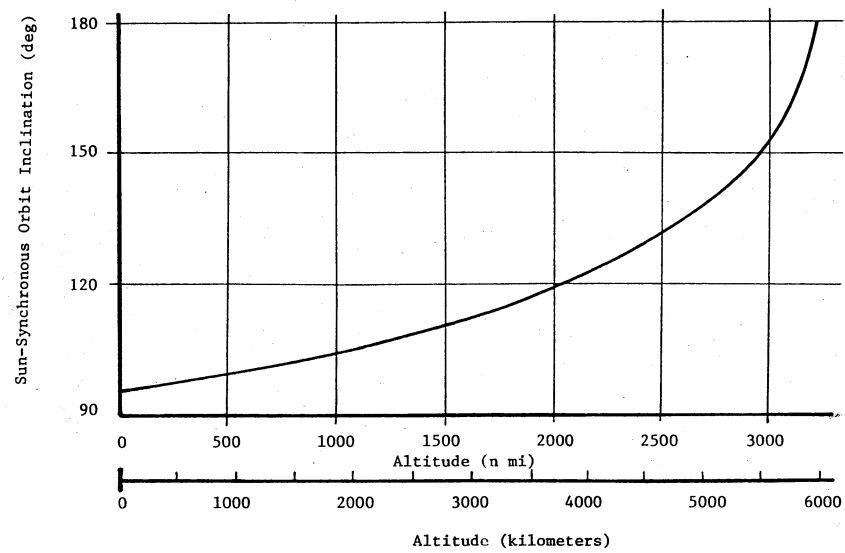


Figure 3.5: Sun-Synchronous Inclination vs. Circular Orbit Altitude [22, p.284]

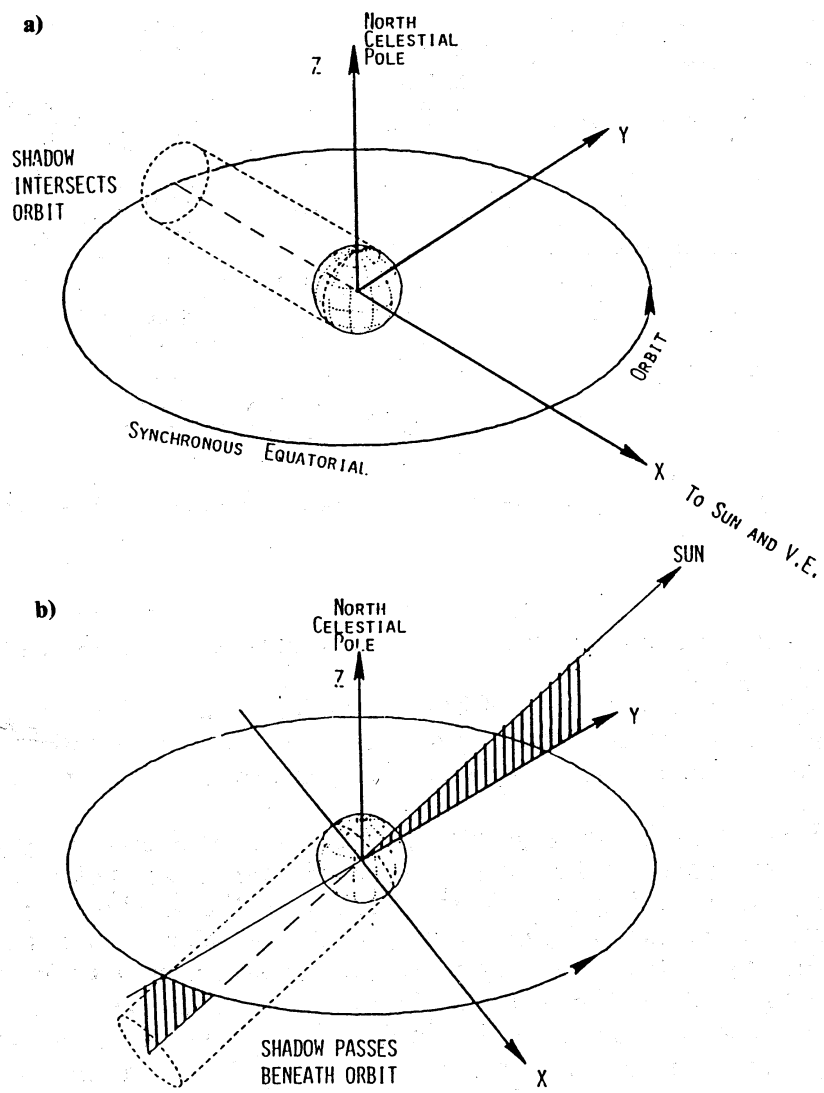


Figure 3.6: Geosynchronous Orbit Geometry [22, p.282]: a) vernal equinox shadow; b) summer solistic shadow (summer in the northern hemisphere)

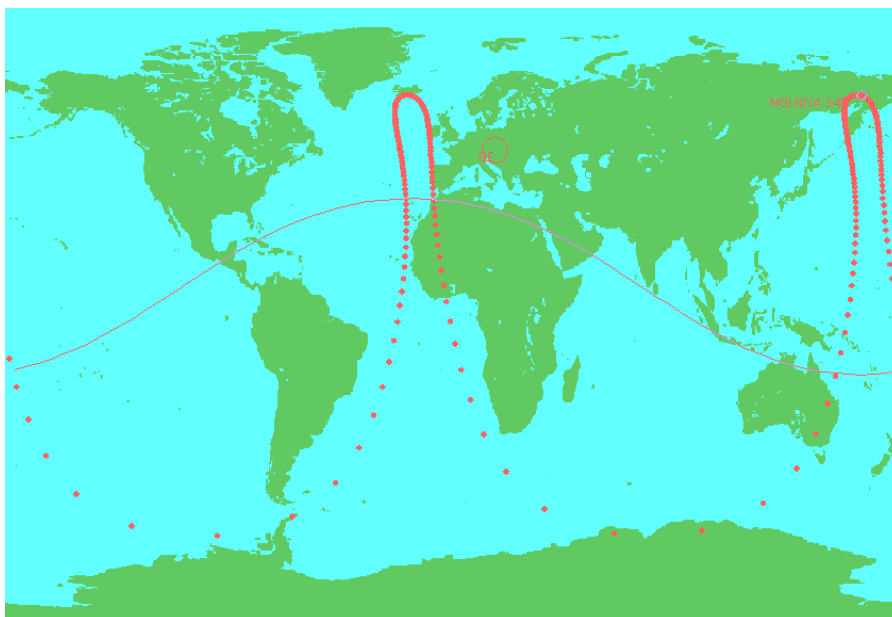


Figure 3.7: MOLNIYA 3-45 Ground Track from 2003/04/12. Created with WinOrbit using two line elements, downloaded from Celestrak [30], [21].

3.3 Solar Cell and Module

Most information in this section is (if not cited differently) taken from the script, lecture and workshop “Solar Cell Physics” in the summer semester 2002 at the Atomic Institute Vienna; lecture held by Dr. Johann Summhammer [49]. Special thanks to Dr. J. Summhammer also for his support of this project by answering all the author’s additional questions about solar cell physics.

This section is mainly focused on Si solar cells and contact materials explained later relate to Si solar cells.

Most Earth orbiting spacecrafts use solar energy to generate the required power (photovoltaic). It is a safe primary energy source without danger for mankind. The sun is a stable power source with the radiation characteristics near a 5900 K hot black body.

A typical solar cell is a pn - junction (or a stack of junctions for multi junction cells) with an anti reflective surface on one side and normally a reflector on the back - side.

To conduct the current to the load, a metal grid is used on the top - side (e.g. Ti-Pd-Ag to reduce the resistance and form a resistive contact to the n - doped layer) and a full metal coverage—acting as reflector and conductor—on the back (typical Al-Ag). The contacts are sintered through the Si - oxygen layer that forms immediately in the air during production process. It is important, that the contact material matches physically to the layer (p- or n-layer), because a semiconductor to metal connection forms a Schottky - diode, but it is unwanted to have a diode in series with each cell Ti is used for the n - doped layer.

The anti reflective layer can be made of TiO₂ or silicon nitride (passivation of surface). The absorption rate can be improved by using anisotropic etching, creating an inverted pyramid surface structure (20x20 μm²). It is possible to reduce the reflection to below 2%. (Values for Si cells)

It should be noted, that some totally different types exist which have totally different structures. The commonly used space cells are (at the time of this thesis) Si, GaAs/Ge, GaInP₂ and thin film cells, typically illuminated from one side only. The structure of a Si solar cell is shown in figure 3.10 on page 21.

With increasing temperature, the voltage drops and the current rises, but the total power decreases.

It is interesting that illuminated cells which deliver the maximum power are cooler than cells which are open- or short circuited. That is because they can transport the energy to the load, otherwise the generated electric energy heats the solar cell. So for Si cells typically 15% less thermal energy is produced through solar irradiation if used in Maximum Power Point (MPP) .

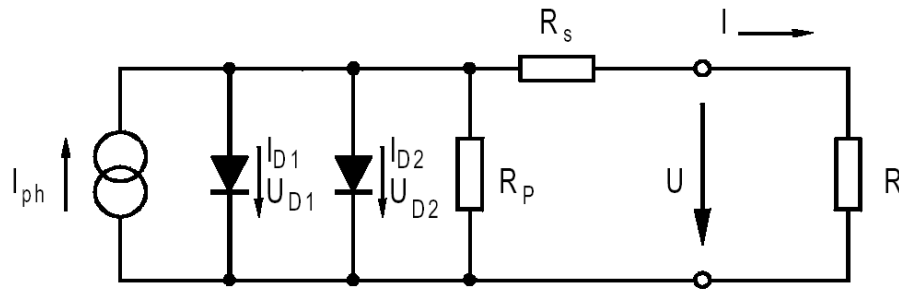


Figure 3.8: Two Diode Solar Cell Equivalent Circuit [54]

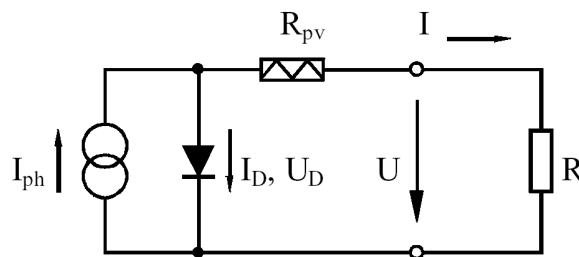


Figure 3.9: Equivalent Circuit Diagram for Effective Solar Cell - Characteristic [54]

3.3.1 Silicon Cell

Silicon is a so-called indirect semiconductor and not only a photon, but also a phonon²⁰ is required to create an electron-hole - pair (Other cell types like GaAs do not require a phonon). It is not very likely that a photon and phonon will meet to create the electron-hole - pair and convey their energy, therefore the photon has to travel a long way through the material (0.1 mm or more). Thus thicker materials are required. At low temperatures (liquid nitrogen), the doping does

Table 3.2: Available Cells from SPECTROLAB; data at 28 °C (End Of Life (EOL): 1 MeV Electron Fluence (1×10^{15} e/cm²)). Begin Of Life (BOL) and EOL irradiation with the spectrum and energy found at a sun distance of 1AU.

cell type	description	efficiency	
		BOL (%)	EOL (%)
Si	K6700B	13.7	10.5
GaAs/Ge	single junction on Ge substrate	19.0	14.5
GaInP ₂ /GaAs/Ge	dual junction on Ge substrate	21.8	18.1
GaInP ₂ /GaAs/Ge	triple junction cell	26.8	22.43

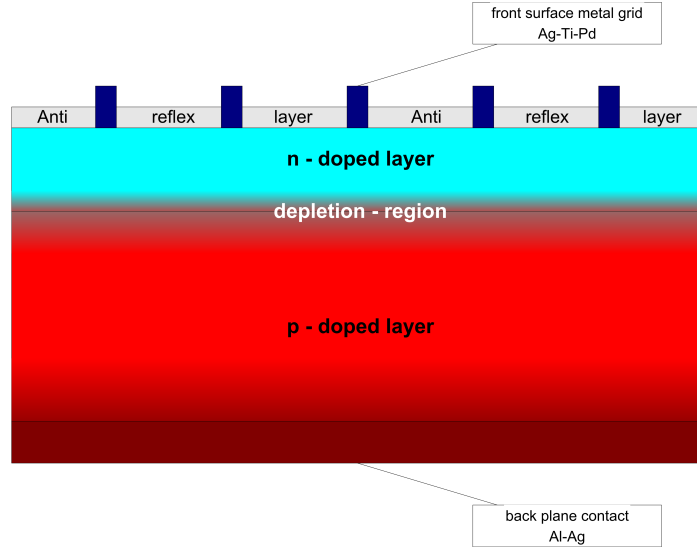


Figure 3.10: Structure of a Solar Cell (not to scale)

not create an internal field. The internal field is required to separate the charges so that the solar cell does not work. To form the junction the silicon material is p-doped boron (B), a higher concentration of phosphor forms the n-doped part (only a few hundred nm thick) and an even higher p-endowed area at the back (Al plane is sintered in).

For silicon cells the minimum photon energy is 1.09 eV which relates to wavelengths of less than 1150 nm for generating electric currents. Shorter wavelengths have more energy than required to create a electron-hole pair and the rest of energy is converted to thermal energy.

Typical losses of the absorbed solar energy are 24% because the wavelength is too long ($\lambda > 1100$ nm) and 33% losses because of too high photon energy [49, ls]. Other losses in the cell are because of recombination²¹ or ohmic losses.

The formula for the 2 diode solar cell equivalent circuit figure 3.8 on the page before, which does not give a clear expression:

$$I = I_{ph} - I_{D1} \left(e^{\frac{U+IR_s}{U_{T1}}} \right) - I_{D2} \left(e^{\frac{U+IR_s}{U_{T2}}} \right) - \frac{U + IR_s}{R_p} \quad (3.2)$$

Where U_{T1} and U_{T2} are thermovoltage ($U_T = \frac{q}{kT}$) with the Boltzmann constant $k = 1.3806503 * 10^{-23} J/K$, the electronic charge $q = 1.602176462 * 10^{-19} C$ and the temperature in Kelvin. Usually U_{T2} is double the value of U_{T1} , which is equal to U_T . I_{D1} and I_{D2} are the reverse saturation currents for the diodes. [54, 10]

²⁰vibration in crystal lattice (Quantum mechanics)

²¹electron and hole recombination creating thermal energy or photon—depending on semiconductor - material

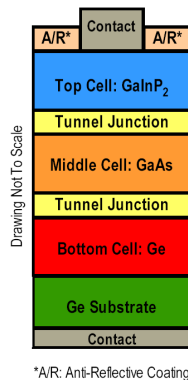


Figure 3.11: Triple Junction Solar Cell with an open cell voltage of 2.545V [47]

It is difficult to measure all these values, but this circuit gives a very good approximation of the real solar cell.

An easier way to approximate the cell is with a single diode and a so-called photovoltaic resistor R_{PV} . The resistor can—something that is physically impossible—have negative values. With this equivalent circuit (figure 3.9 on page 20), it is possible to approximate and calculate the voltage explicitly with an accuracy of 1%. For a description see [54].

3.3.2 Other Cell Types

In general, the effects of other cell types are similar to silicon cells and only the values differ. Triple junction cells are like stacked single cells and a higher cell voltage is possible. Each junction is optimised to a different wavelength, that way a higher cell efficiency will result. Materials for a triple junction cell can be seen in figure 3.11 For direct semiconductors no phonon is required, so they fully absorb the light in a few μm and less of the expensive material is needed.

It should be noted, that bifacial solar cells, and solar cells without a pn - junction (Metal-Isolator-Semiconductor (MIS) exist as well [7, p.2]).

3.3.3 The Irradiation Angle

The angle to the radiation source (sun) is important for all cell types. The solar flux Φ is a constant for a given distance to the sun and an angle different to 90° reduces the amount of solar power on the solar cell surface by,

$$P_{cell} = A\Phi \cos \theta \quad (3.3)$$

where A is the solar array area and θ ($< 90^\circ$) the off-normal - angle to the solar cells. To calculate the electrical power the efficiency of the cell has to be multiplied

with the irradiated power P_{cell} . A small decrease at normal irradiance can occur due to slightly higher reflection rate of the cover glass.

3.3.4 Radiation Degradation on Solar Cell

Radiation in Space will create defects in the crystal lattice. Defects in the crystal structure will “decrease the minority carrier - lifetime. And it is known that solar cells with short minority carrier - lifetime mainly cause a reduced voltage.” [49, 23.4.2003]. The minority carrier diffusion length L depends on the carrier lifetime τ and on the diffusion constant D , where D is directly related to the temperature.

$$L = \sqrt{D\tau} \quad (3.4)$$

If the diffusion length decreases, less minority carriers can make it from their point of origin to the np - junction. Therefore, a reduced minority carrier - lifetime causes a reduced current, but a higher temperature increases the value of the diffusion constant and therefore the current. But overall a higher temperature will decrease the output power (voltage will drop because of a higher current I_D in figure 3.9 on page 20 with rising temperature) [10, p.6], [16, p.5].

It is possible to correct the displacement in the crystal lattice of GaAs (not Si) solar cells by annealing, but that is not very practical in space [49, 11.11.2002], [51, p.153]. None the less, GaAs/Ge cells are less sensitive to radiation.

For other cell types like MIS or thin film, the aging effect might be different.

3.3.5 Typical Efficiency of Solar Cells

Cell types and values, available from SPECTROLAB, are shown in table 3.2 on page 20. For the triple junction cell, SPECTROLAB specifies a MPP voltage degradation of around 14% and the current degradation of 4%.

3.4 Sizing the Energy Storage

The required energy and power for the energy storage has to be estimated with the power budget (section 4.1.1 on page 44). In order to calculate the power budget, eclipse time and power requirements of the satellite subsystems has to be known. The main energy storages are batteries and for some applications capacitors. Other types of energy storage (e.g. bidirectional fuel cells) are not part of this thesis.

3.4.1 For Batteries

The subsections describe how to select the right battery size. It is assumed, that the batteries have no losses. Some factors, which has to be defined to determine the battery size:

- DOD – percentage of Ah discharged from the battery, relative to capacity (specified battery capacity [Ah]²²)
- Discharge rate R_D ²³
- Charge rate R_C
- The battery nominal $V_{BAT_{nom.}}$ and minimum voltage $V_{BAT_{min.}}$

To get the required size of the battery, the calculations from section 3.4.1.2 on the next page, section 3.4.1.3 on page 26 and section 3.4.1.4 on page 26 has to be done, and the biggest value for the capacity has to be used. The discharge current must not exceed the maximum charge- or discharge current specified by the battery manufacturer. The DOD should also not be exceeded which would lead to an accelerated aging.

Note, that these calculations are based on constant current discharge without any losses. And for more accurate calculation, losses, aging and the shape of the current has to be taken in account.

3.4.1.1 The “C” - Rate

“A” common method for indicating the charge and discharge current of a battery is the C rate²⁴, expressed as:

$$I = M * C_n \quad (3.5)$$

²²Capacity unit for capacitors is $[F = \frac{As}{V}]$, where for batteries [Ah] are commonly used.

²³Value for charge- and discharge rate can be taken from the battery - datasheet. Commonly designated as C - rate—note that there are inconsistencies with the units in the C - rate system cf. [36, 3.4].

²⁴Traditionally, the manufacturers and users of secondary batteries have expressed the value of the current to charge or discharge the cell as a multiple of the capacity. For example, a

where I is the discharge current in [A], C_n is the numerical value of rated capacity of the battery in [Ah] for a discharge time of n hours and M is a multiple or fraction of C.

For example, the 0.1C discharge rate for a battery rated at 5Ah is 0.5A. Conversely, a 250mAh battery, discharged at 50mA, is discharged at the 0.2C rate.

It is to be noted, that the capacity of a battery decreases with increasing discharge current.

[36, 3.4-3.5]

3.4.1.2 Battery Charging with known DOD

The equation for recharging the battery is:

$$\text{Energy Removed} = \text{Energy Replaced} \quad (3.6)$$

$$\text{Capacity} * \text{DOD} = I_C * t_C \quad (3.7)$$

where the Capacity is the rated capacity of the battery [Ah], DOD is the percentage of the capacity withdrawn, I_C is the charge current [A] and t_c is the charge time in [h]. So that:

$$I_C = \frac{\text{DOD}}{t_c} * \text{Capacity} \quad (3.8)$$

This is the way the IEC recommends to designate the charge and discharge current.

A charge rate R_C expresses the number of times per hour which the battery's full capacity can be re-loaded into the battery. R_C is calculated as:

$$R_C = \frac{I_C}{\text{Capacity}} \text{ with units } \frac{[A]}{[Ah]} = [h]^{-1} \quad (3.9)$$

For satellite applications, the charge rate is usually not a problem. Typically the charge time exceeds 30 minutes while the DOD is 10-20%. The worst case charge rate is therefore:

$$R_C = \frac{0.2}{0.5} = 0.4 \quad (3.10)$$

current of 1A used to discharge a 5Ah battery would be expressed as $\frac{C}{5}$ or 0.2C (or in the European convention as $\frac{C}{5}$ A or 0,2CA). This method for designation of current has been criticized as being dimensionally incorrect. For more information on how the International Electrotechnical Commission (IEC) describes a new method to designate this current can be found in [36, 3.4].

3.4.1.3 Sizing due to Required Energy

Using equation 3.6 on the preceding page and substituting the formula for charging would lead to:

$$I_D = \frac{DOD}{t_D} * \text{Capacity} \quad (3.11)$$

$$\text{Capacity} = \frac{I_D * t_D}{DOD} \quad (3.12)$$

where I_D is the required current in [A] at the defined nominal battery voltage and t_D is the time, where the power is required. Therefore the equation for given power and DOD is:

$$\text{Capacity} = \frac{P_D * t_D}{V_{BAT_{nom.}} * DOD} \quad (3.13)$$

where $V_{BAT_{nom.}}$ is the battery nominal voltage and P_D is the required power.

3.4.1.4 Sizing due to Required Power

The discharge current (see section 3.4.1.1 on page 24) is calculated, based on equation equation 3.9 on the preceding page, as:

$$R_D = \frac{I_D}{\text{Capacity}} \quad (3.14)$$

leading to:

$$\text{Capacity} = \frac{I_D}{R_D} \quad (3.15)$$

For a given power requirement, the capacity is:

$$\text{Capacity} = \frac{P_D}{V_{BAT_{min.}} * R_D} \quad (3.16)$$

where $V_{BAT_{min.}}$ is the battery nominal voltage and P_D is the required power.

3.4.2 Sizing Capacitors

Typical Values of Supercapacitors can be found in section 3.5 on page 28. The sizing of capacitors is slightly different to batteries due to their voltage (U) vs. energy (W_C in [J] or [Ws]) - relation:

$$W_C = \frac{CU^2}{2} \quad (3.17)$$

Some factors, which has to be defined to size the capacitor:

- Minimum voltage of the capacitor stack
- Maximum voltage of the capacitor stack

The size of the capacitor depends on the signal form of the load current, which is usually not constant. Therefore, only a rough estimation for capacitors without losses is made. *Note, that for real capacitors, the internal resistance causes losses depending on the discharge current (see section 4.3 on page 54 for an example with constant load).* Also note that the minimum voltage, and the required maximum power can lead to high currents. Usually DC/DC converters are used, which themselves have losses and an elaborately analysis is necessary.

The rough capacitor size without losses is:

$$C_r = \frac{2W_{requ}}{U_{max}^2 - U_{min}^2} = \frac{[VAs]}{[V^2]} \text{ with units } \frac{[As]}{[V]} = [F] \quad (3.18)$$

Note, that the energy is required in Ws to get the right result. The most practical way is to do a simulation of the whole system after a rough sizing of the capacitor stack.

3.5 Supercapacitors

A Supercapacitor, also known as Electric Double Layer Capacitor (EDLC) , Ultracapacitor or Pseudocapacitor, is an energy storage device with high power density. *Described over 100 years ago as a double-layer capacitor, the ultracapacitor stores energy by moving charged ions close to an electrode with the opposite charge. This potential is then considered stored energy. A double layer capacitor accomplishes this energy-storage task by moving positive charges in one direction, negative charges in the other, and hence the double layer.* [11]

Due to the high surface area (2500 m²/g) of activated carbon materials and organic electrolyte, capacity values of 120F/g are possible with voltages in the area of 2.5V leading to $\frac{120F * 2.5^2 V^2}{2} = 375J$ per gramm. [53, p.343]

The operation of a double-layer capacitor and a comparison to battery and normal capacitor is shown in figure 3.12 on the next page.

Description on other Supercapacitor - types like polymer or metal oxide can be found in [53, p.487-501] and typical values for Supercapacitors are shown in figure 3.13 on page 30. It should also be noted that NASA did an evaluation of Ultracapacitors from Maxwell e.g. [38].

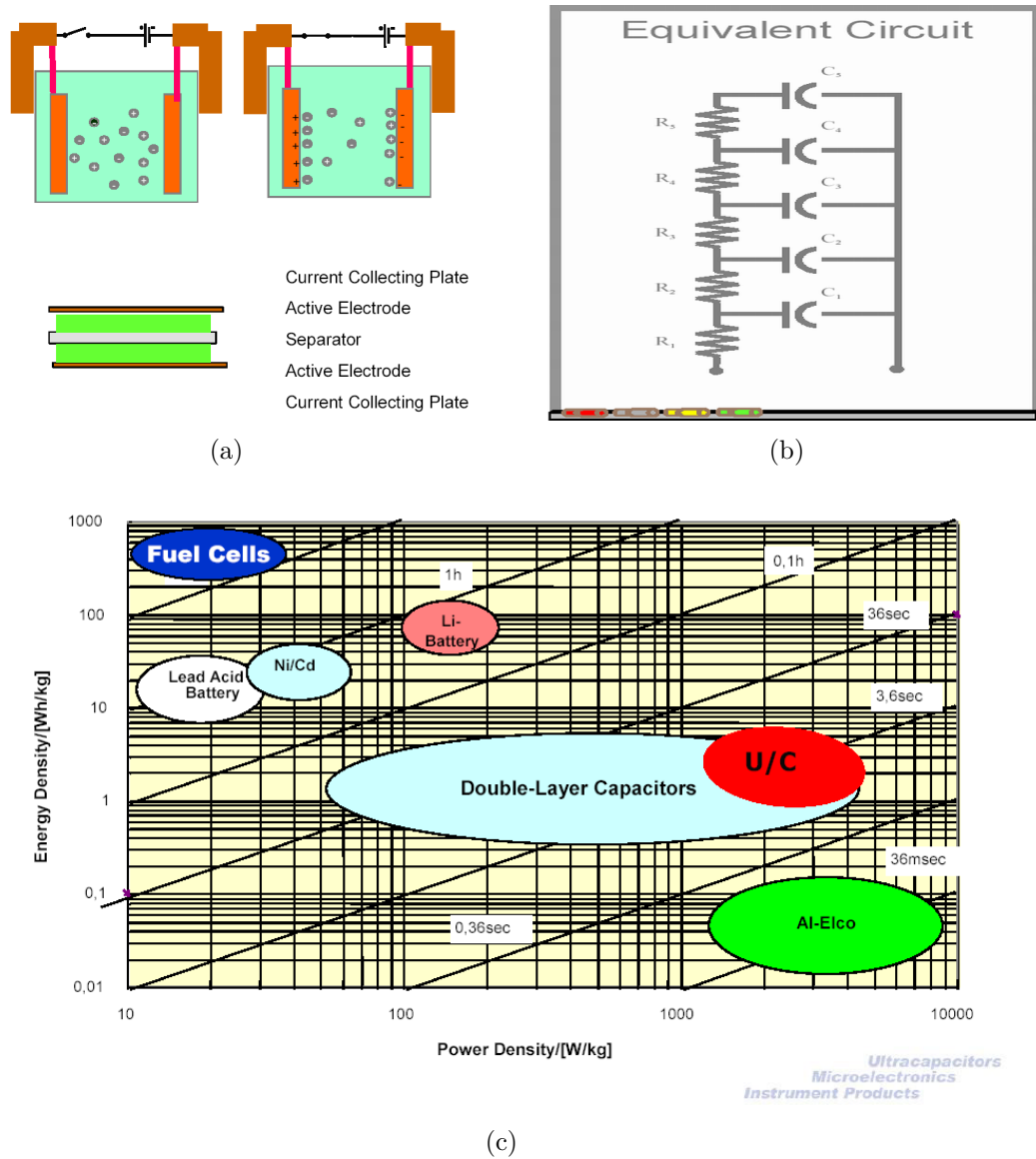


Figure 3.12: The Supercapacitor: (a) storing energy by applying a potential; (b) equivalent circuit and (c) comparison between double-layer capacitor, battery and Al-Elco (electrolytic capacitor). Pictures from [39]

Voltage (V), capacitance (C), ESR (R), specific energy (E), maximum specific power (P_{MAX}), weight and time constant (RC)

Supercapacitor	V V	C F	R mΩ	$E=\frac{1}{2}CV^2$ Whkg ⁻¹	$P_{MAX}=V^2/4R$ kWkg ⁻¹	Weight g	RC s
Single Cell							
EPCOS UltraCap 1200	2.3	1200	1.3	2.2	2.5	400	1.6
EPCOS UltraCap 1200	2.3	3600	3.0	4.1	0.7	650	11
NESS NESSCAP60C	2.3	60	25	3.1	3.8	14	1.5
NESS NESSCAP3500P	2.3	3500	0.4	3.2	4.1	800	1.4
MONTENA BCAP0011A01	2.5	800	2.4	3.3	3.1	210	1.9
MONTENA BCAP0010A03	2.5	2600	0.7	4.3	4.3	525	1.8
Maxwell PowerCache PC2500	2.5	2700	1	3.2	2.2	725	2.7
Matsushita-Panasonic UPB	2.3	1200	2.5*				3.0
Matsushita-Panasonic UPA	2.3	2000	3.0*				6.0
Module							
Maxwell PowerCache PC5.5 (2 cells)	5	1.8	800	0.8	1	8	1.4
Matsushita-Panasonic UPB	12	200	15*				3.0
Matsushita-Panasonic UPA	12	330	18*				5.9
EPCOS UltraCap (6 cells)	14	450	6.5	2.7	1.7	4500	2.9
EPCOS (17 cells)	40	67	23	1.9	2.2	8000	1.5

* ESR measured at 1 kHz

Figure 3.13: Comparison Between Different Capacitors [53, p.485]

3.6 Lithium-Ion Cells

Table 3.3: Major Advantages and Disadvantages of LiIon Batteries. Taken from [36, 35.2]

Advantages	Disadvantages
Sealed cells; no maintenance required	Moderate initial cost
Long cycle life	Degrades at high temperature
Broad temperature range of operation	Need for protective circuitry
Long shelf life “(discharged at low temperature)”	Capacity loss or thermal runaway when overcharged
Low self discharge rate	Venting and thermal runaway when crushed
Rapid charge capability	Cylindrical design typically offer lower power density than NiCd or NiMH
High rate and high power discharge capability	
High coulombic and energy efficiency	
High specific energy and energy density	
No memory effect	

Lithium-Ion (LiIon) cells are a relatively new cell chemistry. They are widely used in commercial products. Most laptop batteries are made of LiIon cells. For satellites, special, large space qualified cells are used. AEA follows the approach to use selected commercial cells in space. This thesis is not focused on the big and expensive, space qualified cell approach but on commercial cells, specially on round cells of the “18650” type.

Information for space qualified cells can be found in books like [36, 35.47] or on the webpages of cell manufacturers like SAFT. Information on big LiIon cells (not in mass production like the standard laptop cells) and their behaviour can be found in [14], [25] or [13].

3.6.1 Charging and Discharging of LiIon Cells

The energy in LiIon cells is stored through exchange of lithium ions (Li^+) between positive and negative electrode. The process is shown in figure 3.14 on the next page

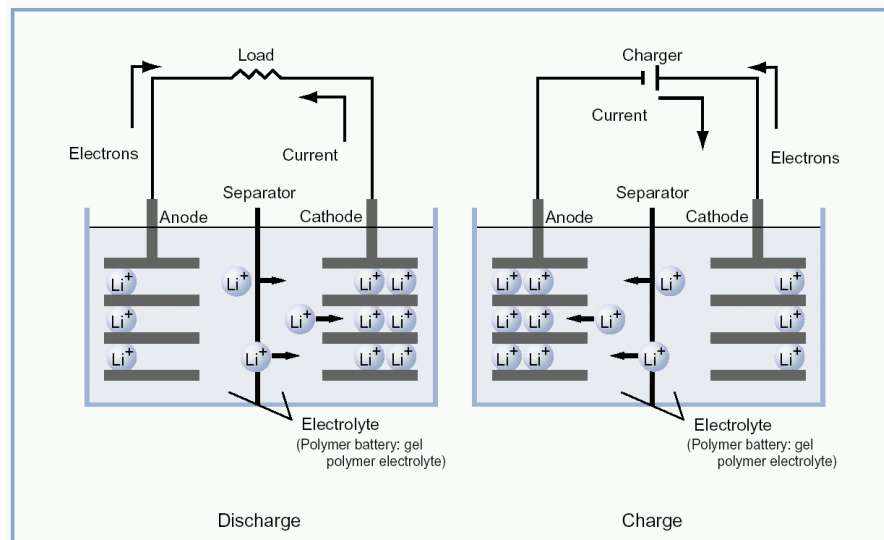


Figure 3.14: Charge and Discharge Mechanism of LiIon Cells. Negative electrode: Carbon (Graphite, Hard&Soft carbons, etc). Positive electrode: LiMO_2 ($M = \text{Co, Ni, Mn}$)

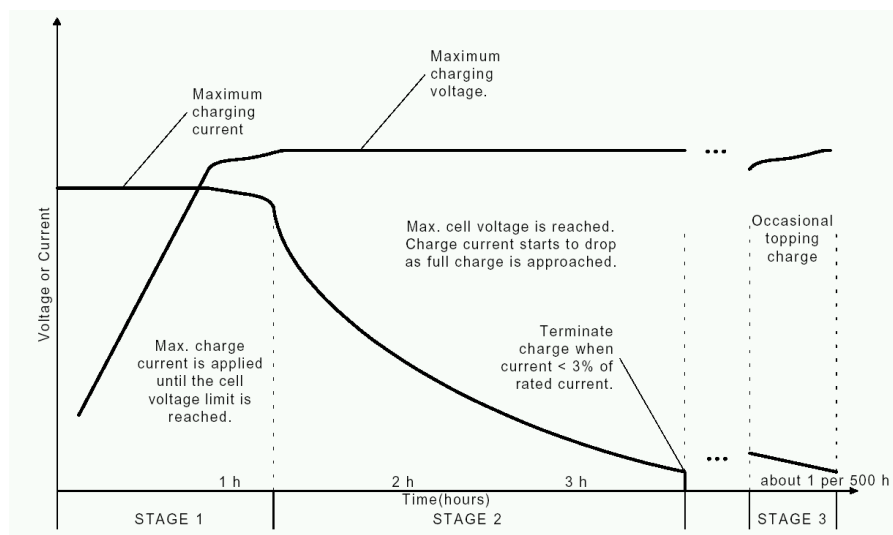


Figure 3.15: Charge Curve of a LiIon Cell. Taken from [20]

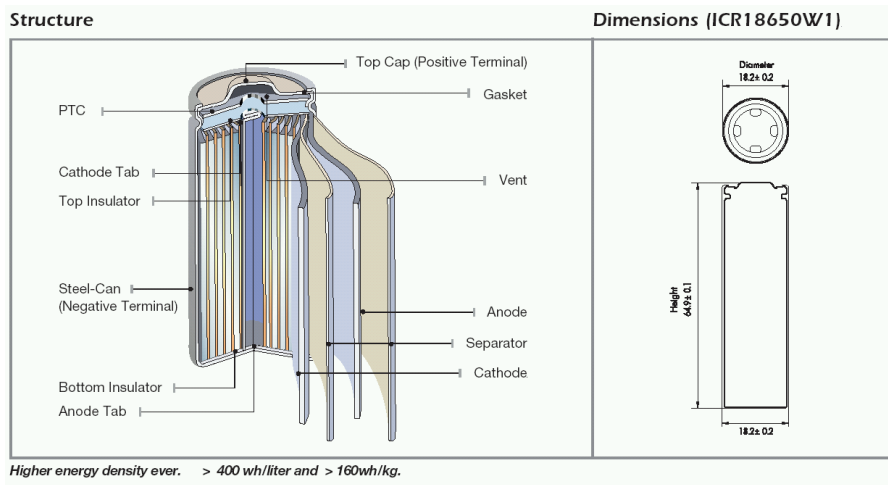


Figure 3.16: Structure of a LiIon Cell taken from [35].

The maximum charge voltage for LiIon cells is between 4.1V and 4.2V. The charge and discharge rate limits from the cell manufacturers has to be followed, or degradation of the capacity is accelerated.

The required charge technique is a constant current - constant voltage (CC-CV) method. The constant current at the beginning of the charge process is to limit the current to the specified charge current. The constant voltage stage is required to charge the cell completely. It is not recommended to use a higher voltage than the maximum charge voltage to reach the full state earlier. A typical charge curve is shown in figure 3.15 on the preceding page. According to AEA, the battery can stay connected to the charger if the voltage is strict limited to the maximum charge voltage, leading otherwise to gas production and open circuit failure (section 3.6.3 on page 35).

For discharge, the end of discharge voltage is between 2.5V and 3V. As mentioned, the discharge current degrades the performance and also the number of cycles and the Depth Of Discharge (DOD) .

Typical self discharge of LiIon batteries is 0.3%/day and the energy efficiency is 96% $\left(\frac{\text{discharged energy}}{\text{charged energy}}\right)$ [2].

3.6.2 Buildup of Lilon Cells

The electrode active materials are a combination of carbon and lithium-metal-oxide (LiMO_2). Different types of materials are shown in figure 3.14 on the preceding page. The positive electrode consists of Al foil coated with the active material (LiMO_2), where the negative is made of copper coated with carbon or graphite [36, 35.31]. The electrodes are electrically isolated through a microporous film [36, 35.29]. The structure of a round LiIon cell is shown in figure 3.16 and

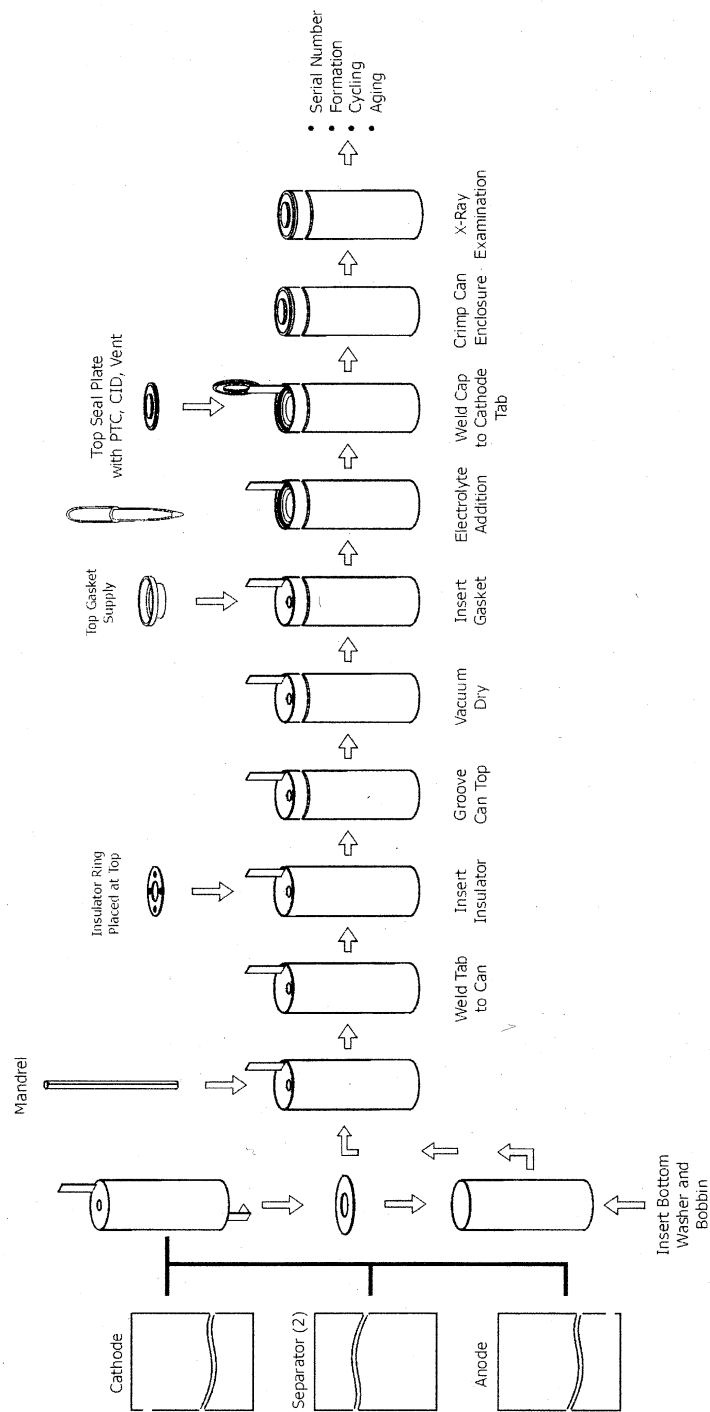


Figure 3.17: Stylized Depiction of the Assembly Process for Cylindrical LiIon Cells taken from [53, p.280].

the production process in figure 3.17 on the preceding page. The top cap is shown in section 3.6.3

3.6.3 Safety Mechanism of 18650 Cells

The safety mechanisms of round cells of the 18650 types are:

- Over charge protection (Circuit breaker)
- Protection from explosion (Pressure vent; valve disc)
- Protection from thermal runaway (Shut down separator; acts as thermal fuse)
- Short circuit protection (PTC)

The circuit breaker breaks an internal connection, if the internal pressure is too high. The circuit breaker stops the charge, and if the charge current was small ($<1C$), the pressure should not rise to a value, high enough to open the pressure valve. The circuit breaker is a non-reversible protection.

The pressure valve opens if the cell pressure is very high to prevent a uncontrolled explosion. If the valve opens, leakage of electrolyte is expected. The pressure valve opens at a higher pressure than the circuit breaker, so the electrical connection to the electrode should be disconnected by the time the pressure valve opens. This is a non-reversible mechanism.

The shutdown separator is the micro porous film, isolating the two electrodes. The separator melts at more than $130^{\circ}C$ and shuts down the reaction in the cell. Also this mechanism is non-reversible.

The only reversible protection is the PTC²⁵, which limits the current.

Pictures of a disassembled top cap and the safety devices can be seen in figure 3.18 on the following page.

Battery management is used in almost all LiIon battery packs with more than one round cell (section 3.6.6 on page 37). Passive, thermal activated switches (e. g. KLIXON from Texas Instruments) are used as additional protection.

3.6.4 Aging Effects on LiIon Cells

As already mentioned, the charge and discharge current, the DOD, the number of cycles and also the temperature depending on the State Of Charge (SOC) causes capacity loss [8]. During normal operation LiIon cells should never produce gas, and therefore the circuit breaker should never open (cf. section 4.6 on page 63

²⁵Positive Temperature Coefficient



Figure 3.18: The Top Cap of a Panasonic 18650 Cell. (a) The top cap from top side; (b) the top cap from bottom side, rest from metal can removed; (c) top side, top of cap removed with grinder, pressure valve visible, plastic removed; (d) metal of top seal plate (figure 3.17 on page 34) weakened; (e) parts of the top cap, bottom the plastic removed in c, top the isolation between valve disc and circuit breaker, left to right: outer metal part of top cap – visible in a, PTC, valve disc, circuit breaker, inner metal part of top cap – visible in b; (f) pressure valve left and circuit breaker right.

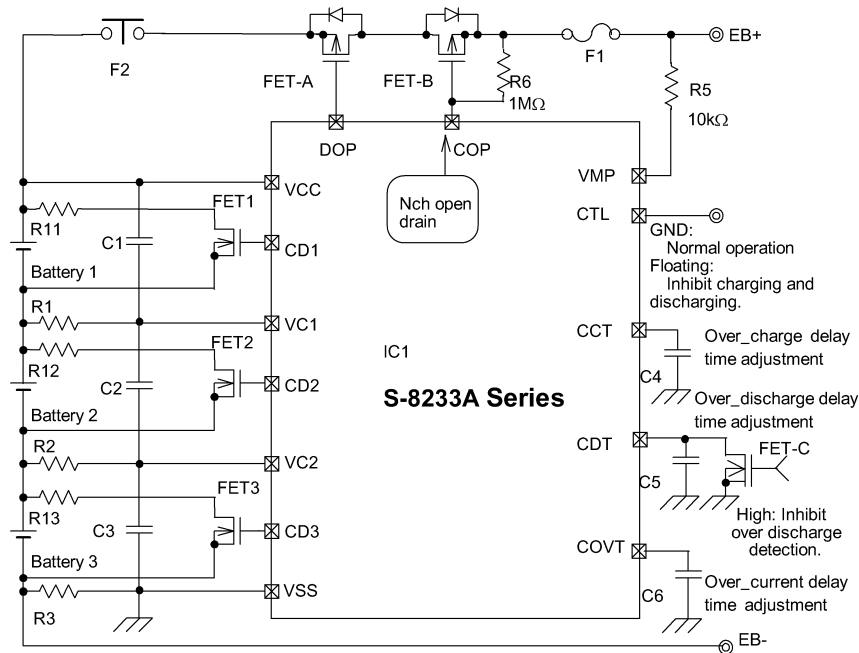


Figure 3.19: S-8233A - Battery Protection Circuit [45]

where in practice other behaviour was found) [5]. Information on “Aging Mechanisms and Calendar-Life Predictions in Lithium-Ion Batteries” can be found in [53, p.393]

3.6.5 Classification of Cells

Classification of LiIon cells is shown in table 3.4 on the next page.

3.6.6 Cell and Battery Management

Cell management includes cell monitoring and equalization.

A patent of AEA Technology [44] termed “Lithium cell recharging” involves bypassing the cells for equalization using a MOSFET and a resistor, controlled by a control circuit. Another patent [32], focused on “Battery charging apparatus” describes different ways of charging and balancing batteries.

A Review of cell equalization methods can be found in [42]. One example of integrated circuits for LiIon battery protection²⁶ and equalization with controlled resistors (dissipative method) is shown in figure 3.19. For circuit board effects on LiIon protection circuits please consult [31].

²⁶This IC was found in an analysed battery pack, see section 4.6.2.2 on page 68

Table 3.4: Codes for Rechargeable Li-Systems [1]

Classification according to IEC	
Code	Description
1. position	Describes the negative Electrode: I: Li-Ion L: Lithium metal or Li-alloy
2. position	Describes the positive Electrode C: based in cobalt N: based on Nickel M: based on Mangan V: based on Vanadium
3. position	Battery shape: R: Round P: Prismatic
Cell size for round cells	
4.+5. position	Diameter in mm
6.-8. position	Height in 1/10 mm
Example	ICR 18650 Round Li-Ion cell pos. cobalt based Electrode. Diameter ca. 18 mm, High: 65 mm
Cell size for prismatic cells	
4. + 5. position	Width in mm
6. + 7. position	Thickness in mm
8. + 9. position	Height in mm
Example	ICP 340848 Prismatic Li-Ion cell with pos. cobalt based electrode. Width: 34 mm, Thickness: 8mm, Height: 48 mm
<p><i>Additional</i> If the size is more than 100 mm then the number groups are separated by a slash. The groups can then be enlarged as necessary. In case of thin prismatic cells, a T can separate the groups. Then the size is given in 1/10 mm units.</p>	

3.7 Nickel Cadmium Cells

Table 3.5: Major Advantages and Disadvantages of Sealed Nickel-Cadmium Batteries. Taken from [36, 28.1]

Advantages	Disadvantages
Long cycle life	Voltage depression or memory effect in certain applications
Good low-temperature capability	Higher cost than sealed lead-acid battery
Good high-rate discharge capability	Poor charge retention
Long shelf life in any state of charge	Contains toxic cadmium
Rapid charge capability	Lower specific energy than other batteries

Nickel Cadmium (NiCd) cells used to be widely used in commercial products. Now LiIon and Nickel-Metal Hydride cells are more common in commercial products because they do not contain any toxic materials like Cadmium.

For satellite applications NiCd cells are interesting because they are more resistant to overcharging and trickle charging of the battery can be used to equalize the cells.

According to the [40, p.577], the lifetime for NiCd cells is 21'000 cycles for a DOD of 25% or 3000 cycles for 50% DOD. The cell voltage is 1.25V and temperature range -10 to +40°C. A good discussion on NiCd cells can be found in [50, p.35-151] or in [36, c.28]. The typical self discharge of NiCd batteries is 1%/day and the energy efficiency is 72% ($\frac{\text{discharged energy}}{\text{charged energy}}$), so [2]. In [36, 28.22] a charge efficiency of 85% can be deducted from figure 28.27.

The advantages and disadvantages of this cell chemistry are shown in table 3.5

3.8 Nickel Hydrogen Cells

Table 3.6: Major Advantages and Disadvantages of the Nickel-Hydrogen Battery.
Taken from [36, 32.1]

Advantages	Disadvantages
High specific energy (60 Wh/kg)	High initial cost
Long cycle life, 40'000 cycles at 40% DOD for LEO applications	Self-discharge proportional to H ₂ pressure
Long lifetime in orbit, over 15 years for GEO application	Low volumetric energy density: 20 - 40 Wh/l (battery)
Cell can tolerate overcharge and reversal	
H ₂ pressure gives an indication of state of charge	

Nickel Hydrogen (NiH₂) cells are used in satellites because of their long cycle life. In [40, p.577] the cycle life is specified with > 10'000 cycles for 50% DOD where [36, 32.1] mentioned 40'000 cycles for 60% DOD. NiH₂ cells use pressurized gas, kept in a pressure vessel. Typical self discharge of NiH₂ batteries is 10%/day and the energy efficiency is 70% ($\frac{\text{discharged energy}}{\text{charged energy}}$) [2]. Other sources like [36, 35.47] mention an energy efficiency of 80 to 85%. The advantages and disadvantages of this technology are shown in table 3.6

3.9 Power System Structures

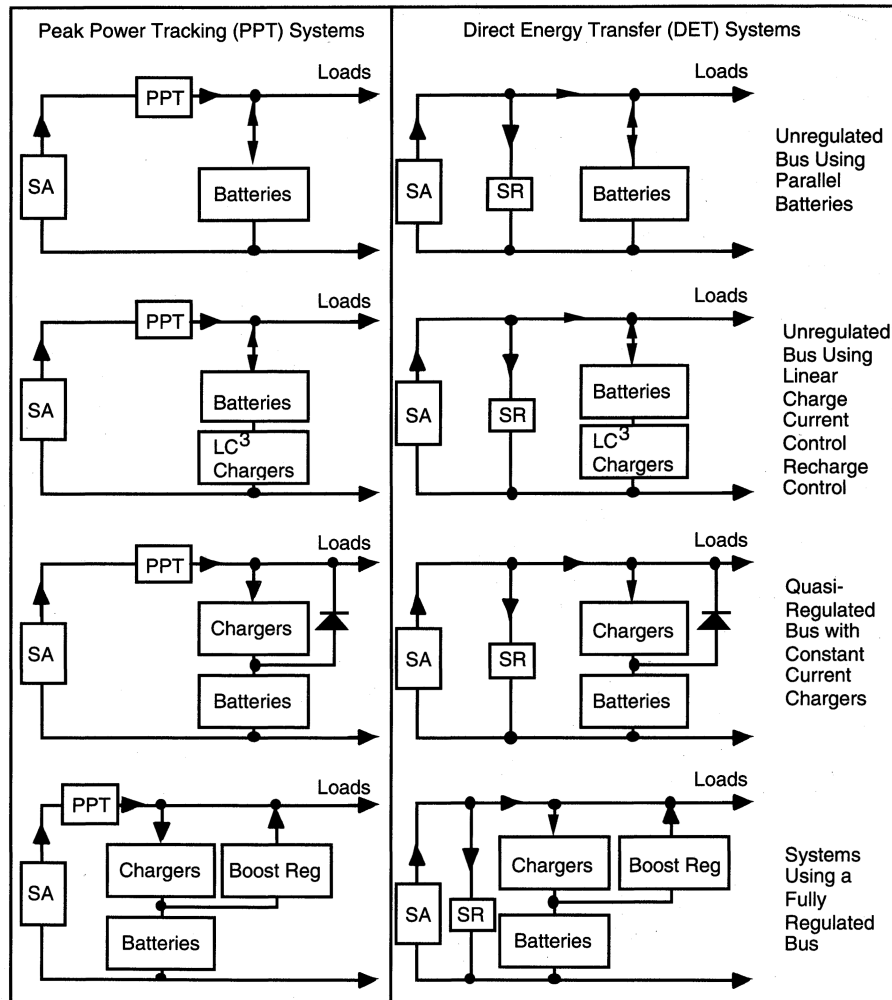


Figure 3.20: Techniques for Power Regulation. The two basic approaches for the power structure of satellites, taken from [34, p.408]. SA refers to Solar Array and SR relates to Shunt Regulator

Different power structures are used in satellites. Some satellites use a Direct Energy Transfer (DET), where the solar array is connected through a DC - path to the satellite power bus. The second approach is the use of a Peak Power Tracker (PPT), also known as Maximum Power Point (MPP) - tracker. Both basic approaches are shown in figure 3.20. For more information please refer to [34, p.391-409], [40, p.566-586].

3.10 High Power - Low Duty Cycle Application SAR

SAR²⁷ - satellites are used to take images of the Earth without being influenced by clouds. Radar pictures can be used, e.g., to distinguish between different types of Earth surfaces for civil applications. Radarsat is a satellite with a SAR imager [6].

Radar systems have high power requirements and therefore energy storage with high power capabilities is required. A low duty cycle is practical for small satellites; otherwise a big solar array is used. With an imaging time of 120 seconds and a 100 minute orbit, the duty cycle is only 2% leading to a required energy of 84Wh for a imaging power of 2500 W. The average over a 100 min orbit is, therefore, only 50W.

The high power requirements are a main factor for selecting the energy storage.

²⁷Synthetic Aperture Radar

4 Practical Work

The practical work starts with a typical design process for power subsystems [34, tab.11-30]. During the work on the thesis project the power source was not selected. The most realistic approach is the use of GaAs or Si solar cells for LEO or GEO satellites. A tool to simulate the power generated by solar cells in different Earth orbits was developed. Different ways of energy storage were evaluated for a specific satellite with high power requirements. Commercial LiIon cells were analysed and a cell selection process was developed. Test equipment was built to test the electrical characteristics of LiIon cells very accurately.

4.1 SAR - Analysis of power requirements

The analysis of requirements in a power system is a very important part. This section shows the process flow for a power budget analysis. A EXCEL - sheet was developed to calculate the required power by specifying the modules in the satellite and different operation modes.

4.1.1 Power Budget

Device	Voltage [V]	Current min [mA]	Current avg [mA]	Current max [mA]	Power min [mW]	Power avg [mW]	Power max [mW]
Solar Module	14				0	-200,000	-200,000
Magnetometer						300	500
Horizon sensor						3,000	3,500
Fine sun sensor						3,000	3,500
PSD Sensor						1,000	1,000
Star camera						2,000	3,000
Torque coils						12,000	25,000
Reaction wheels						6,000	75,000
PCU	12		130	130			
ADCS						2,500	3,000
OBC	14		100	100			
VHF RX	14		91	91			
TX UHF	14		1,610	1,610			
SAR	50		30,000	50,000			

Figure 4.1: Power requirements of different modules

The power budget is a list of power requirements of all modules in the satellite. The power budget contains maximum power and average power. With the power-budget one can size the solar module and energy storage. It should be possible to define operating modes (which modules should be on at the same time) to optimize the power system, because it is uncommon to have all the subsystems switched-on at the same time.

The supposed power requirements are shown in figure 4.1. In figure 4.2 on the following page several modes are defined with their “on-time”, and the duty cycle of each module. The results are shown in figure 4.3 on page 46.

	Time							
	M0	1 h		During launch				
	M1	2 days		Not stabilized in orbit				
	M2	1 sec		Bat low voltage				
	M3	99 min		Normal sun exposed				
	M4	1 min		Normal eclipse				
	M5	120 sec		Imaging				
	M6	8 min		Transmitting data				
	M7	0 days		not defined				

	During launch	Not stabilized in orbit	Bat low voltage	Normal sun exposed	Normal eclipse	Imaging	Transmitting data	not defined
Device	M0	M1	M2	M3	M4	M5	M6	M7
	duty cycle	duty cycle	duty cycle	duty cycle	duty cycle	duty cycle	duty cycle	duty cycle
Solar Module		0.3	1	1		1	1	
Magnetometer			0.4	1				
Horizon sensor			0.3	1		0.7		
Fine sun sensor			0.3	1		0.9		
PSD Sensor			0.1	1	0.4	0.2		
Star camera			0.1	1				
Torque coils				0.1				
Reaction wheels			1	1				
PCU		0.2		1	1		1	
ADCS		1	1	1	1	1	1	
OBC	1	1	1	1	1	1	1	
VHF RX		1	1	1	1	1	1	
TX UHF				1			1	
SAR				0		1		

Figure 4.2: Specification of the different modes

4.1.1.1 Maximum Power

To calculate the maximum power some values were assumed. The value for imaging was assumed to be 2500W. The total power requirements of the modules for all the different modes were calculated. The mode with the highest power requirement defines the maximum¹ power requirement for the satellite power system. In a SAR satellite the radar is the part consuming the most power. As seen in figure 4.3 on the following page there’s a big difference between imaging and all the other modes.

High voltages require more cells (solar array and battery) to be connected in series, if linear regulators are used to charge the battery. A single failure in a longer string (higher voltage) causes a higher total performance loss. On the other hand high currents require thicker wires (extra weight) and high currents can cause magnetic forces, which can turn the satellite (this effect is used in torquer coils). A standard nominal voltage is 28V—for LiIon 29.6V, which can vary from 20V to 33.6V. For small satellites (100W) four LiIon cells in series (14.8V) are fine.

¹Short radar pulses with higher power values, typ. 15μs and 10kW, are handled within the power amplifier

4.1.1.2 Average Power and Time

To select the right capacity for the energy storage, the average values have to be known. On average there has to be more energy from the solar panel than is consumed by the satellite subsystems. The average power strongly influences the size of the solar array, therefore a reduction of the average power reduces the solar array size and also the cost thereof.

4.1.2 Sizing the Solar Array

A first approximation for the solar panel size (A) in m^2 is given by:

$$A = \frac{P_{requ}}{P_{cell}\eta} \frac{1}{d_{sun}} \quad (4.1)$$

where P_{requ} is the required average power [W]. P_{cell} is the power (irradiation angle - corrected) which is absorbed by the cell (see equation 3.3 on page 22). The solar flux² (Φ), required by equation 3.3 on page 22 is ≈ 1353 [W/m²] at a distance of 1AU. And the efficiency (η) is typically 0.15 for Si cells, and d_{sun} is the duty cycle for sun exposure per orbit (nearly constant in sun-synchronous LEO).

At aphelion (5th July) the generated power is less due to the bigger distance (1.017AU). At perihelion (January 2nd) most power is generated (distance is 0.983AU). To calculate the minimum power, we assume, that the power radiated from the sun stays constant. We also assume, that the solar flux at 1AU is the solar constant with $\Phi = 1353$. With a change in distance, the surface becomes bigger and Φ becomes less, because the total radiated power is now distributed over a bigger surface (cf. surface of a sphere equation 4.2).

$$A_r = 4\pi r^2 = \pi d^2 \quad (4.2)$$

We can find the relation:

$$\Phi_r = \Phi_{1AU} \frac{A_{1AU}}{A_r} = \Phi_{1AU} \frac{4\pi 1^2}{4\pi r_{AU}^2} = \frac{\Phi_{1AU}}{r_{AU}^2} \quad (4.3)$$

where r_{AU} is measured in AU. If we use $\Phi_{1AU} = 1353$ [W/m²] then we get 1308 [W/m²] at aphelion (1.017AU) which is 3.33% less than at 1AU.

It is important to size the solar array for the power required at End Of Life (EOL) . It is not a good choice to use the Begin Of Life (BOL) parameters to match the solar cell array - voltage—recommended in [52]—to the battery voltage because the degradation of the solar cell characteristics is also in cell voltage.

²Value of 1353 and 1370 found in [40, p.567] or 1358 in [34]

A solar module was analysed, focusing on the degradation of the MPP³ - voltage during a five-year LEO mission. The celltype was GaAs/Ge and the array was sized according to the required energy at EOL. The 23 cells in series had a MPP BOL - voltage of 19,9V at 3,37A, calculated through the cell - datasheet. The BOL degradation Factors (cover glass, wiring . . .) were not included in this calculation. The EOL calculation for the selected 5 year LEO was offered with MPP EOL - voltage 16V although the required voltage is 17.2V. The cells can deliver the required power, but could deliver more power at a lower voltage—according to the offer. Degradation during the mission due to UV & Micrometeorites is estimated at 2.5%.

It is recommended to use 1300 W/m² with EOL efficiency for a fixed output voltage—if no MPP - tracking regulator is used—to size the solar array. It is important, that the EOL voltage is high enough to charge the battery completely.

4.1.2.1 Selecting the Solar Cell Type

Si cells are typically the cheapest cells, but GaAs - cells offer a better degradation behaviour. Triple junction cells offer double the efficiency of Si cells, but they are more expensive. If the required solar array size (power) is known and the dimensions for the solar array is limited, the cell with the cheapest cell technology should be used, that can supply the required power at the EOL for the given area.

The selection process for satellites where the cells are not mounted on the satellite structure is more difficult because cheaper cells require a bigger area which leads to a bigger structure which, because of the extra weight, is more expensive. Thus, more factors influence the total cost and it is a more extensive calculation.

4.1.3 Selecting and Sizing the Energy Storage

Selecting a battery for a SAR satellite is only possible if the required number of discharge - cycles, time of SAR - imaging and the required calendar lifetime for the satellite are known. For LiIon and short imaging time, LiIon batteries have to be oversized due to their low discharge rate (2C to 3C).

4.1.4 Conclusion of SAR Power Requirements

It was shown how the power budget was done and the influence distance from the sun was discussed. It was seen that detailed specifications of the orbit and mission are needed to size the power system. Work was only done on sun-synchronous orbits—for other orbits the irradiation time varies in a wide range.

³Maximum Power Point

4.2 Matlab Model for Power Simulation

To simulate the power that is available with a defined solar module, a MATLAB Simulink model was developed. The Model contains:

1. A fixed orientation of the solar module in the orbit coordinate system
2. A given orbit (NORAD 2 line element)
3. A defined solar module size

The following subsections explain how the work was done.

4.2.1 NORAD Two-Line Element

For each object in the USSPACECOM⁴ list, orbit parameters are available as a “Two Line Element”. The SUNSAT⁵ NORAD⁶ element is taken as an example to explain the data fields in that structure.

SUNSAT

```
1 25636U 99008C 01128.97266161 +.00000715 +00000-0 +19965-3 0 05158
2 25636 096.4723 260.1847 0149953 231.6439 127.1180 14.41855678116021
```

The name of the object is not part of the two-line element. Each line contains exactly 69 characters. The first line:

1 The line number *1*.

25636U The NORAD ID *25636* plus a character *U* for unclassified object. The letter *S* = secret, is used for satellites that are in military use. One wouldn't find such a satellite in a public system like the Internet.

99008C The third field is used for international identification. The first two digits indicate the year of launch *99*. SUNSAT was payload *C* at the *008*th Rocket start in the specified year. World Data Centre-A for Rockets and Satellites (WDC-A-R&S) allocate the number for the rocket start.

01128.97266161 The next field specifies the reference time t_0 for the variable orbit parameters. The content of this field is the year *01*, the day of the year *128* and after the dot the UT⁷ in day units $.97266161 \approx 0.973 * 24 \approx 23:21$ o'clock.

+.00000715 To calculate the average change of the orbital rate.

⁴US Space Command

⁵Stellenbosch University Satellite

⁶North American Aerospace Defence Command

⁷Universal Time

+00000-0 Also to calculate the average change of the orbital rate.

+19965-3 Aerodynamic circumstances for the object.

0 Number to indicate the orbit model to extrapolate the orbit data from measurements. The Number 0 was defined for the SGP4⁸ - Model.

05158 Is the number of the data set *0515* plus a digit *8* to verify the data in this line.

To calculate the checksum, all the digits must be summarized. For each minus sign the value 1 must be added. The checksum is the result of a modulus 10 division. The second line:

2 The line number *2*.

25636 The NORAD ID *25636*

096.4723 The inclination in degrees

260.1847 Right ascension of the ascending node in degrees

0149953 The eccentricity (only numbers behind decimal point are shown)

231.6439 Argument of perigee in degrees

127.1180 Mean anomaly in degrees

14.41855678116021 The mean motion *14.41855678* [Revs per day], the revolution number at epoch *11602* [Revs] and the checksum *1*.

Norad data as well as a more detailed description of the NORAD elements could be found via the Internet[21].

4.2.2 Vector System for Matlab Model

The coordinate system is centred on the spacecraft and defined in figure 4.4 on the following page. It is used to define the solar panel normal vector \vec{s} and sun pointing vector \vec{n} . Vector components are shown in equation 4.4.

$$\vec{n} = \begin{pmatrix} s_x \\ s_y \\ s_z \end{pmatrix} = \begin{pmatrix} \text{Velocity component} \\ \text{Neg. orbit plane norm. component} \\ \text{Nadir component} \end{pmatrix} \quad (4.4)$$

⁸Simplified General Perturbations V.4

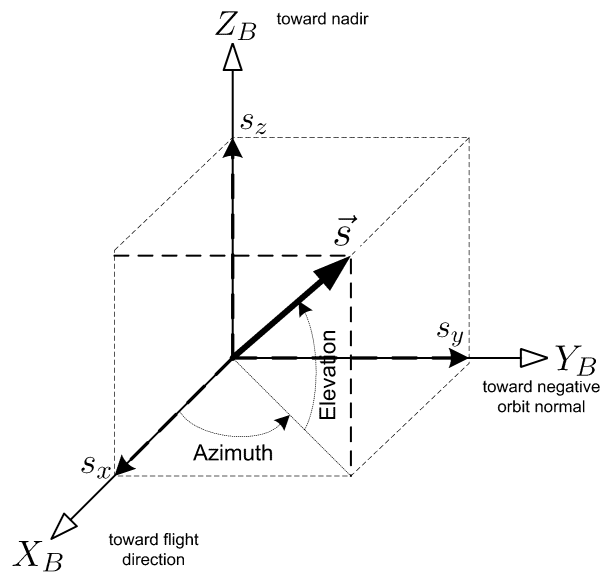


Figure 4.4: Spacecraft Coordinate System

4.2.3 SunSpace Simulink Model - NORAD

To simulate the power from the solar panel, the NORAD 2 line element with a SimuLink S - function from SunSpace was used. This model uses NORAD data as input to simulate the satellite orbit.

A vector \vec{n} in the orbit coordinate system, pointing to the sun, is one of the outputs of this Simulink S - function [48].

4.2.4 MATLAB Model for Simulation

An existing Simulink block was used and extended, so that numerous parameters could be changed and data displayed.

- Sun to solar panel normal angle
- Solar energy Wh produced by solar panel
- Solar power W produced by solar panel
- Solar energy from back side Wh
- Solar power from back side W

The complete MATLAB - model is shown in figure 4.5 on the following page. The following text describes the model.

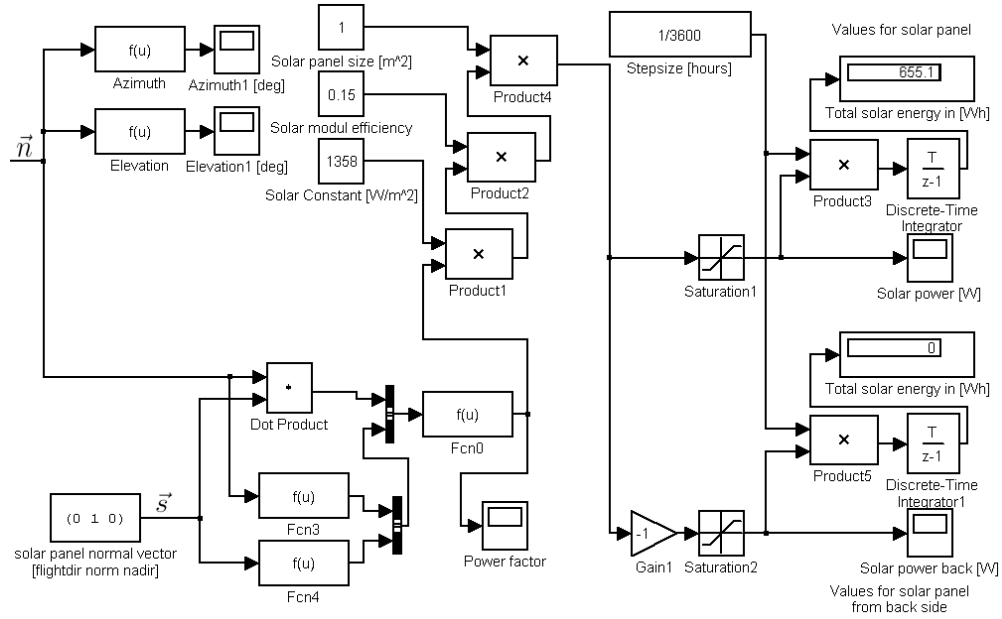


Figure 4.5: Complete MATLAB Model for Solar Simulation

The input vector \vec{n} points to the sun in an orbit coordinate system described in section 4.2.2 on page 50. The function block Azimuth calculates:

$$f(\vec{u}) = \frac{180}{\pi} * \arctan \frac{u[2]}{u[1]} \quad (4.5)$$

The function block Elevation calculates:

$$f(\vec{u}) = \frac{180}{\pi} * \arctan \frac{u[3]}{\sqrt{u[1]^2 + u[2]^2}} \quad (4.6)$$

They are used to display the angles to the sun. The outputs of these formulas are shown on a scope.

The input vector \vec{n} is zero if the satellite is in solar eclipse and otherwise has a size of 1. The solar panel normal vector \vec{s} defines the direction of the solar panel. It has the same coordinate system as \vec{n} . The component which is normal to the nadir- and velocity - axes could have a negative value depending on the flight direction of the satellite—especially in sun synchronous orbits.

Function Fcn3 and Fcn4, which are the same functions,

$$|f(\vec{u})| = \sqrt{u[1]^2 + u[2]^2 + u[3]^2} \quad (4.7)$$

calculate the magnitude of \vec{n} and \vec{s} . Together with function Fcn0 (see figure 4.5 on the preceding page) and the dot product of the vectors, the solar power factor is calculated .

$$\cos \Phi = \frac{\vec{s} \cdot \vec{n}}{|\vec{s}| |\vec{n}|} \quad (4.8)$$

This factor is multiplied with by solar constant, solar module efficiency and solar panel size, which are satellite mission specific parameters.

For positive values the data can pass the Saturation1—which filters all negative values out—and is displayed at the Solar power scope. The accumulated value is shown on the Total solar energy display. The whole system as it is, also generates data for a solar panel, which is turned around (i.e. back-to-back with the panel displayed above). Because it was no extra work the results are multiplied by -1 and shown separately.

In the simulation of figure 4.5 on the page before the following parameters were defined:

- Solar module size $1m^2$
- Solar module efficiency 15%
- Solar constant $1358 \frac{W}{m^2}$
- Solar panel normal vector $\begin{pmatrix} 0 \\ 1 \\ 0 \end{pmatrix}$
- The orbit parameters of SUNSAT⁹ were used to produce \vec{n}

The simulation time was 8h 20min. The output of the simulation is shown in figure 4.5 on the preceding page. The screenshot of the scopes Azimuth1 (figure A.5 on page 117), Elevation1 (figure A.6 on page 118), Solar power (figure A.7 on page 118) and the scope for the solar power factor (figure A.8 on page 119) are shown too.

⁹Satellite in sun-synchronous orbit NORAD no. 25636

4.3 Capacitor Stack - Performance Analysis

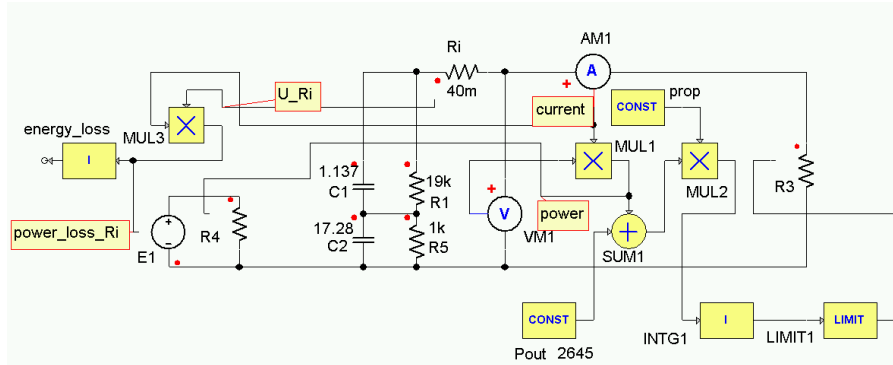


Figure 4.6: Circuit in Simplerer to analyse a Capacitor Stack

Supercapacitors are used in the automobile industry for temporary energy storage. This section analyses a capacitor stack to store the energy required by a SAR - satellite with special focus on capacity mismatching, efficiency and requirements to the equivalent input resistance of a DC/DC - converter, required to gain a stable power bus voltage. Capacitor mismatching and degraded characteristics are assumed for this analysis. 30 seconds of imaging time (2.3kW plus 15% losses in the DC/DC - converter) should be practically attainable.

4.3.1 EOL Simulation with Simplerer®

This subsection describes the simulation of the circuit, shown in figure 4.6. A Student version of SIMPLORER® was used to analyse the capacitor stack and therefore the number of components are limited and nineteen capacitors had to be substituted by one.

The capacitor stack with 20 capacitors in series (type TC2700 from MAXWELL with 2700F) was simulated by two capacitors. The capacitor C1 simulated nineteen capacitors with 20% degraded capacity¹⁰. The capacitor C2 is assumed with an even more degraded (extra 20%) capacity. The series resistance of all capacitors is represented through Ri equal to 40mΩ. The starting condition of the capacitors for the simulation was 2.5V for C2 and nineteen times this value for C1 (47.5V). To reduce the simulation time, the capacity was reduced to $\frac{1}{100}$ of the datasheet values minus degradation. Thus the capacity of C1 was:

$$C_1 = \frac{2700F * d}{100 * n} = 1.137F \quad (4.9)$$

¹⁰Degradation factors used from BCAP0010A03 (Montena); 500'000 cycles. The Equivalent Series Resistance (ESR) was conservatively estimated as 2mΩ—According to the datasheet 200% of BOL would lead to 1.4mΩ for DC.

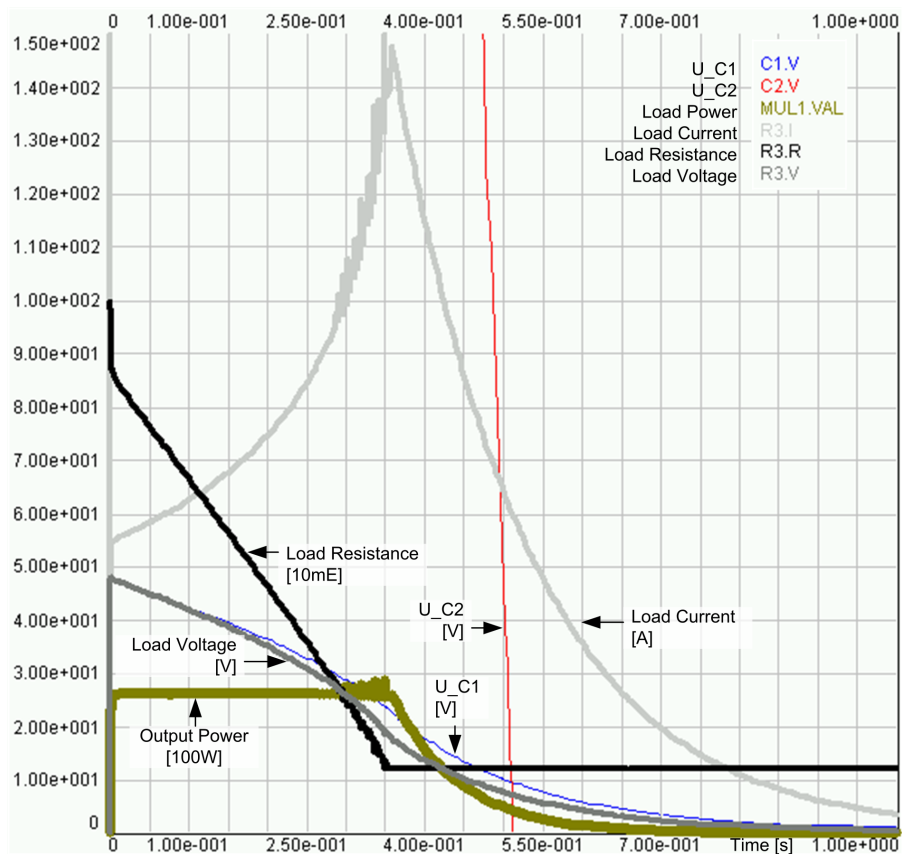


Figure 4.7: Simulation of the load behaviour for 2645W constant power discharge. Different scale factors were used to fit all graphs in the same figure. For example, the Output Power stays nearly constant at 2600W (26 from y-axis multiplied with 100W). The Load Resistance drops from around 900m Ω to above 100m Ω (90 from y-axis multiplied by 10mE)

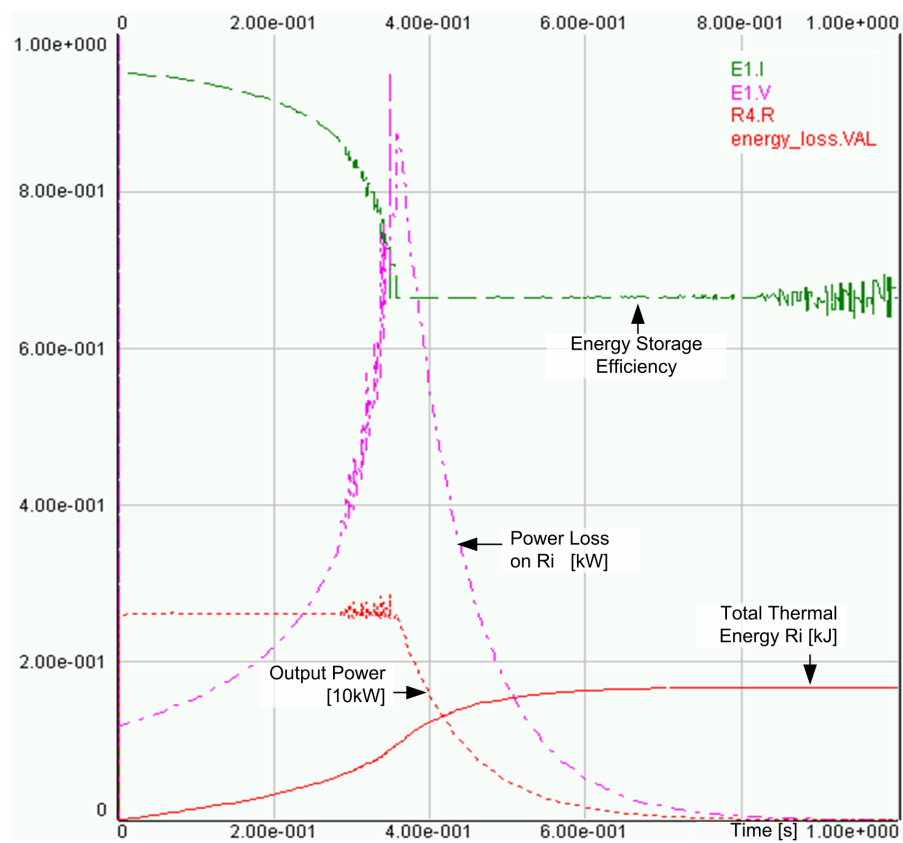


Figure 4.8: Simulation of thermal losses, and the efficiency of a capacitor stack as a means for energy storage

where d is the degradation factor 0.8 and n the number of cells (nineteen). For C2 the degradation factor was 0.64 and n was one.

The resistors R1 and R5 (parallel to the capacitors) did not influence this test. The variable resistor R4 is used together with the controlled source E1 to measure the efficiency of the energy storage. The value of R3 is regulated in such a way that the power loss is 2645W (2300 + 15%) for resistances bigger than 100m Ω . The start condition of the integrator was set to one, leading to a resistance of one ohm at time zero.

4.3.2 Results of the Simplorer[®] Simulation

As already mentioned in section 4.3.1 on page 54, the capacity for the real capacitors is 100 times bigger and therefore the timescale in figure 4.7 on page 55 and figure 4.7 on page 55 has to be multiplied by a factor of 100. The simulation was done once with the real values, longer simulation time and same time steps for the simulation, with the result of a smaller calculation error (noise on the signals between 300ms and 350ms) and a much longer simulation time.

As shown in figure 4.7 on page 55, the load resistance required for a load with a power of 2.6kW varies between 900m Ω and 100m Ω . 100m Ω were defined as the minimum load resistance (LIMIT1) to limit the maximum current. A capacitor stack, made of 20 in series connected Supercapacitors (see figure 3.13 on page 30) can deliver 2.6kW for more than 35 seconds. In practice 20 seconds or less is used because the voltage change of the power source is therefore in the range of 50V to 35V and the current does not exceed 80A.

The mismatched capacitor C2 (-20% capacity) is discharged after 50ms, which is far beyond the time required for the stack to deliver the requested 2.5kW, within the defined limits.

As shown in figure 4.8 on the page before, the efficiency of the capacitor stack, excluding wiring resistance, is quite good. Within the first 200ms (20s for the real 2700F capacitors) the efficiency is above 90%¹¹. The total thermal energy for the complete discharge is around 170J for the simulated capacitor and 17kJ for the real capacitor stack. If only 20 seconds are used, the simulated stack generated less than 50J (equivalent to 5kJ for the real stack).

The relevance of these results is shown in section 4.4 on the following page.

¹¹worst case condition $R_i = 2\text{m}\Omega$ was used

4.4 Lithium-Ion versus Capacitor in High Power Application

The content of this section is the comparison between LiIon and Supercapacitor. An EXCEL - sheet (see figure 4.9 on the next page) was designed to do the calculations. For the LiIon cells, average costs for space-qualified batteries were used, where for the Supercapacitors the price for low quantities of commercial products was used. It was assumed, that the fully sealed capacitors are fine for the vacuum environment. The work-study was based on research done on the Internet. No physical tests were done on any Supercapacitors.

4.4.1 Discharge Rate

The recommended discharge rate for LiIon batteries, based on commercial cells is below 2C. The Supercapacitors can be discharged through a short circuit, if they are kept within the specified temperature range. The practical discharge time for constant power (see section 4.3 on page 54) is in the range of 20 to 30 seconds or more. If 20 seconds are used, the discharge rate compared to LiIon is:

$$\frac{C_{Cap}}{C_{LiIon}} = \frac{3600s}{20s} = 90 \quad (4.10)$$

where the discharge rate is $C = \frac{Q}{t_{discharge}}$ with unit $\frac{[Ah]}{[h]} = \frac{[As]}{[s]}$ cf. section 3.4.1.1 on page 24. A LiIon cell can be discharged in 30min, where a Supercapacitor can be discharged in 20s.

If the power is only needed for times less than 30 minutes, the discharge current is the sizing factor, which drives the minimum battery capacity. Therefore, for short imaging times, the battery capacity is the same. An other factor which determines the size of the battery is the DOD (section 4.4.2 on the following page).

For discharge times longer than 20 or 30 seconds, the capacity is the sizing factor for the Supercapacitors. These effects can be seen in figure 4.9 on the next page, where for the LiIon battery a capacity of 26.46Ah is required due to discharge rate while for Supercapacitors only 0.59Ah are required. To calculate the Ah - capacity of the battery, the battery was substituted by a constant voltage source. For the Supercapacitor the required energy was calculated and the capacitor was sized, using:

$$W_C = \frac{CU^2}{2} \quad (4.11)$$

which leads to double the Ah - size for the capacitor if same discharge rate or DOD is used.

		to complete				
Power bus voltage	50 V					
Average power (imaging)	2646 W	including power losses because of				
Imaging time	35 s	internal resistance and power losses in Power - converter				
LiIon: [average values incl SAFT, AEA]						
Battery volume [l/Wh]						
Battery discharge rate [C]	2	Battery capacity due to discharge rate	26.46 Ah			max of these two values is used
Battery discharged to [%]	85	Battery capacity due to DOD	3.43 Ah			
Battery voltage	50	Battery capacity needed	26.46 Ah			
Cell voltage	3.6	Energy capable to store	4762.8 kJ	1323	Wh	
Wh/kg	110	necessary to provide the energy	0.23 kg			
W/kg	220	necessary to provide that power	12.03 kg			
kg		Weight (Energy capable to store)	12.03 kg			
Wh/Litre	150	No of cells:	13.89			
		Price per Wh	1380 ZAR/Wh			
		Battery Price	1,825,740 ZAR			
		Battery Volume	8.8 dm ³			
PowerCap: BCAP0010A03						
Capacity of cell [F] (EOL)	2080					
'Battery' volume [l/Wh]						
'Battery' discharge rate [C]	180	Battery capacity due to discharge rate	0.59 Ah			
'Battery' discharged to [%]	18	Battery capacity due to DOD	1.25 Ah			
'Battery' voltage	50	Battery capacity needed	1.25 Ah			
Cell voltage	2.5	Energy capable to store	112.94 kJ	31.37	Wh	
Wh/kg	3.439153	necessary to provide the energy	7.48 kg			
W/kg	619.0476	necessary to provide that power	4.27 kg			
Capacitor cell weight [kg]	0.525	Weight (Energy capable to store)	9.12 kg			
Litre per cell	0.42	No of cells:	20			
RND/Cell	2000	Price per Wh	1107.69 ZAR/Wh			
Wh/Litre	4.298942	Battery Price	34750 ZAR			
		Battery Volume	10.07 dm ³			
		Energy per Capacitor	1.81 Wh/Capacitor			
	2078.078	Farad needed (EOL)				
	0.999076	Strings parallel (EOL)				
Pulswidth (radar puls)	1.50E-05 s	Power @ 10kW pulses & 10kHz	1500.00 W			
Minimum frequency (radar)	4000 Hz	Maximum puls power @ average power	44100.00 W			
Maximum frequency (radar)	10000 Hz	Minimum puls power @ average power	17640.00 W			
This area isn't used in the calculation		Average energy [J]	2646			
		Maximum puls energy [J]	11.025			
		Minimum puls energy [J]	1.764			

Figure 4.9: LiIon and Capacitor Comparison Tool. Price for +/- 0.5% matched Montena BCAP0010A03 capacitors. Power bus voltage is used to size the capacity.

4.4.2 Depth of Discharge

Another factor sizing the LiIon battery is the DOD for the battery. A DOD of 10 to 20% is used for LEO satellites, which means that after the discharge cycle, 85% of the energy is left on a new battery. However, during the mission of the satellite, the capacity can degrade by 60 or 70% and the battery will still be able to deliver the required energy.

Supercapacitors can be cycled completely without strong effects on the degradation. For practical use, a remaining energy of 18 to 20% (DOD of 80%) is sufficient and will result in a remaining voltage of 21V for a 50V capacitor stack. Capacitors with a slightly smaller capacity will be discharged to a lower voltage if all the capacitors were charged to the same voltage end of charge voltage (cell equalization required). The capacity mismatching influences the storeable capacity less, if the

capacitors are charged to the same end of charge voltage. By selecting the DOD with 80%, the weaker capacitors can be protected from reverse voltage conditions.

4.4.3 Specific Energy

The specific energy of LiIon is between 100 and 130Wh/kg for space qualified batteries and up to 160Wh/kg for commercial LiIon single cells. (Lithium polymer cells can reach 260Wh/kg)

The specific energy of Supercapacitors is in the range of 3 to 5Wh/kg

4.4.4 Specific Power

The specific power of the LiIon battery is in consequence of the discharge rate a more or less fixed value of 200 to 300W/kg.

For Supercapacitors the specific energy depends on the state of charge (voltage) and the equivalent series resistance (ESR). For fully charged capacitors, the maximum output power is given if the load resistance is equal to the ESR. A capacitor (BOOSTCAP BCAP0010A03) with 2600F, an ESR of 0.7mΩ and a weight of 525g, charged to 2.5V would give a maximum power output of:

$$P_{out}/kg = \frac{(2.5V)^2}{4 * 0.7m\Omega * 0.525kg} = 4252W/kg \quad (4.12)$$

The datasheet specified a specific power of 4300W/kg.

4.4.5 Lifetime of Energy Storage

Commercial LiIon cells are specified to around 500 full cycles. For space, especially LEO, much more cycles are needed. Low DOD leads to a longer lifetime, thus it is possible to use them as energy storage. Capacitors and also Supercapacitors can withstand many more full charge/discharge - cycles. The datasheet of the supercapacitors specifies a lifetime of more than 500'000 cycles—enough for any LEO orbit.

4.4.6 Extra Circuit Requirements

The capacitors in a stack require cell equalization to store a maximum amount of energy. Nonetheless, all LiIon battery- and cell manufacturers (except the AEA) recommend cell equalizing, or at least cell monitoring for LiIon too.

4.4.7 Conclusion

Supercapacitors and LiIon cells are products with extreme performances. LiIon cells offer a very high energy density while their specific power is bad. Supercapacitors are useful at high power, low duty cycle applications.

For specific applications in satellite power systems, capacitors seem to be an interesting approach. A special application can be global imaging in a sun-synchronous orbit with more satellites (low cost) and short imaging times (below 1min) for three or more times per orbit (1300km long image per orbit).

Before these capacitors are used in space, it should be analysed if the capacitors are sensitive against radiation and vibration during launch.

In the future, tests on capacitor stacks can be made to prove if a matching of the capacitors can reduce the amount of required electronics (equalization), and charge management on stack level is possible.

4.5 MPP vs. Analogue

A higher power output, especially at BOL with Maximum Power Point (MPP) - tracking is possible. Unfortunately, a switching Circuit is required, which needs more components than a single shunt regulator. A single event can have hazardous effects on the switching control circuit. Most MPP - tracking regulators measure current and voltage and use a closed loop to get out most power from the solar cell. An interesting way for “voltage-based maximum power point tracker” for small satellite power supplies is discussed and described in [41].

4.6 Analysis of Commercial LiIon Batteries

LiIon cells have a high specific energy density and they can contain highly flammable electrolytes. It is therefore not recommended to disassemble batteries or open the cells. This work only shows how it was done and it was not supported by any manufacturer. Maybe a safer way exists, but no battery or cell manufacturer wanted to supply any information about disassembling a cell.

To get know-how on LiIon cells and their possible failures, old damaged laptop batteries were disassembled and analysed. The information in this section should support future satellite projects at Stellenbosch University. The point of failure of laptop battery packs should also be analysed to evaluate possible risks of using Commercial Off The Shelf (COTS) LiIon cells. During the analysis of the LiIon cells, it was considered necessary to analyse the cell protection circuit, too, in order to find out if a damaged electronic caused LiIon cell damage.

4.6.1 The Analysed Material

Unfortunately, the poor cooperation of the cell manufacturers meant that it was not possible to get single cells for tests (see section 4.8 on page 72). The circuit diagram for a 2P4S and a 3P3S configuration—used in the laptop packs—is shown in figure 4.11 on page 66. Unfortunately, all the battery packs were made of Panasonic cells. A variety of manufacturers would have been preferable.

The battery packs were 2 x IBM (in a 3P3S topology), 1 x ASUS (CGR18650H cells in a 3P3S topology) and a battery (CGR18650H in a 2P4S topology) from a unknown laptop - type.

4.6.1.1 Two IBM Laptop Batteries

These two laptop batteries were obtained from computer service centres in Vienna (Austria). Both were defective. No history about the usage of these batteries was available. The cell type in these batteries were CGR18650HM in a 3P3S - topology.

4.6.1.2 Loose Cells from unknown Source

Some spare LiIon cells were found in the laboratory in Stellenbosch; unfortunately, their source and history is unknown. The cover plastic of these cells was grey, and it is not presumed that Panasonic produced them. The cover plastic of all the other cells showed that Panasonic produced them.

4.6.1.3 Laptop Pack from ASUS (3P3S) and unknown Type (2P4S)

A battery trading company in Cape Town (South Africa) made these two batteries available. No history on these cells was available. The ASUS - battery was made

Table 4.1: Results of Battery Analysis (PANASONIC CGR18650H). “high Z” refers to high impedance of the cell (Open Circuit cell). The corrosion with an intensity of one was only visible under the microscope, two was visible on less than half the area near the gasket and three was used to indicate strong corrosion on the cells around the gasket

Cell Number	LiIon Cells				Protection Electronics	
	Cell Voltage	Corrosion intensity	Production Line	Internal Voltage	Under Voltage	Over Voltage
P1-1a	high Z	1	D	3.897	2.268	4.178
P1-1b	high Z	1	D	3.955	2.268	4.178
P1-2a	3.685	—	D	—	2.298	4.181
P1-2b	3.685	2	D	—	2.298	4.181
P1-3a	3.435	1	D	—	2.311	4.163
P1-3b	3.435	3	D	—	2.311	4.163
P1-4a	3.701	1	D	—	2.310	4.190
P1-4b	3.701	—	D	—	2.310	4.190
P2-1a	high Z	3	H	2.542	2.420	4.323
P2-1b	2.425	—	H	—	2.420	4.323
P2-1c	high Z	—	H	2.510	2.420	4.323
P2-2a	high Z	3	H	2.493	2.394	4.322
P2-2b	high Z	2	H	2.411	2.394	4.322
P2-2c	high Z	—	H	2.525	2.394	4.322
P2-3a	2.410	3	H	—	2.409	4.333
P2-3d	high Z	3	H	2.870	2.409	4.333
P2-3c	2.410	—	H	—	2.409	4.333

by CGR18650H cells in a 3P3S - topology and the unknown type had a 2P4S structure with the same cell - type. A photo of the ASUS - Pack is shown in figure 4.10(a) on the following page.

4.6.2 Analysis of the Laptop Battery Packs

The Protection mechanism of LiIon cells is described in section 3.6.3 on page 35.

4.6.2.1 The Lilon Cells

After opening the battery pack, the cells (of the ASUS and unknown laptop) were

1. serialised,
2. the voltage was measured,

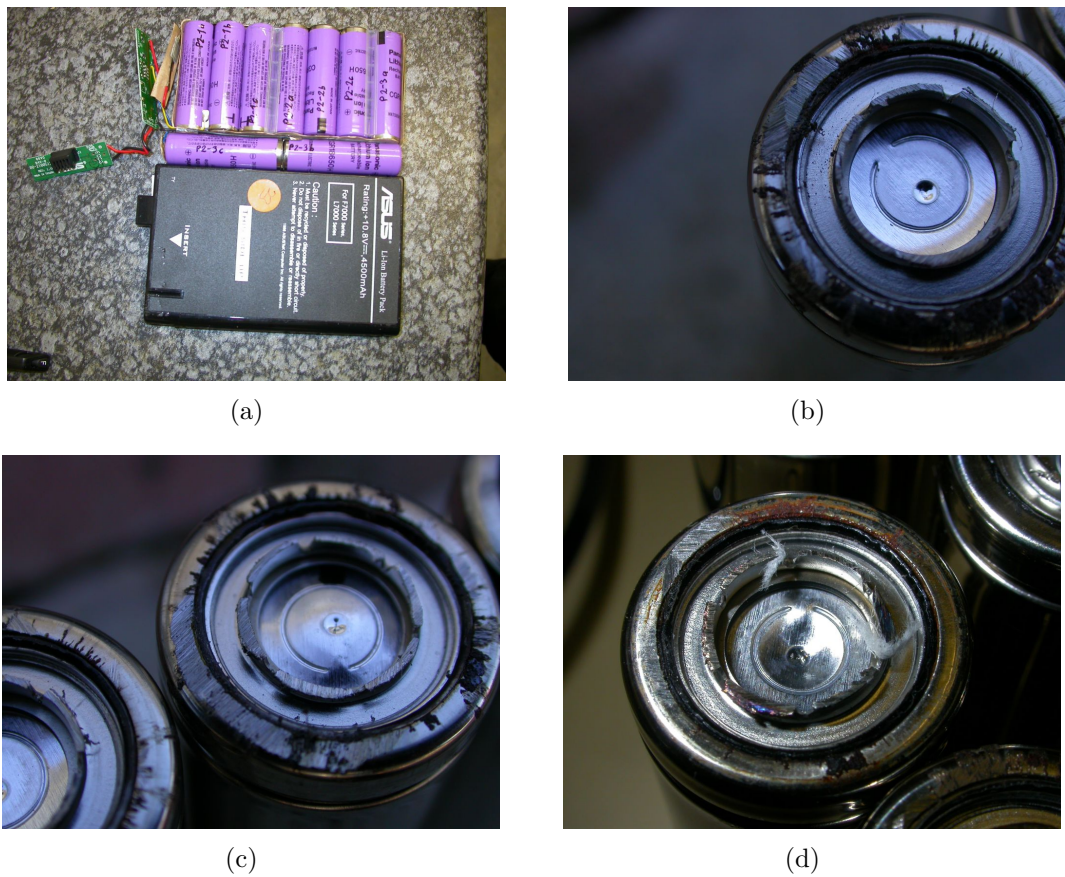


Figure 4.10: Picture of: (a) the ASUS - Pack and Partly Opened Cells (b) Normal Operation, (c) an Open-Circuit Cell and (d) a Reactivated Cell.; The difference between (b), (c) and (d) is the pressure disk in the middle of the top cap. (b) is domed to the outside (open circuit), while (c) is flat (normal operation) and (d) is pressed in to reconnect the circuit breaker

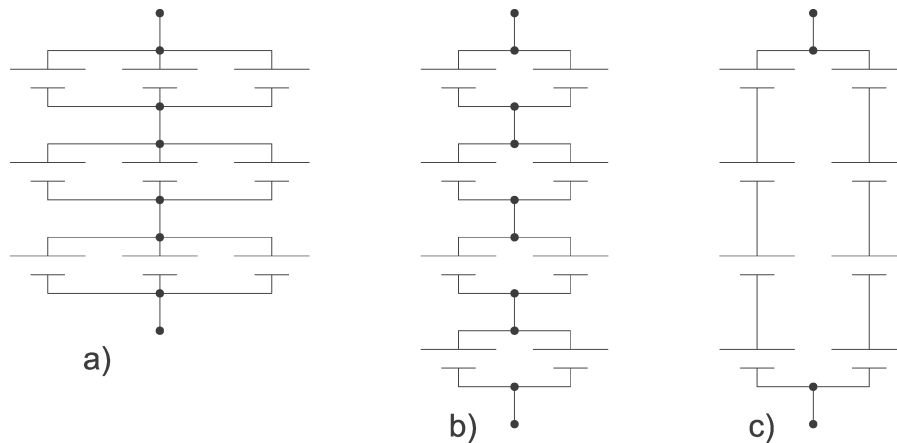


Figure 4.11: Circuit a) shows a 3P3S configuration; b) shows a 2P4S configuration; c) shows a 4S2P configuration (structure used by AEA - Technology)

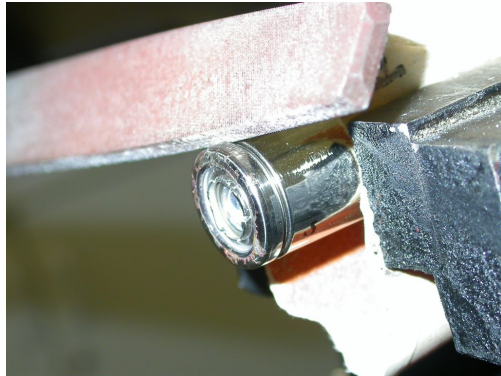
3. the plastic around the cell was removed,
4. inspection for indications of cell leakage (corrosion at the gasket examples shown in figure A.9 on page 120) was done,
5. cells with open circuit failure were partly opened to verify that the pressure disk was activated (see figure 4.10 on the page before),
6. the pressure disk was pushed in to reactivate the cell (figure 4.10(d) on the preceding page),
7. the cell voltage of the reactivated cells was measured (Internal Voltage).

The results are shown in table 4.1 on page 64.

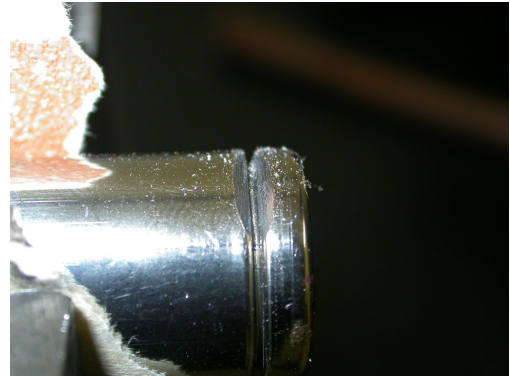
The destroyed LiIon cells of the CGR18650HM - type were all partly or completely opened. For the *partly opened* cells, only the cap of the positive connector was removed, in a way, which did not destroy the hermetic sealing of the cell. The cap was removed using a grinder. Many short sequences with breaks in between were used to protect the cell from overheating (only allowed to be lukewarm). The goal was to see the outer pressure disk, to verify that the open circuit failure was caused by the safety mechanism.

It is *more dangerous to open a cell fully*, especially if the cell is open circuit. The state of charge is not known and if the cell is fully charged, it can be very dangerous. The following procedure was used to open the cells: (Protective goggles and gloves are strongly recommended for safety reason, also the work should only be done in a well ventilated area without flammable materials—see figure 4.12 on the following page)

1. discharge the cell (if possible) completely without exceeding 2C;



(a)



(b)



(c)



(d)



(e)

Figure 4.12: Opening the Cell Fully.

2. decrease the material thickness around the top cap using a file (cell could be under pressure and contain aggressive electrolyte—work with care using protective goggles and gloves);
3. remove the top cap and do not short the wound core (anode wire to case);
4. cut the anode connector (do not cause a short circuit);
5. measure the cell voltage;
6. discharge the cell using a resistor (discharged cell is safer);
7. if interested, remove the wound core carefully.

Work slowly and always watch the cell temperature. If the cell heats up itself, back away immediately.

4.6.2.2 The Cell Protection Electronics

The cell protection electronics were tested and the results are also shown in table 4.1 on page 64, next to the cell data. The electronics were tested using the setup shown in figure 4.13 on the following page. The 10E resistor was used to measure the current, flowing in the V_m - inputs, no equalizing current could be measured. The ASUS - pack used an 8233 - type protection IC (see figure 3.19 on page 37).

4.6.3 The Results

4.6.3.1 The Cells

All failures were open circuit failures caused by higher pressure in the cells. According to all the information found on the Internet or in books, the cell pressure should not rise if the cell is used in the specified operating area. Some sources say that over discharge leads to decompose of the electrolyte, but the cells operated within the specified range.

Although there was no cell equalization in the ASUS - pack, in all parallel-connected cells, one or more defective cells were found. No runaway because of single cell failure—causing failure of other cells which are connected in parallel to the defective one because of capacity imbalance in the pack—took place in the ASUS - pack.

Another effect found on all the cell types was leakage at the gasket. The leakage of electrolyte corroded the metal case of the cell near the gasket. Examples of leakage and corrosion are shown in figure A.9 on page 120.

Mr. Bachmann from BMZ Germany mentioned via telephone, that 4.33V is a high voltage, but he has no idea why all the cells (From different sources Austria,

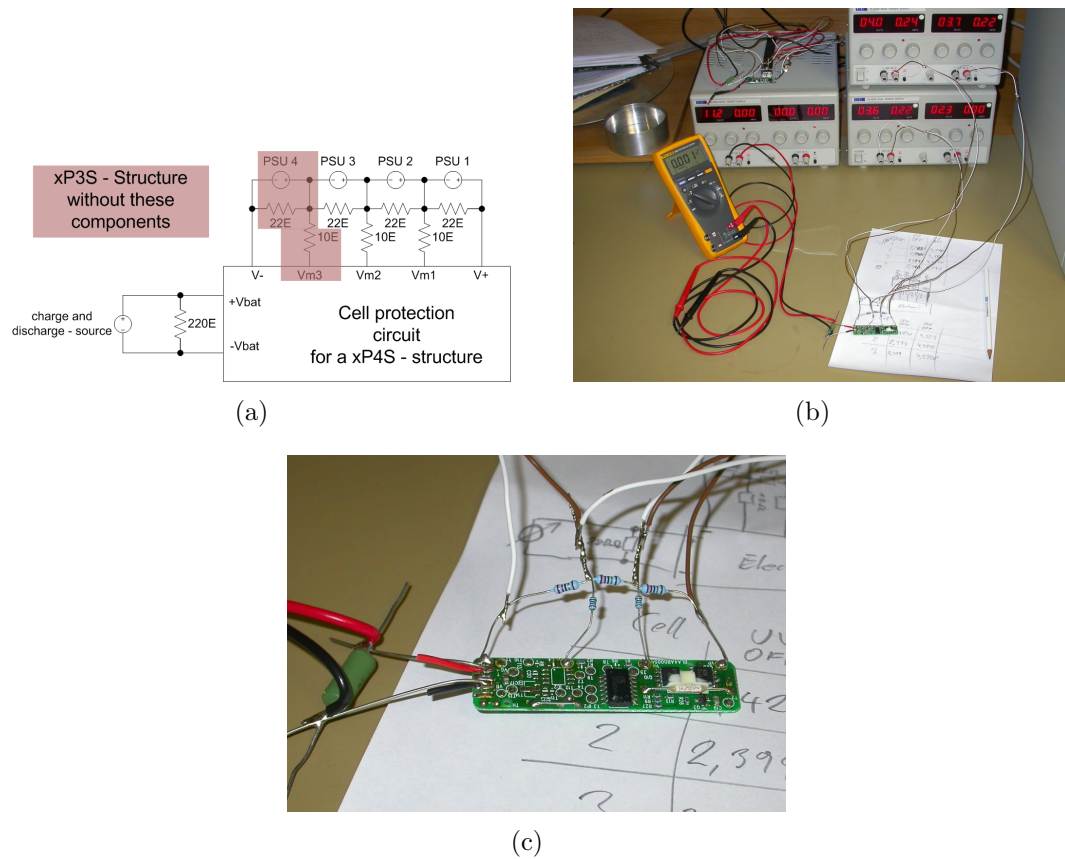


Figure 4.13: Cell Protection Electronics - Test. (a) the setup with 4 independent adjustable voltage sources and 22E to simulate the behaviour of a LiIon cell and the 220E as load resistor; (b) picture of the test setup; (c) the cell protection electronics

Cape Town and Stellenbosch) showed the same error. Leakage at the gasket was never experienced at BMZ. Mr. Wehning from Panasonic Germany could not give me an explanation why the cells are open circuit either.

With regards to leakage, Mr. Wehning mentioned that the electrolyte has the ability to leak through the gasket if the cell voltage is less than 2V—but the cell voltage was higher than that value. There are only two ways the cells can produce gas (according to both): 1) a too high current, or 2) overcharging. Overcharging should not be possible because of the protection. Neither none of the sources had an answer to the flaws that were found. But the fact of too high current could be the reason for failure in the IBM packs because if one cell fails, the other cells have to supply a higher current which will lead to accelerated aging of the remaining cells.

4.6.3.2 Protection Circuit

The latest analysed battery packs (see section 4.6.1.3 on page 63) showed that the cell protection circuit held the cell voltage within the range¹² by enabling and disabling the charge and discharge current. No cell equalization circuit was built in.

Compared to the ASUS - pack, the over discharge voltage of the unknown laptop battery pack was set to a value, which was 100mV less.

4.6.4 Conclusion

Leakage, found on more than 50% of the analysed cells, cannot be accepted for use on satellites. Also open circuit failures cannot be accepted for the use in spacecrafts. More testing and analysis of LiIon cells from different manufacturers is required. In order to analyse the behaviour of cells in the future, testing at different SOC is recommended. The effect of working at low and high SOC on cell lifetime should be made before cells are used in space. The focus of these tests should be on the internal pressure of the cells. Cells should also be analysed for the leakage of electrolyte and rise of internal pressure at different charge- and discharge rates. The cell measurement circuit described in section 4.8 on page 72 is fit for electrical analysis.

¹²specification from the cell manufacturer

4.7 Analysis of Space Qualified Lilon Battery from AEA

AEA Technology is the only supplier (as far as the author knows), which sells space qualified LiIon batteries made of commercial cells. The cells used are Sony US18650HC - type. "This cell is the first commercially produced cell and it has not changed since 1995"[18]. According to an email from AEA (Rob Spurret), AEA matches the cells within +/- 20mV. An electric equivalent of a 4S-6P battery - structure (structure description see figure 4.11 on page 66) was measured during a few charge- and discharge cycles. The maximum cell difference was +15mV and -12mV at a battery voltage of 10.7V. On the fully charged battery, the cell difference was 1mV or less. The measured values can be seen in figure A.10 on page 122. AEA LiIon batteries only need charge control on battery level. This is an approach which no other battery or cell manufacturer recommends. Unfortunately, no thermo graphic photo of a working cell in a vacuum chamber could be taken but the information on this specific battery showed that thermal analysis was done and a mechanism to transport the heat from the cells to the satellite structure is implemented.

Leakage of electrolyte could not be analysed on the AEA battery due to the closed structure. It was not possible during the research to do long-time - tests on the battery and therefore no results are available.

However, the AEA battery shows well matched cells and AEA have had batteries in Space for more than one year now. So it should be presumed that they are fine for use in space.

4.8 Lithium-Ion Cell Measurement Process

Special thanks to Chris Mouton who wrote a user-friendly software for the test equipment. (see section 4.8.8 on page 91) LiIon cells are a relative new technology and therefore limited information is available. Unfortunately, no source for LiIon cells was found which can deliver single cells from one batch—the problem was not to find a cell manufacturer, there are plenty, but the company - politics. Only two cell manufacturers in China agreed to send us single cells, but transport costs were too high. The design flow for the LiIon cell measurement equipment is described in this section.

This equipment was built to be able to measure the behaviour of LiIon cells under different operating conditions and to select cells with equal characteristics from a batch.

4.8.1 Requirements for Cell Measurement Equipment

The following requirements were defined for the Cell Measurement Equipment.

- Measuring of the charge and discharge curve (Capacity...)
- Cycling of cells
- Individually measuring multiple cells at a time (up to 8)
- Programmable charge- and discharge conditions
- Programmable limits
- Measurement of cell impedance with different frequencies (50Hz to 10kHz) and programmable signal form.
- Highly accurate measurement (cell matching)
- Very high accuracy for measurement of cell differences (verification of cell matching)
- Small influence on cells due to measurement
- Modularity and reuse of components
- Capability to measure all cell types (maximum voltage of all cells in series is 35V)
- Capability of charging and discharging cells at high rate (up to 10A)
- Low cost (Budget except Laboratory Equipment below \approx €400)

Table 4.2: The Possible Cell Configuration Modes for the two Relays

Mode	PAR_SER	ABS_DIFF	Description
—	OFF	OFF	<i>not implemented</i>
S	OFF	ON	<i>Serial mode</i>
D	ON	OFF	<i>Differential mode</i>
P	ON	ON	<i>Parallel mode</i>

4.8.1.1 Low Cost

Reading the specified requirements would give the impression that low cost is impossible. Low cost in this case was an amount of \approx ZAR 3400 for material. Some standard components (wires, resistors and diodes) were not part of this amount. Half of the components bought can be easily reused for other purposes. The extra amount for an accurate multimeter was funded separately.

The design is low cost but not low quality. Unconventional ways were used to meet these requirements—but isn't that the way engineers should go anyway?

4.8.1.2 Measuring of the Charge and Discharge Curve

For measuring the charge and discharge curve it is necessary to sample current and voltage for the cell. A timestamp was saved for each measurement to be able to verify the time between the measurements. Current measurement was done by voltage drop measurement on a known resistor.

4.8.1.3 Cycling of Cells

Cycling of cells should be programmable and measurements should be taken over the complete duration of the test. The test had to run autonomously, therefore a PC - based system was selected to do the test. To control the setup a digital IO - card is used.

4.8.1.4 Measuring of Multiple Cells at a Time

Two possible ways of testing multiple cells are:

- Full equipment (source, load, measurement equipment) for each cell with a bus - type interface for the data.
- + Fast tests of nearly unlimited number of cells.
- Non unique measurement error.
- price for a larger amount of cells is higher.

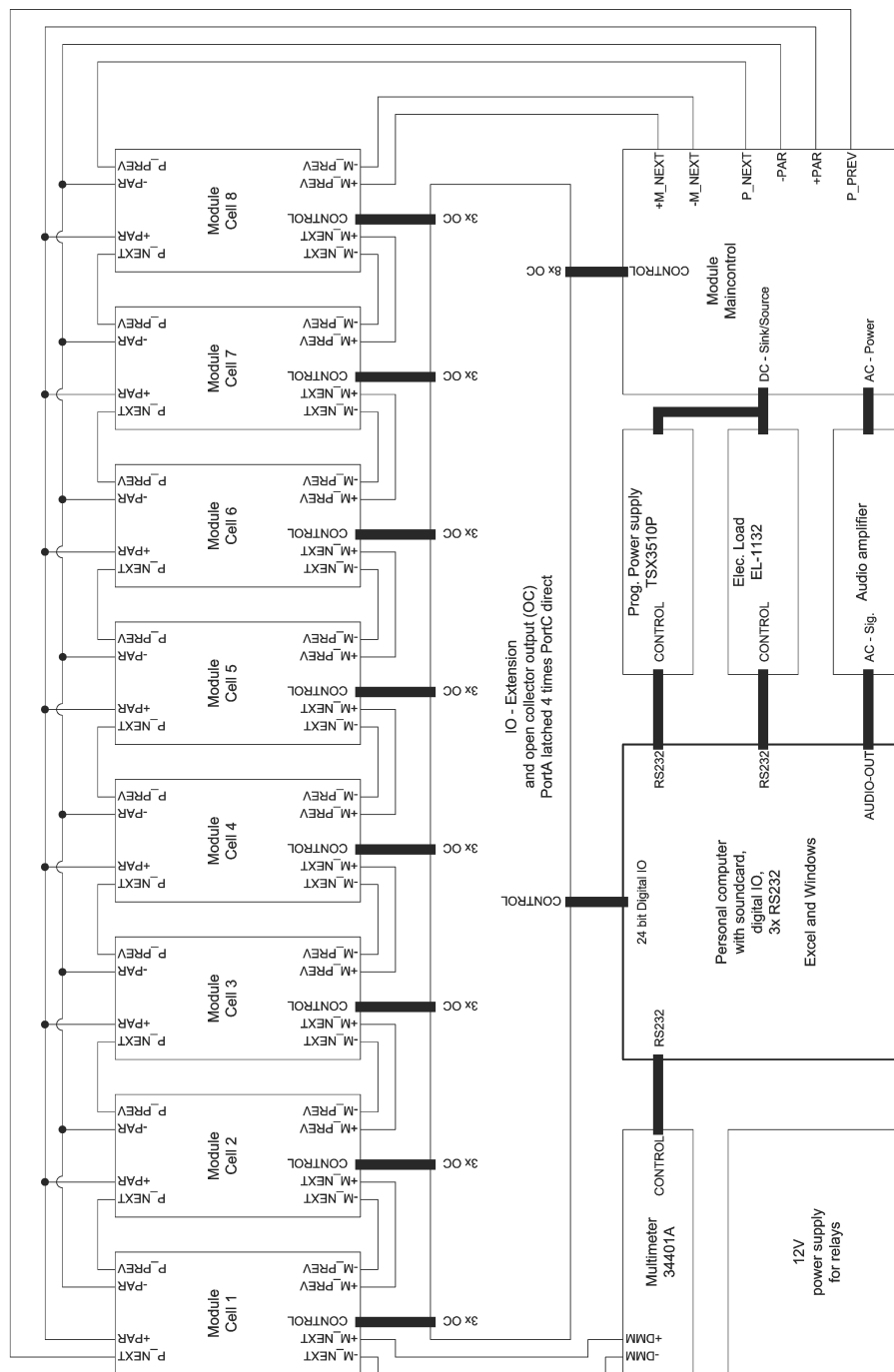


Figure 4.14: The test setup for the cell measurement electronics.

- Single equipment and sharing the facilities
 - + Same measurement - error for all measured cells.
 - + Only one measurement setup needed.
 - More cells reduce the sampling rate.
 - Impossible to measure all the cells at the same time.

The second approach was used for the this project.

4.8.1.5 Programmability

Free programmability of the following parameters for each test step (part of a longer test process, which is programmed through a sequence of test steps):

- the charge current (constant current charge),
- the maximum source - voltage (constant voltage charge),
- the discharge current (constant voltage discharge),
- the minimum load - voltage (to protect the cells from deep discharge),
- the AC resistance with freely programmable frequency (20Hz to 10kHz) and waveform,
- number of cycles for a defined number of test steps,
- sample rate for the cell voltage and current measurement,
- cell configuration (see section 4.8.1.8 on the following page),
- abort criteria¹³:
 - minimum cell voltage,
 - maximum cell voltage,
 - minimum cell difference (to abort if the cell voltages are within a certain limit),
 - maximum cell difference (to abort if the differences are too big)
 - time

¹³Abort - criteria voltage is only verified on the cells with the same configuration as the PAR_SER - relay (cells in "P" - mode, if the PAR_SER - relay is activated)

4.8.1.6 Impedance Measurement

For impedance measurement, the AC - voltage over the defined and well-known shunt resistor and the AC - cell voltage are measured. The waveform is freely programmable with MATLAB or other software which can create 10s wave files. A soundcard and amplifier are used to generate the required signal with low impedance. Capacitors are used to decouple the DC - voltage.

4.8.1.7 High Accuracy

High accuracy for the measurement is gained by using a highly accurate multimeter (HP 34401A) with a multi-slope AD - measurement (integrates AC - signal like noise on the measured voltage). This approach was used because measurement utilities measure accurately and one can trust the results. The high input resistance of the multimeter also affects the measurement positively (minimal change of the cell voltage due to measurement).

For accurate results, a 4 - way measurement was used with spring forced probes to connect the cells (see figure A.12 on page 124).

4.8.1.8 Very High Accuracy Cell - Difference Measurement

To measure the difference in the cell voltage very accurately, it is necessary to connect the positive or negative terminals of the cells together and measure the voltage between the other two terminals. The measured voltage is therefore $U_{Cell1} - U_{Cell2} = U_{diff}$. In this setup, the cell with the highest ID (for 6 cell - testing, cell6) is specified to operate in “P”¹⁴ - mode, acting as a reference cell and all the other cells are specified to operate in “D”¹⁵ - mode to measure the voltage difference to the reference cell. It is important that no charge or discharge current flows, therefore the source/load has to be disconnected (ON-OFF - relay).

4.8.1.9 Small Influence due to Measurement

Low influence due to measurement is achievable as a result of the high input resistance of the multimeter and the fact that the multimeter is connected to the cell only for a low duty cycle of $\frac{1}{11}$ for a one cell setup to $\frac{1}{18}$ for an eight cell setup with maximum sample rates, or less for lower sample rates. The input resistance of the multimeter can be set to $10G\Omega$ leading to at least $100G\Omega$ equivalent resistance for a maximum sampling rate. For the first tests, the multimeter is used with $10M\Omega$ input resistance. The additional 2x 150Ω resistor in the sense path influences the measurement by 0.03 per mill.

¹⁴Parallel - mode adds a cell to the parallel configuration—make sure, that all cells have the same voltage, because no current limiting function is supplied, only fuses with 10A

¹⁵Differential - mode, to measure the cell voltage, or take the cell out of the test.

Assuming, that for long term measurement, the sample rate is 30 measurements per hour, and one measurement takes 1.2 seconds, a duty cycle of 0.01 leads to an equivalent resistance of $1\text{G}\Omega$ ($10\text{M}\Omega$ mode) or $>1\text{T}\Omega$, if the $10\text{G}\Omega$ input resistance is selected. With a LiIon cell voltage of 4V, that leads to an equivalent current of 4nA for the $10\text{M}\Omega$ input range or less than 4pA for the $>10\text{G}\Omega$ - range. A constant current of 4nA needs 50000 years to discharge an 1800mAh cell. The self-discharge of the cell is probably higher than the influence of the multimeter. Relays were used to switch between the cells because they offer the lowest influence on the measured signal—no additional current or voltage. But problems can occur if the current over the relay contact is too small. For selecting the relays, see section 4.8.3 on the following page.

4.8.1.10 Modularity, Reusability and Reconfigurability

A highly accurate multimeter is used for charging and discharging, a programmable power supply and a programmable electronic load were used. For control and impedance measurement, a PC with digital IO and sound card (with audio - amplifier) was used. The external circuit for IO-extension and relays were built up on a LEGO base plate using modified LEGO - blocks to connect the cells. The relays for the power path were used with relay socket terminal blocks. For all other relays, a multifunctional PCB - layout was made—also with screw terminals (see figure A.11 on page 123 for scematic and figure 4.16 on page 80 for a picture of the PCB). Changing the multimeter, load, power supply or amplifier to reach other currents or voltages is easily possible.

NOTE: More small LEGO - Blocks stick better to the ground plate than a big one, thus it is recommended to use more small blocks instead of one big one (see figure A.13 on page 125)

4.8.1.11 Measuring of all Cell Types

Because the voltages and currents are freely programmable and depend mostly on the used power supply or load, all cell types¹⁶ can be measured. For NiCd, maybe the software has to be changed for end of charge - detection. It is also possible to test entire battery packs with currents up to 10A (connecting them as a cell).

4.8.1.12 Charging and Discharging at High Rates

The rate depends on the power supply and electronic load as well as on the spring forced probes and relays. The relays and probes are rated at 10A and to use a higher current, more cells have to be used in parallel and another power supply and load is required.

¹⁶Also measurement of Supercapacitors with currents up to 10A is possible

4.8.2 The setup

As seen in figure 4.14 on page 74, the strongly modular design enables one to change the setup for a wide range (more cells, other power source or load). It is also possible in the future to replace the expensive power supply and the load by cheaper self-made and less accurate circuits and to replace the highly accurate voltmeter by a cheaper one if less accurate results are required.

4.8.3 The Cell Module

The cell module is the circuit which is required by each (LiIon) cell. Each circuit contains four relays. The power relay (PAR_SER¹⁷) with three contacts is required to switch between parallel and serial configuration of the specific cell (see section 4.8.5 on page 81). The first state (e.g. PAR for PAR_SER) is the activated state. The relay is activated by setting the digital IO to high, leading the open collector - output to conduct (see section 4.8.6 on page 84).

One relay is required to select the measurement of this specific cell (SELECT-MEAS) where otherwise the measurement signal is routed through this module. SELECT-MEAS is activated (measurement of this cell), if the digital IO is set to high. One relay is used to select between absolute or differential measurement (ABS_DIFF). *NOTE: To connect the cell in parallel, the measurement - mode "Absolute" has to be selected, which is automatically done by the software*

Because of the low current in the measurement path (e.g. $\frac{4V}{10ME} = 400nA$), switching these small currents is a problem. Normal relay contacts build up a non-conducting oxide or dust layer, which can lead to a contact malfunction. Gold contacts are much better but are only specified to currents above $10\mu A$. For smaller currents mercury wetted contacts should be used. For our application, mercury wetted contacts are much too expensive, and sealed relays with gold plated contacts are used, being aware of the fact that they will be operating beyond their specifications.

The power relays (see figure A.13(d) on page 125) are neither sealed nor gold plated and, therefore, in some configurations problems¹⁸ can be expected. For configurations with very low current over the power relays (e.g.. differential mode measurement) a parallel-connected small signal relay is used (Au plated contacts). To prevent circuit shorts or contact overload on the small signal relay because of different switching times (the contacts should only work for low current), 150Ω resistors were connected in series to each contact. If necessary, the drop over the resistance can be calculated, and the measured value can be corrected. For the worst case configuration (differential measurement) the series resistance is around

¹⁷do not get confused with PAR_SER for the cells and SER_PAR in the main control - module

¹⁸If the voltage/current over the contact is too low, the oxide- or dust - layer will lead to a undefined contact resistance, which can be very high

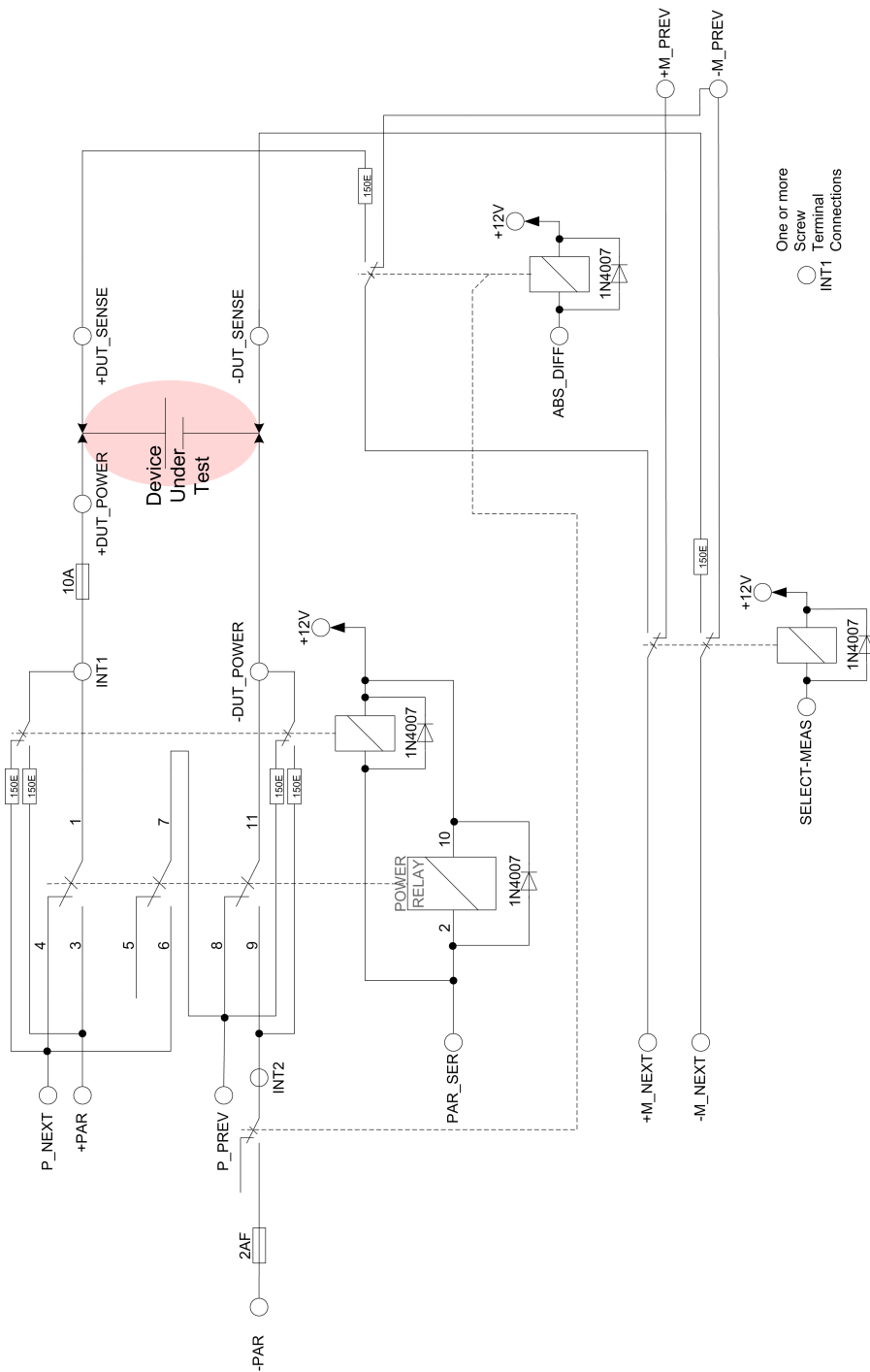


Figure 4.15: The schematic of the circuit, required by each cell.

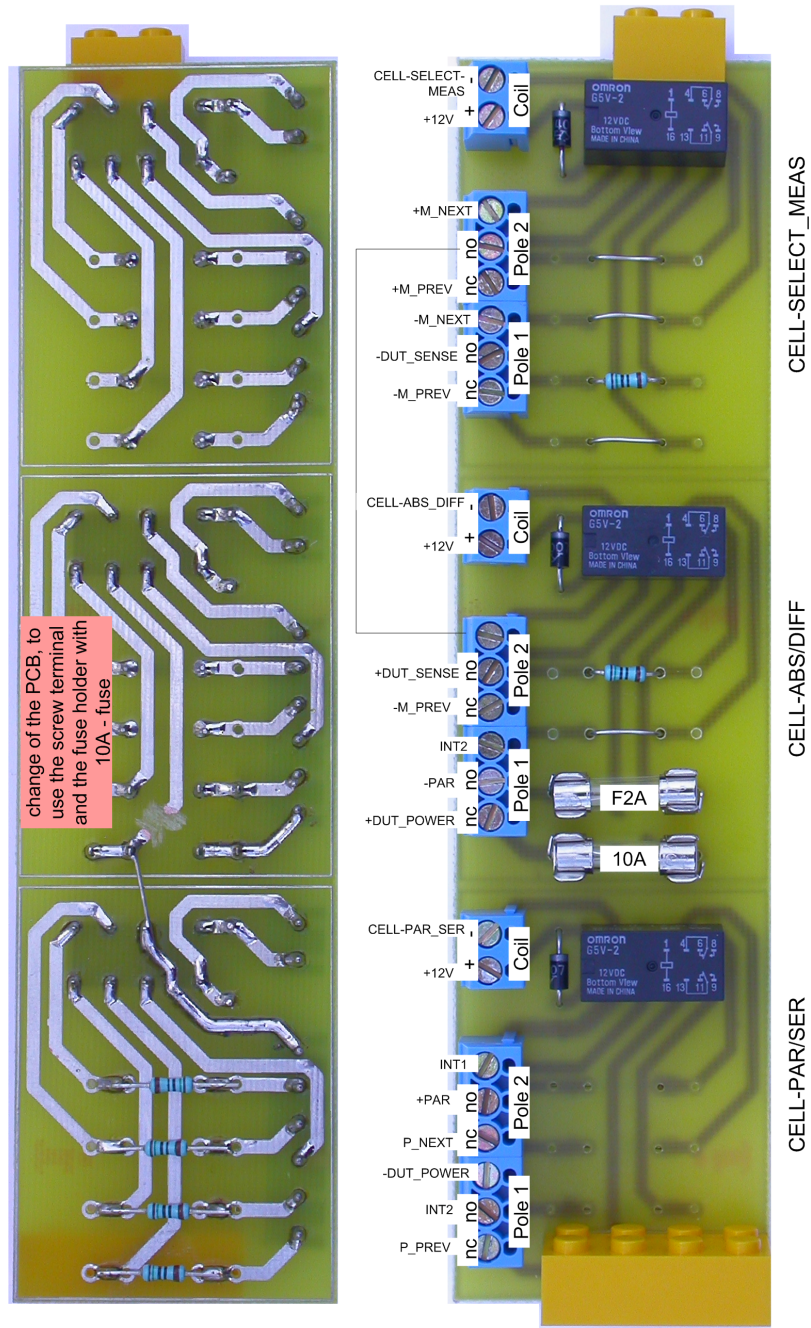


Figure 4.16: PCB with 3 times the same layout, slightly modified to save wiring effort.

600E and therefore the influence due to the input resistance is 0.06 per mill, which is of no further relevance for our measurement. The picture of the PCB¹⁹ with the three small signal ($I < 2A$) relays is shown in figure 4.16 on the preceding page.

4.8.4 The Main Control - Module

The main control - module is also based on the same PCB, with the small signal relays and the same power relays as in the cell modules. One is used to select the source (AC or DC with the ON-OFF - relay) and supplies it to the series, or parallel connected cells (selection by SER-PAR - relay). It is also possible to disable the power source/load (no matter if AC or DC is selected) with the ON-OFF - relay. Small signal relays in the main control - module are used to measure:

- a 10Ω reference resistance to check the measurement - chain,
- the temperature (function not used for the first tests, but are strongly recommended if temperature- or fast discharge - tests on the cells are done)—relay TEMP_10E,
- charge/discharge - current by measuring the voltage drop on a shunt resistor—relay CURRENT,
- measuring the voltage of the cells connected in series and parallel—relays PAR_SER_V and V_I,

All these values are read again with inverted signal by exchanging the signal wires (VOLTAGE-INV - relay).

4.8.5 The possible Configurations

The four possible configurations for the relay PAR_SER and ABS_DIFF (required by each cell, see section 4.8.3 on page 78) and the name for the mode is shown in table 4.2 on page 73.

The “not implemented” mode. The use could be to measure the voltage drop over the contacts between cells in the serial configuration. Nothing is connected to the parallel string.

The serial mode, where also nothing is connected to the parallel string. If the measurement for this module is selected, the cell voltage is measured. The advantage is, that the exact same current is flowing through all the cells in serial configuration. The following cell test can be made in this mode:

¹⁹Printed Circuit Board

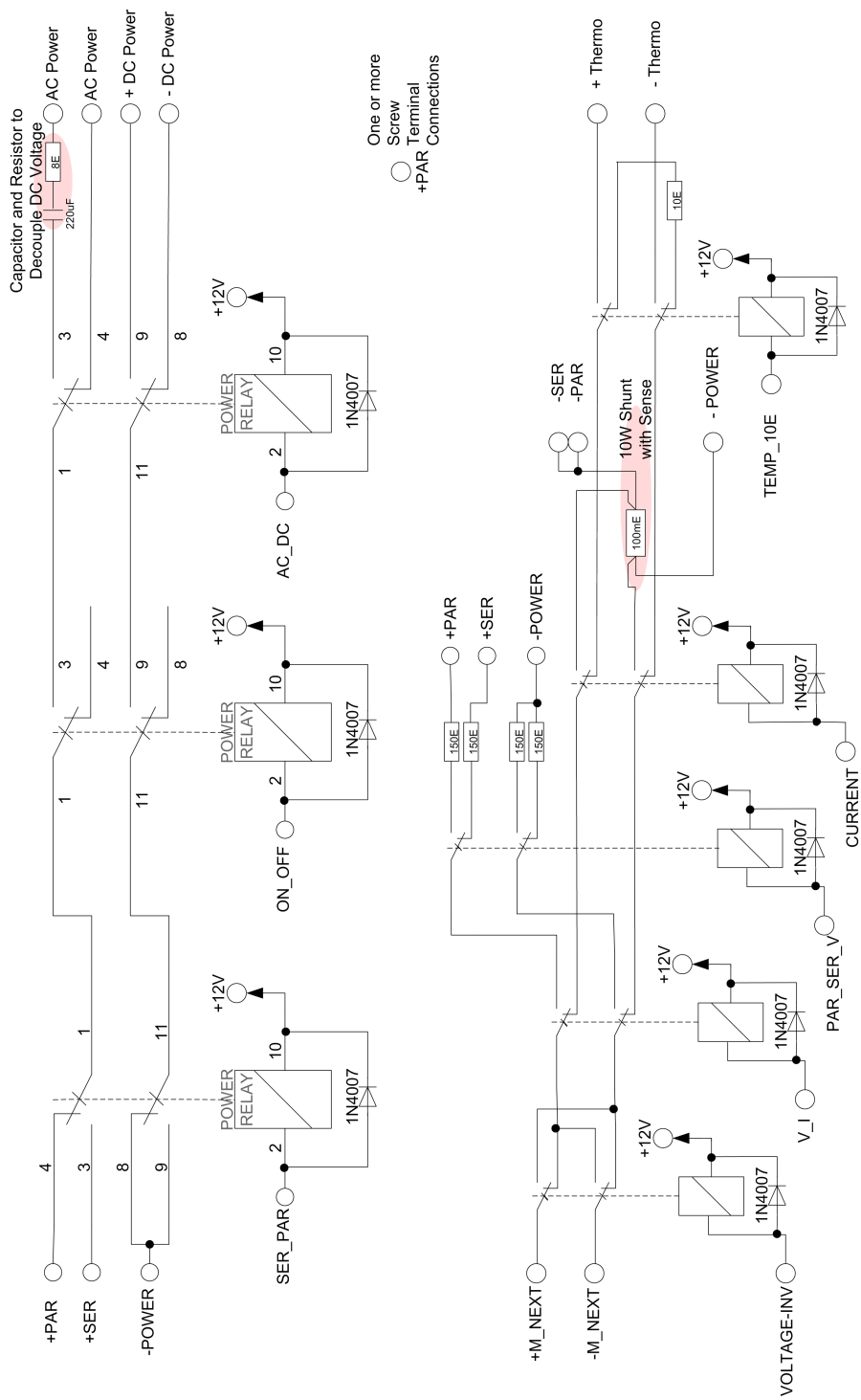


Figure 4.17: The Main Control Schematic

- Cell behaviour at different SOC can be measured. Charge efficiency at different SOC or self-balancing effects can be analysed.
- Quality of cell matching can be analysed.
- Cell behaviour at different temperatures (heating one side of the test setup) at cells which are in series connection can be made.

The differential mode, where only the positive terminal of the cell is connected to the parallel string. The negative point is measured to the next higher cell ID, where also the measurement was selected. It is practical to select an absolute measurement for the cell with the highest ID (P - mode), and for the other cells this mode. It is important that the measurement has to be selected for a cell with a higher ID.

The voltage difference is measured.

The module is bypassed for the serial string through a short between P_NEXT and P_PREV (corresponding to a cell with 0V and R_i of 0Ω).

Charge and discharge should be disabled through ON_OFF in the main control - module.

The Advantage is that very small differences in cell voltage (mV) can be measured very accurately. This is a plain measurement mode. The following results can be achieved by using this mode:

- Cell voltage vs. temperature behaviour.
- After charging the cell to the exact same voltage, and a few charge/discharge - cycles in serial configuration, the change in cell voltage can be measured.
- Different self discharge behaviour of the cells can be analysed.
- This measurement can be used whenever small differences in the cells should be measured.

NOTE: The voltage of cells in differential mode is not used as abort criteria

The parallel mode To cycle all the cells through the same voltage swing, it is important that the cells are low impedant connected in parallel. Therefore, no series resistance was designed into the circuit and the only protection against over current is a fuse. Before the cells are connected in parallel, the voltage difference should be a minimum (less than 200mV) to reduce the current to 2A through the wiring resistance and the resistance of the

fuse, the contacts and the spring forced probes. Charge all cells individually to the same voltage before connecting them in parallel. If measurement is selected for this module, the cell voltage is measured. The module is also bypassed for the serial string. This mode is used:

- for cycling the cells through the same voltage swing.
- to equalize the cell voltage.
- to give the cells the same history for the last few cycles.
- to measure the capacity and charge/discharge curve between two voltages exactly. (in serial configuration not possible, weakest cell estimates the abort time)
- for single cell tests. (Without removing the other cells from the setup)

4.8.6 The IO-Extension

On the IO-extension board (figure 4.19 on page 86), octal D-type latches and flip-flops with 3-state - output (74HC373 and 74HC374) were used to expend the number of IOs. The principle structure is shown in pinterface. To drive the relays, BC546 - transistors were used with a base resistor of 2k2 (to switch currents up to 200mA).

As seen in table 4.3 on page 87, Port A (PA) is used to control the cells. The extra output is not used at the moment. The state for the PAR_SER and ABS_DIFF relays of Cell(module)1 to Cell8 are written to PA0 to PA7 and stored through a rising edge on PB0 (W-PAR_SER) and PB1 (W-ABS_DIFF). The value for the extra output is also stored through a rising edge on PB2 (W-EXTRA-OUT). The value for the measurement selection is transparently guided through the 74HC373 while PB3 (W-SELECT-MEAS) is high (values latched with a change to low). The signals for the main control - module (Port C) are guided through the 74HC373 all the time (Latch is constant enabled).

NOTE: All the outputs are normally high impedance and no base current is supplied to the transistor. Therefore all relays are switched off (disabled). To enable all relays, PB4 (/ENAB-OC) has to be set to LOW!

4.8.7 The Software Requirements

4.8.7.1 The Test Step

The cell test is built of single tests, called test steps. One test step is defined in one line of the testsetup in the Charge/Discharge Setup - window in the software (see section 4.8.8 on page 91). Abort criteria and other definitions are already described

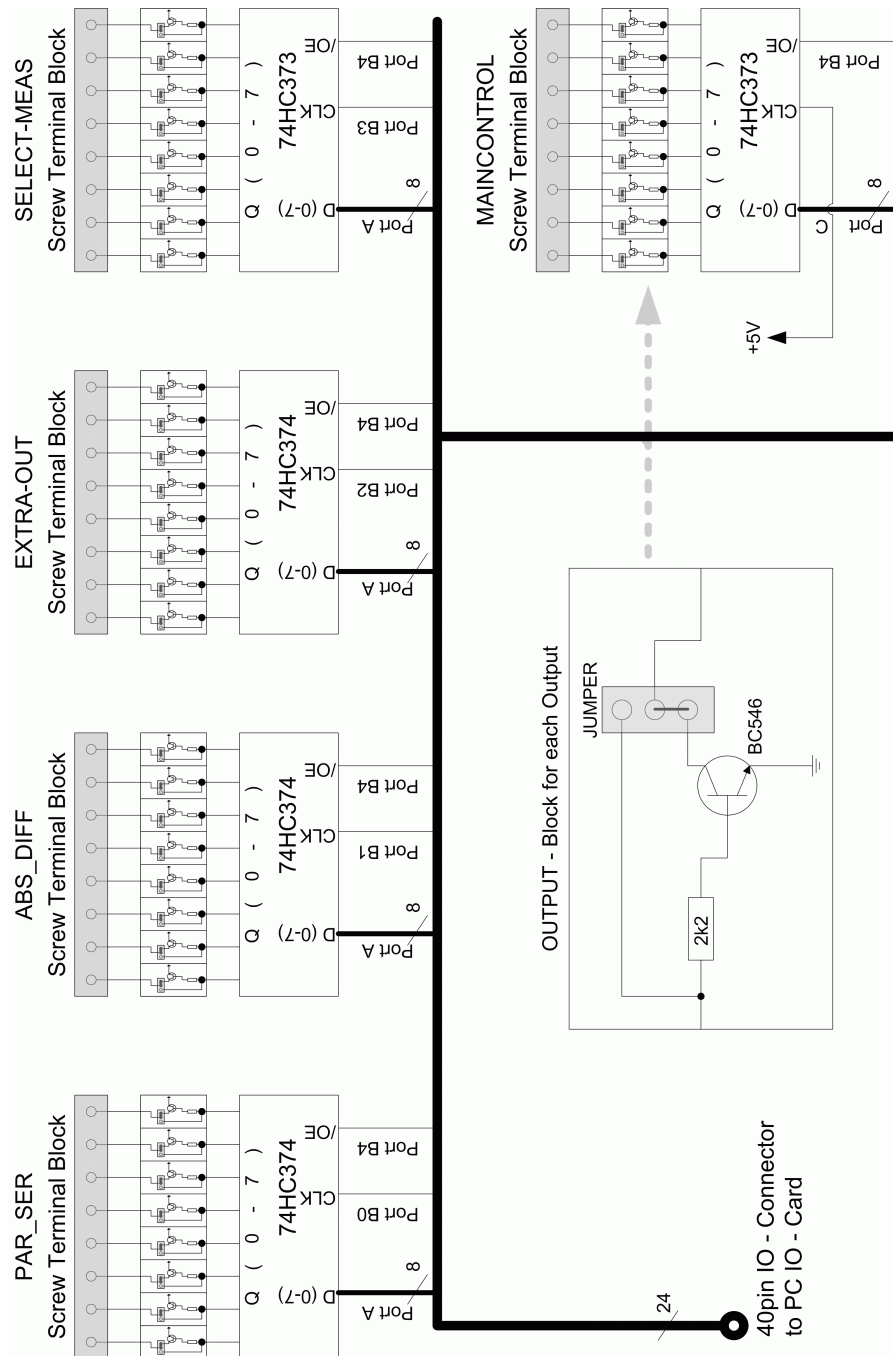


Figure 4.18: The IO - extension with Open Collector (OC) output. /OE is Output Enable (low active), CLK is CLock signal (rising edge) to store the data, LE is Latch Enable. For pinouts of the connector see table 4.3 on page 87

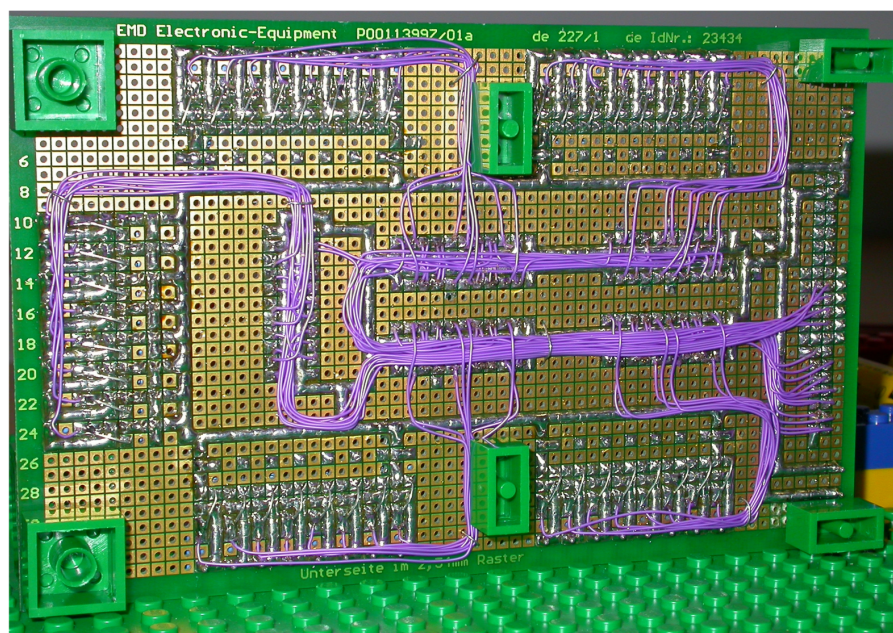
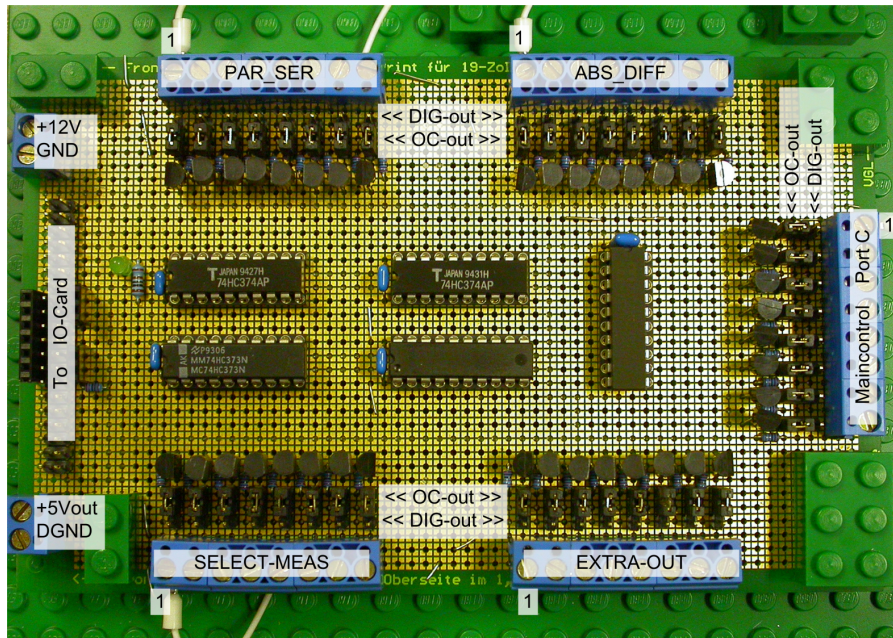


Figure 4.19: The IO - Extension - Board

Table 4.3: The Pinning of the Connector to the IO - Card

Function	Name	Pin	Pin	Name	Function
Cell1	PA0	1	2	PA1	Cell2
Cell3	PA2	3	4	PA3	Cell4
Cell5	PA4	5	6	PA5	Cell6
Cell7	PA6	7	8	PA7	Cell8
W-PAR_SER	PB0	9	10	PB1	W-ABS_DIFF
W-EXTRA-OUT	PB2	11	12	PB3	W-SELECT-MEAS
/ENAB-OC	PB4	13	14	PB5	
	PB6	15	16	PB7	
VOLT-INV	PC0	17	18	PC1	V_I
PAR_SER_V	PC2	19	20	PC3	CURRENT
TEMP_10E	PC4	21	22	PC5	SER_PAR
ON-OFF	PC6	23	24	PC7	AC_DC
	DGND	25	26	—	
	—	27	28	—	
	—	29	30	—	
	—	31	32	—	
	—	33	34	—	
	—	35	36	—	
	+5V	37	38	DGND	
	—	39	40	—	

in section 4.8.1.5 on page 75 and can also be seen in section 4.8.8 on page 91. For information how to enter a test step, please look up at section 4.8.7.2 on page 90. All the relays used for measurement are shown in table 4.4 on the next page. The test step itself runs as follows (*only signals for the relays where names are shown in the enumerated list below, are high if not otherwise specified*):

1. measure the cell voltages up to the maximum specified cell by applying Port A and SELECT-MEAS with a HIGH for the measured cell. *Always keep the highest Cell at measure - state (SELECT-MEAS is HIGH) for possible differential measurement.* (1 to 8 cycles, depending on the number of cells in the setup.)
2. measure serial string voltage (V_I)
3. measure parallel string voltage (PAR_SER_V and V_I)
4. measure the current with multimeter in voltage - measurement mode (CURRENT)
5. measure the temperature with multimeter in voltage - measurement mode (TEMP_10E)
6. measure 10Ω reference resistance (multimeter in resistance - measurement mode) with all relays off.
7. measure all the last 5 values again with inverted signal by setting VOLTAGE-INV to high for the following five tests!
8. calculate the minimum and maximum cell voltage and the minimum and maximum cell difference between any two cells (only voltages from cells with the same mode as the SER_PAR - relay in the main control - module are used)
9. verify the abort criteria
10. verify, if the time since the last measure of the first cell is longer or equal to the sampling rate.
11. do the last two tests every second until one verification is positive. Then act as follows:

Abort criteria: Enter the next test step

Sampling time: Restart with (1.)

After switching the relays, make sure that the multimeter measures the new value (command to the multimeter or enough delay time). Save all the values for a data evaluation at a later stage.

Table 4.4: List of all the Relays. If two abbreviations are combined with a “_”, the first state is the active one (Digital output is H; OC is conducting)

Relay Name	Function
SER_PAR	This relay is used to connect the source to either the parallel string or the serial connected cell string.
ON_OFF	This relay is to break the connection between the cells and the power supply/load.
AC_DC	Selects the type of source (AC or DC)
PAR_SER	Configuration of the cells. Each cell - module has one of these relays. PAR_SER1 to PAR_SER8.
ABS_DIFF	Measurement mode. This is set once at the beginning of a test step. Each cell - module has one of these relays. ABS_DIFF1 to ABS_DIFF8.
SELECT-MEAS	These relays are for measuring and are switched with the sample rate. They are used to select the measurement at the specific cell. (e.g. SELECT-MEAS3 will select to measure the voltage of Cell3 or if the cell mode is “D”, the difference to a cell with a higher ID where also the measurement is selected.)
VOLT-INV	Is used to measure the following values in this table with crossed signal wires. This should enable one to verify that values are measured correctly also for an inverted signal.
PAR_SER_V	Selects between measurement of the voltage of all the cells in serial mode and parallel mode.
V_I	Selects between string voltage measurement (line above) and all the following relays.
CURRENT	Selects to measure the voltage over the shunt resistor.
TEMP_10E	Selects between temperature measurement or reference resistance.

4.8.7.2 Hazardous Program Situations

The software can control all the relays, and wrong settings can lead to circuit shorts. Next, three hazardous transitions follow, as well as safe ways to handle them:

start of test is problematic due to the fact that switching off and enabling all relays at the same time, can cause problems because of different switching times and therefore unwanted configurations. To handle this properly:

1. set all relays to LOW (Ports with write signal).
2. enable the relays with LOW on PB4 (/ENAB-OC).
3. proceed with the routine for “change between test steps”.

end of test can cause problems because of unwanted setup of the test equipment (charge, discharge. . .) or problems similar to “start of test”. Handle the end of the software in the following way:

1. set ABS_DIFF for all Cells to LOW (differential mode).
2. set ON_OFF to LOW (power disconnected).
3. disable all relays (HIGH, or high impedance on PB4).
4. set all relays to LOW.

change between test steps is also problematic because of different switching-times of the relays and many configuration possibilities of the relays. If handled as follows, no problems should occur:

1. set ABS_DIFF to LOW for all Cells ('00000000' on Port A, followed by a rising edge on PB1 (write signal W-ABS_DIFF))
2. set ON_OFF to LOW
3. delay 100ms
4. set all relays (except ABS_DIFF and ON_OFF) according to the new test step
5. set multimeter, power supply and electronic load to the new value
6. set ABS_DIFF according to the new test step

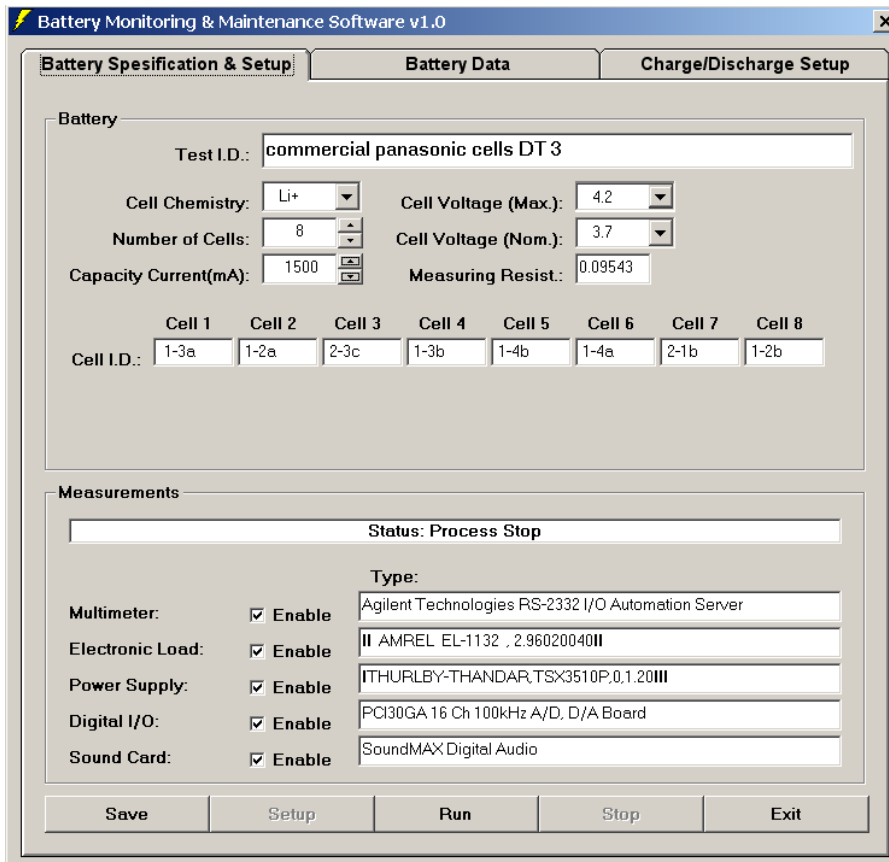


Figure 4.20: Specification of the used Equipment and General Settings.

7. set ON_OFF according to the new test step
8. set EXTRA-OUT according to the new test step

NOTE: Only one write signal should be HIGH at a time (except for switching all relays OFF). Set all write - signals (PB0 to PB3) to LOW and write that state to the digital IO, before setting a write signal to HIGH

4.8.8 The Software—Screenshots

The basic settings, in the window “Battery Specification & Setup” (see figure 4.20), and the test procedure (in the “Charge/Discharge Setup” - window) have to be defined before a test can be done. A picture of that window can be seen in figure 4.21 on the next page and a full test description can be seen in figure 4.25 on page 97. The output during the test is displayed in the window called “Battery Data” (see figure 4.22 on page 93).

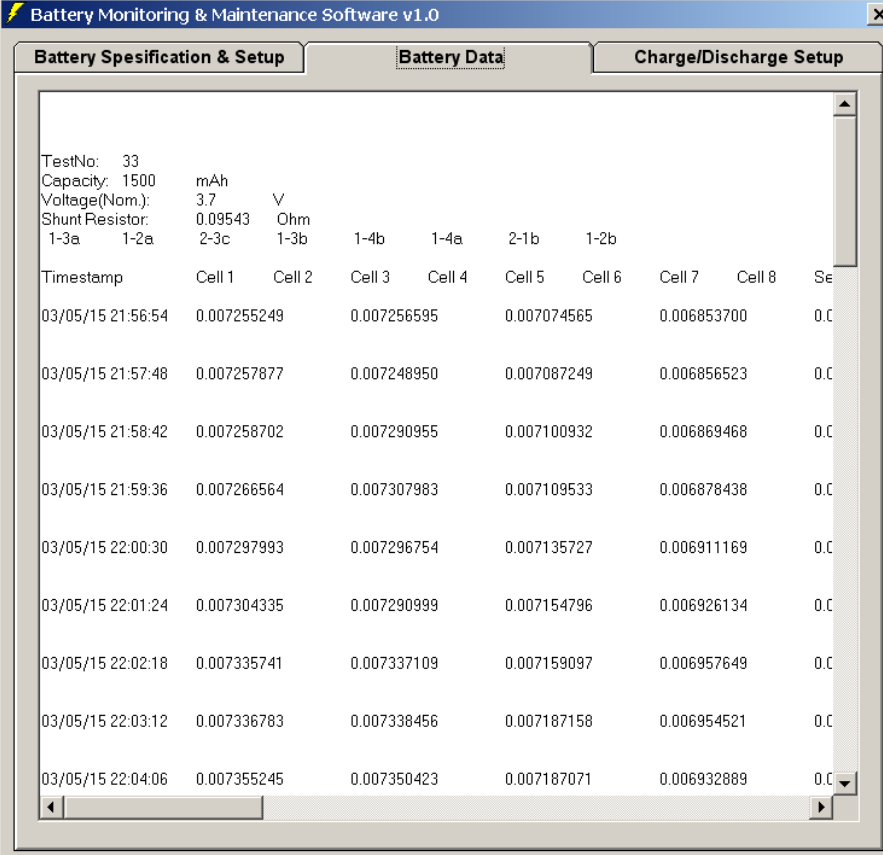
Battery Monitoring & Maintenance Software v1.0

Battery Specification & Setup Battery Data Charge/Discharge Setup

Microsoft Office Spreadsheet

	A	B	C	D	E	F
1					Cycle	
2	No.	Description:	Duration[s]	Sample[s]	Amount	Start
15	13	Discharge	6000	15	1	1
16	14	Meas Ri	720	15	1	1
17	15	Charge	6000	15	1	1
18	16	Meas Ri	720	15	1	1
19	17	Discharge	6000	15	1	1
20	18	Meas Ri	720	15	1	1
21	19	Charge	6000	15	1	1
22	20	Meas Ri	720	15	1	1
23	21	Charge	8000	15	1	1
24	22	Meas Ri	720	15	1	1
25	23	Difference measurement	1800	15	1	1
26	24	Meas Ri	720	15	1	1
27	25	Discharge	6000	15	1	1
28	26	Discharge	6000	15	1	1
29	27	Discharge	6000	15	1	1
30	28	Discharge	6000	15	1	1
31	29	Discharge	6000	15	1	1
32	30	Discharge	6000	15	1	1
33	31	Discharge	6000	15	1	1
34	32	Discharge	6000	15	1	1
35	33	Meas Ri	720	15	1	1
36		End				

Figure 4.21: Setup Window for Test Procedure.



The screenshot displays the 'Battery Data' tab of the 'Battery Monitoring & Maintenance Software v1.0'. The interface includes three tabs: 'Battery Specification & Setup', 'Battery Data', and 'Charge/Discharge Setup'. The 'Battery Data' tab shows a table of test results for a battery with the following specifications:

- TestNo: 33
- Capacity: 1500 mAh
- Voltage(Nom.): 3.7 V
- Shunt Resistor: 0.09543 Ohm

The table below shows the data recorded during the test, with columns for Timestamp, Cell 1, Cell 2, Cell 3, Cell 4, Cell 5, Cell 6, Cell 7, Cell 8, and a partially visible 'Se' column.

Timestamp	Cell 1	Cell 2	Cell 3	Cell 4	Cell 5	Cell 6	Cell 7	Cell 8	Se
03/05/15 21:56:54	0.007255249		0.007256595		0.007074565		0.006853700		0.0
03/05/15 21:57:48	0.007257877		0.007248950		0.007087249		0.006856523		0.0
03/05/15 21:58:42	0.007258702		0.007290955		0.007100932		0.006869468		0.0
03/05/15 21:59:36	0.007266564		0.007307983		0.007109533		0.006878438		0.0
03/05/15 22:00:30	0.007297993		0.007296754		0.007135727		0.006911169		0.0
03/05/15 22:01:24	0.007304335		0.007290999		0.007154796		0.006926134		0.0
03/05/15 22:02:18	0.007335741		0.007337109		0.007159097		0.006957649		0.0
03/05/15 22:03:12	0.007336783		0.007338456		0.007187158		0.006954521		0.0
03/05/15 22:04:06	0.007355245		0.007350423		0.007187071		0.006932889		0.0

Figure 4.22: Data can be Seen during the Test to Check for Correct Operation.

4.8.9 The Integration

There were no mentionable problems during the integration of test soft- and hardware. The shunt resistor was measured, using a fluke calibrator (see figure 4.24(c) on page 96), set to 1.99999A, to force a current through the resistor. The voltage on the sense line of the resistor was measured with the AGILENT multimeter to calculate the resistance of the shunt which was built using 5x 470m Ω in parallel. The shunt resistor can be seen in figure 4.23(b) on the next page at the right top of the IO-extension.

4.8.10 The first Test

Firstly, fixed resistors were used to prove the measurement for the cell series resistance. Measurements indicated that using an AC signal with an amplitude of 1.5A measured a 409m Ω fixed resistor with 410m Ω . The measured value was reproduceable within a difference of +/- 0.4m Ω which is one per mill.

For the first test to prove the flexibility of the circuit, a solar2000 lamp with integrated NiCd battery pack and full protection from over charge and over discharge were used. The solar2000 can also act as power source and a current of less than 2A can be drawn from the battery in the solar lamp. The maximum charge current is 1.5A. The test process, shown in figure 4.25 on page 97, generated during the nearly twelve hour test 2043 sets of data (see figure 4.26 on page 98).

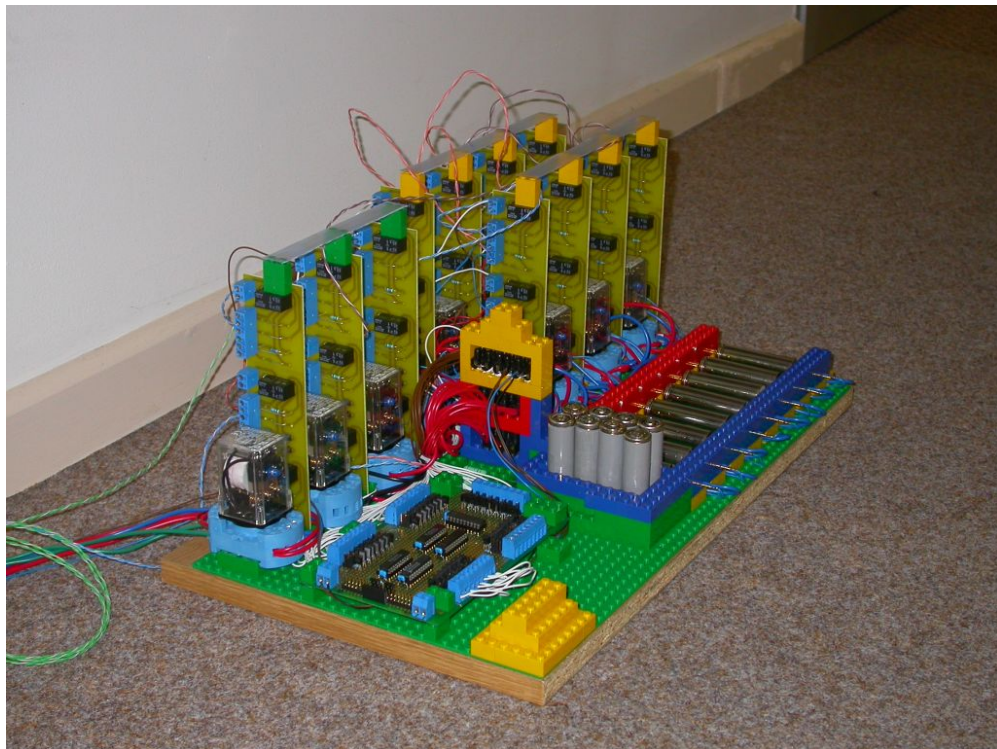
From this data various graphs can be drawn. As example, the terminal voltage and accumulated charge are shown in figure 4.27 on page 99 and the accumulated energy and charge are displayed in figure 4.28 on page 100.

4.8.11 Problems and Solutions

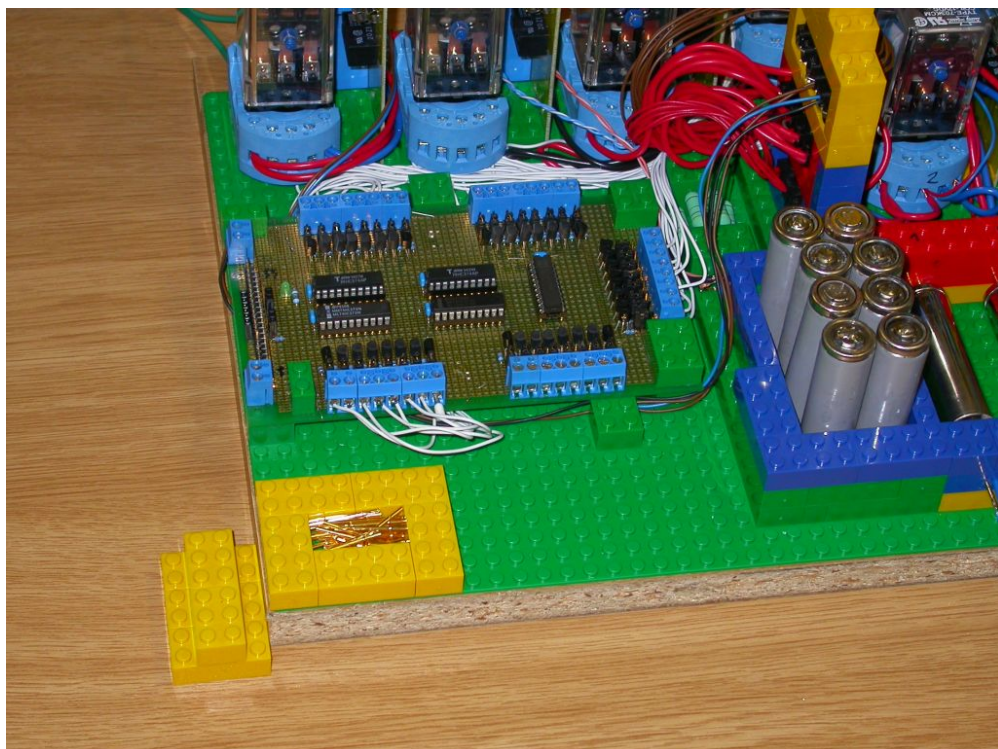
Unfortunately, the PC - loudspeaker did not work with high output power for a longer periode. A solution is the use of a amplifier built for a CAR - HIFI, it should be capable to supply 10W AC - signal constantly.

4.8.12 Conclusion

The test equipment is performing as planned. Tests of a fixed resistor to simulate the series resistance of a LiIon cell had shown that the this equipment generates reproduceable results and the flexibility of the soft and hardware enables the user to do tests on cells or battery packs without being limited to a certain cell type. Unfortunately, the file with the test results for LiIon cells was overwritten by accident and a new test is still running.

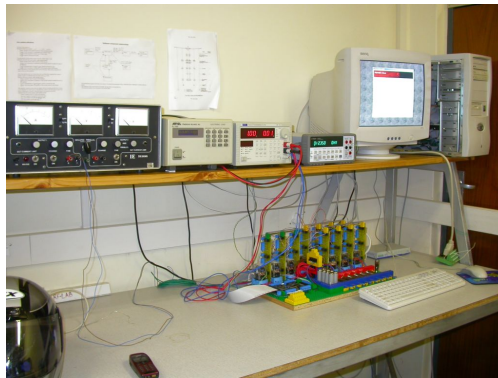


(a)



(b)

Figure 4.23: The Complete Setup is shown in (a). The IO-extension next to relays, screw terminal blocks, shunt resistor and the container for 8 LiIon cells is shown in (b).



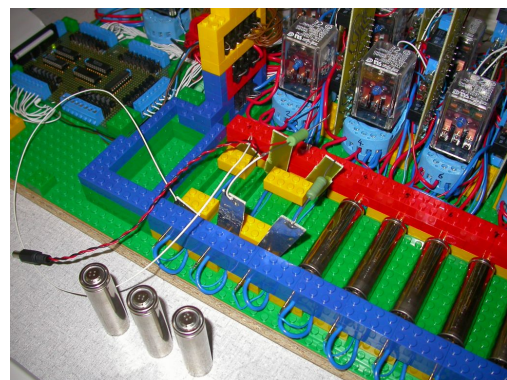
(a)



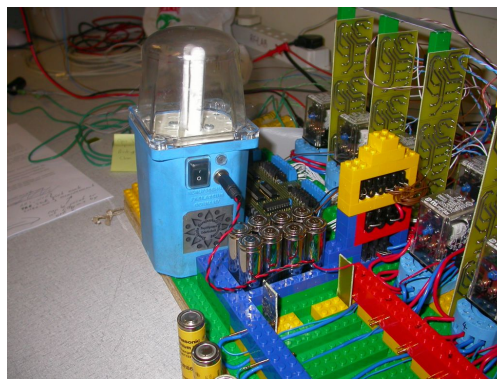
(b)



(c)



(d)



(e)

Figure 4.24: The Integration at the ESL. (a) is the setup at the ESL, (b) is the capacitor required to decouple the DC voltage from the AC source, (c) is the FLUKE 5100B calibrator used to measure the shunt resistor, (d) are reference resistors to prove the series resistance measurement of the test equipment and (e) is the setup with a solar2000 lamp which is described in section 4.8.10 on page 94

A	B	C	D	E	F	G	H	I	J	K	L	M	N	O	P	Q	R	S	T	U	V	W	X	Y	Z	AA	AB	AC	AD	AE			
1	No.	Description:	Duration [s]	Sample [s]	Cycle			Abort Criteria			Multi-meter	Power Supply		Electronic Load		Audio / AC		Digital I/O															
					AS	IE	FI	Umax [V]	Umin [V]	Udiffmax [V]		Udiffmin [V]	Voltage [V]	Current [A]	Mode (C/R/M)	Value	Freq. (Hz)	Mode (Cell1)	Value	S/P	On/Off	AC/DC											
3	1	Meas RI	3	3	1	1	1				AC	0	0	C	0	750	s	d	d	d	d	d	d	d	d	d	d	d	10	s	On	ac	
4	2	Meas RI	120	15	1	1	1				AC	0	0	C	0	750	s	d	d	d	d	d	d	d	d	d	d	d	10	s	On	ac	
5	3	Discharge	16000	15	1	1	1	3			DC	2	2	C	1.3	50	s	d	d	d	d	d	d	d	d	d	d	10	s	On	dc		
6	4	Charge	360	15	1	1	1				DC	10	2.3	C	1	50	s	d	d	d	d	d	d	d	d	d	d	10	s	On	dc		
7	5	Meas RI	3	3	1	1	1				AC	0	0	C	0	750	s	d	d	d	d	d	d	d	d	d	d	10	s	On	ac		
8	6	Charge	17000	15	1	1	1	8			DC	10	2.3	C	1	50	s	d	d	d	d	d	d	d	d	d	d	10	s	On	dc		
9	7	Discharge	200	15	1	1	1				DC	2	2	C	1	50	s	d	d	d	d	d	d	d	d	d	d	10	s	On	dc		
10	8	Meas RI	3	3	1	1	1				AC	0	0	C	0	750	s	d	d	d	d	d	d	d	d	d	d	10	s	On	ac		
11	9	Discharge	1000	15	1	1	1				DC	2	2	C	1	50	s	d	d	d	d	d	d	d	d	d	d	10	s	On	dc		
12	10	Meas RI	3	3	1	1	1				AC	0	0	C	0	750	s	d	d	d	d	d	d	d	d	d	d	10	s	On	ac		
13	11	Charge	500	15	1	1	1				DC	10	2	C	1	50	s	d	d	d	d	d	d	d	d	d	d	10	s	On	dc		
14	12	Meas RI	3	3	1	1	1				AC	0	0	C	0	750	s	d	d	d	d	d	d	d	d	d	d	10	s	On	ac		
15	13	Discharge	1000	15	1	1	1				DC	2	2	C	1	50	s	d	d	d	d	d	d	d	d	d	d	10	s	On	dc		
16	14	Meas RI	3	3	1	1	1				AC	0	0	C	0	750	s	d	d	d	d	d	d	d	d	d	d	10	s	On	ac		
17	15	Charge	1000	15	1	1	1				DC	10	2	C	1	50	s	d	d	d	d	d	d	d	d	d	d	10	s	On	dc		
18	16	Meas RI	3	3	1	1	1				AC	0	0	C	0	750	s	d	d	d	d	d	d	d	d	d	d	10	s	On	ac		
19	17	Discharge	1000	15	1	1	1				DC	2	2	C	1	50	s	d	d	d	d	d	d	d	d	d	d	10	s	On	dc		
20	18	Meas RI	3	3	1	1	1				AC	0	0	C	0	750	s	d	d	d	d	d	d	d	d	d	d	10	s	On	ac		
21	19	Charge	1000	15	1	1	1				DC	10	2	C	1	50	s	d	d	d	d	d	d	d	d	d	d	10	s	On	dc		
22	20	Meas RI	3	3	1	1	1				AC	0	0	C	0	750	s	d	d	d	d	d	d	d	d	d	d	10	s	On	ac		
23	21	Discharge	1000	15	1	1	1				DC	2	2	C	1	50	s	d	d	d	d	d	d	d	d	d	d	10	s	On	dc		
24	22	Meas RI	3	3	1	1	1				AC	0	0	C	0	750	s	d	d	d	d	d	d	d	d	d	d	10	s	On	ac		
25	23	Charge	9000	15	1	1	1				DC	2	2	C	1	50	s	d	d	d	d	d	d	d	d	d	d	10	s	On	dc		
26	24	Discharge	150	15	1	1	1				DC	2	2	C	1	50	s	d	d	d	d	d	d	d	d	d	d	10	s	On	dc		
27	25	Meas RI	3	3	1	1	1				AC	0	0	C	0	750	s	d	d	d	d	d	d	d	d	d	d	10	s	On	ac		
28	26	Discharge	16000	15	1	1	1	3			DC	2	2	C	1	50	s	d	d	d	d	d	d	d	d	d	d	10	s	On	dc		
29	27	Charge	150	15	1	1	1				DC	10	2	C	1	50	s	d	d	d	d	d	d	d	d	d	d	10	s	On	dc		
30	28	Meas RI	3	3	1	1	1				AC	0	0	C	0	750	s	d	d	d	d	d	d	d	d	d	d	10	s	On	ac		
31	29	Measure Voltage	8000	15	1	1	1				DC	10	2	C	1	50	s	d	d	d	d	d	d	d	d	d	d	10	s	off	dc		
32	End																																

Figure 4.25: The Test Program for the SOLAR2000 - Lamp.

	A	B	C	D	E	F	G	H	I	J	K	L	M	N	O	P	Q	R	
1	TestNo:	4																	
2	Capacity:	4500 mAh																	
3	Voltage(Nom.):	V																	
4	Shunt Resistor:	0.0965 Ohm																	
5	Solar2000 No. 01 606																		
6																			
7	Timestamp	Cell 1	Cell 2	Cell 3	Cell 4	Cell 5	Cell 6	Cell 7	Cell 8	Serial String	Parallel String	Shunt Resistor Voltage	Temperature	10E reference Resistor	Serial String	INV Parallel String	Shunt Resistor	INV Return	
8																			
9																			
10	2003/05/12 22:44:32	5.4901249	0	0	0	0	0	0	0	5.9817771	0.03575799	0.097534552	4.9924581	12.220558	-5.873	-0.047	-0.0975	-4.9	
11	2003/05/12 22:44:53	5.7061719	0	0	0	0	0	0	0	6.1615336	0.04542437	0.12610232	4.9924581	12.220364	-6.164	-0.049	-0.1261	-4.9	
12	2003/05/12 22:45:14	5.7340341	0	0	0	0	0	0	0	6.1886601	0.03721646	0.12612688	4.99247	12.220525	-6.191	-0.047	-0.1261	-4.9	
13	2003/05/12 22:45:35	5.7576967	0	0	0	0	0	0	0	6.2111661	0.03663027	0.12616821	4.9924074	12.220752	-6.213	-0.049	-0.1261	-4.9	
14	2003/05/12 22:45:56	5.7780137	0	0	0	0	0	0	0	6.2305019	0.03694123	0.12614455	4.9923696	12.221141	-6.232	-0.049	-0.1261	-4.9	
15	2003/05/12 22:46:17	5.7963719	0	0	0	0	0	0	0	6.2522298	0.03695706	0.12616878	4.9923017	12.221022	-6.252	-0.048	-0.1261	-4.9	
16	2003/05/12 22:46:38	5.8129609	0	0	0	0	0	0	0	6.2644918	0.03646326	0.1261662	4.9923394	12.220515	-6.265	-0.048	-0.1262	-4.9	
17	2003/05/12 22:46:59	5.8276955	0	0	0	0	0	0	0	6.2757706	0.03615259	0.12619959	4.9923459	12.22086	-6.275	-0.049	-0.1262	-4.9	
18	2003/05/12 22:47:20	5.8408346	0	0	0	0	0	0	0	6.2840369	0.03823445	0.12618225	4.9922368	12.220828	-6.284	-0.047	-0.1262	-4.9	
19	2003/05/12 22:47:42	5.8532767	0	0	0	0	0	0	0	6.2927426	0.03519912	0.1262345	4.9922078	12.2214	-6.293	-0.005	-0.1262	-4.9	
20	2003/05/12 22:48:03	5.8644066	0	0	0	0	0	0	0	6.3013057	0.03745421	0.12623362	4.9921959	12.221378	-6.301	-0.048	-0.1262	-4.9	
21	2003/05/12 22:48:24	5.8749326	0	0	0	0	0	0	0	6.3095493	0.03681401	0.12623622	4.9922283	12.221874	-6.31	-0.048	-0.1262	-4.9	
22	2003/05/12 22:48:45	5.8847408	0	0	0	0	0	0	0	6.3175814	0.03526861	0.12627532	4.992238	12.222392	-6.318	-0.046	-0.1263	-4.9	
23	2003/05/12 22:49:06	5.8934991	0	0	0	0	0	0	0	6.3241342	0.03739679	0.12622415	4.9921603	12.222392	-6.325	-0.049	-0.1262	-4.9	
24	2003/05/12 22:49:27	5.9019423	0	0	0	0	0	0	0	6.3320111	0.03702784	0.12624548	4.9922261	12.22195	-6.332	-0.045	-0.1262	-4.9	
25	2003/05/12 22:49:48	5.9098978	0	0	0	0	0	0	0	6.3388595	0.03538818	0.12622577	4.9921646	12.222619	-6.339	-0.046	-0.1262	-4.9	
26	2003/05/12 22:50:09	5.9175458	0	0	0	0	0	0	0	6.3454349	0.03634509	0.12621812	4.9921743	12.222964	-6.345	-0.042	-0.1262	-4.9	
27	2003/05/12 22:50:30	5.9249953	0	0	0	0	0	0	0	6.3519468	0.03750753	0.12626423	4.9921819	12.222867	-6.352	-0.045	-0.1262	-4.9	
28	2003/05/12 22:50:51	5.9321114	0	0	0	0	0	0	0	6.3564197	0.03506975	0.12627974	4.9922402	12.222543	-6.359	-0.047	-0.1263	-4.9	
29	2003/05/12 22:51:12	5.9387516	0	0	0	0	0	0	0	6.3653351	0.03750516	0.12628703	4.9921797	12.22318	-6.366	-0.045	-0.1263	-4.9	
30	2003/05/12 22:51:33	5.9458626	0	0	0	0	0	0	0	6.3717045	0.03599358	0.12634276	4.9920395	12.223612	-6.372	-0.046	-0.1263	-4.9	
31	2003/05/12 22:51:55	5.9518648	0	0	0	0	0	0	0	6.3755738	0.03466754	0.12634405	4.9922874	12.223881	-6.379	-0.049	-0.1263	-4.9	
32	2003/05/12 22:52:16	5.9576558	0	0	0	0	0	0	0	6.3841044	0.03435533	0.12632218	4.9922348	12.223986	-6.385	-0.043	-0.1263	-4.9	
33	2003/05/12 22:52:37	5.9633692	0	0	0	0	0	0	0	6.3897228	0.03499639	0.1263009	4.99217	12.223692	-6.39	-0.043	-0.1263	-4.9	
34	2003/05/12 22:53:16	5.9025086	0	0	0	0	0	0	0	9.9991707	0.06112983	0.000000615	4.9921301	12.224184	-7.242	-0.051	-0.0363	-4.9	
35	2003/05/12 22:53:37	5.9404442	0	0	0	0	0	0	0	6.3755738	0.03579882	0.126261	4.9920006	12.224033	-6.378	-0.044	-0.1262	-4.9	
36	2003/05/12 22:53:58	5.9562266	0	0	0	0	0	0	0	6.39202	0.03476988	0.12625184	4.9920449	12.224631	-6.393	-0.046	-0.1262	-4.9	
37	2003/05/12 22:54:19	5.9690879	0	0	0	0	0	0	0	6.4019471	0.03485204	0.12625033	4.9920028	12.223838	-6.403	-0.045	-0.1262	-4.9	
38	2003/05/12 22:54:40	5.9772476	0	0	0	0	0	0	0	6.4099749	0.034991387	0.12625485	4.9920341	12.224702	-6.41	-0.047	-0.1262	-4.9	
39	2003/05/12 22:55:01	5.9840065	0	0	0	0	0	0	0	6.4164468	0.03613416	0.12624775	4.9920308	12.224658	-6.417	-0.046	-0.1262	-4.9	

Figure 4.26: Output Data, generated during the Test on the SOLAR2000 Lamp.

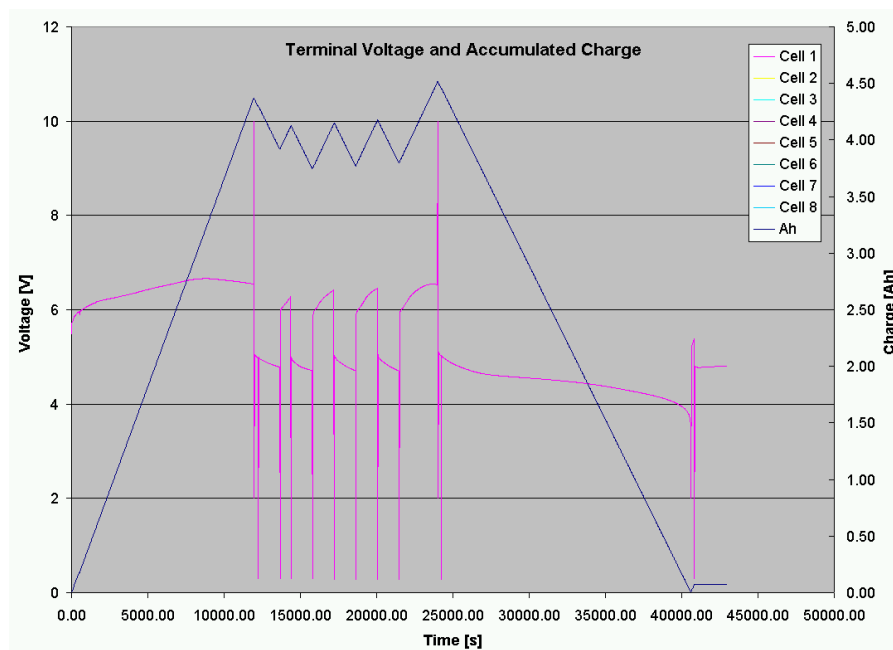


Figure 4.27: Terminal Voltage and Accumulated Charge. The voltage on the terminals rises to 10V, if the solar lamp is fully charged—battery is disconnected to protect it from overcharging (10V is the output voltage of the power supply). The Voltage drops to 2V in case that the lamp is completely discharged (over discharge protection disconnects the battery from the terminal; see figure 4.25 on page 97). The short needles down to some hundred millivolt are due to the measurement of the series resistance where only the AC voltage is measured.

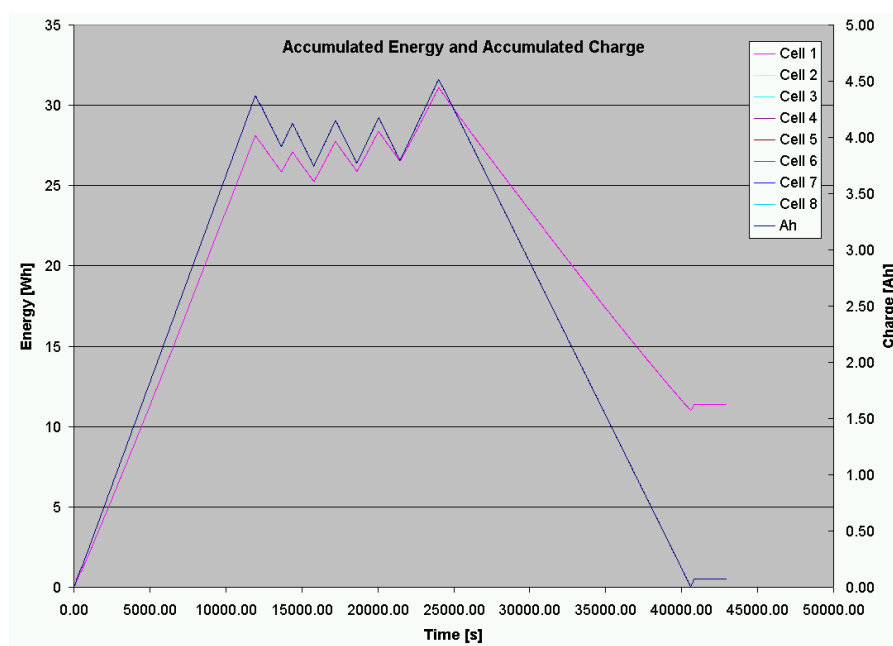


Figure 4.28: Accumulated Energy and Accumulated Charge. It can be seen, that after discharging the same amount of Charge, the accumulated energy is not zero. This is due to the losses in the battery and the protection electronics.

4.9 Radiation Testing of Components

Because of the space environment (see section 3.1 on page 3), components have to be tested before they are used in space. These tests are done on “space qualified” products, which are quite expensive. For commercial products these tests are commonly not done and oneself has to make sure, that the product will last in space.

For devices, which are sensitive to displacement²⁰ damage (e.g. GaAs, JFETs, LEDs, ect), electron accelerators are used; Cobalt 60 sources are used for ionisation damage tests (Si is sensitive to that type of radiation) [27, p.7].

Before the test is started, the parameter of the devices must be measured. During the test, data should also be collected to verify the aging and degradation. It is therefore necessary to stop the radiation for measurement (ESA recommend a maximum pause of 2 hours between exposures) or to measure the data during radiation. The second method should be used whenever possible. It is important to assign the test data to the specific device. Therefore it is important to do a sample serialisation.

ESA²¹ recommended the selection of a minimum of 11 samples of at least 2 different lots, making a minimum of 22 samples. [27, p.10]

In the test described in section 4.9.1, the following tests were not done:

- anneal under bias condition at 25°C (with measurement of the electrical parameters after 12 h, 24 h, and 168 h).
- accelerated aging test (baking the device for 168 h at 100 °C) after the radiation test.

Both tests are recommended by ESA for the “RADIATION EXPOSURE AND TEST SEQUENCE” [27, p.11].

4.9.1 Radiation Test on PROFET[®]

PROFET[®] is a “smart” switch from Infineon Technologies AG. Its main features are

- short circuit protection,
- thermal shutdown,
- current limitation,

²⁰Change of the crystal lattice structure due to energetic, heavy atomic particles. Displacement can only be “cured” by high-temperature annealing. [43]

²¹European Space Agency

- diagnostic feedback (digital) or current sense output (analog),
- CMOS compatible input (for some devices),
- low R_{on} ,
- Electro-Statically Discharge (ESD) protection,

as well as some other features (see datasheets). According to Mr. Andreas Erl from Infineon Germany, no prior radiation test were done on these MOSFETs. There was also no information in the technical marketing or development division about the use of PROFET[®] - devices in space.

The devices BTS 443P and BTS 432E2 were chosen for radiation tests. Infineon Technology (Andreas Erl) recommended using the BTS 6143D instead of the BTS 443P and the BTS 5240L instead of the BTS 432E2 for future designs. Five free samples from each device were received through EBV-South Africa. Unfortunately, the BTS 5240L is still in development and not in full production.

Test conditions were 12k Rad within 6 h at a constant rate of 2k Rad per hour. Each PROFET[®] had a 21W/24V bulb as load. The test circuit for the radiation test contained:

- 3 x BTS432E2
- 3 x BTS443P
- 3 x BTS6143D
- 1 x BTS5240L (because not in full production)

The load of the BTS 432E2 with the 50% duty cycle was used for the BTS 5240L. The on-times of the MOSFETs were 1/3, 1/2 and 2/3 (each MOSFET-type with 3 different on - times) with a cycle length of 6 minutes. Only one analogue channel was used to measure the outputs (sum of all outputs). To distinguish the MOSFETs from the collected data, different starting delays were used.

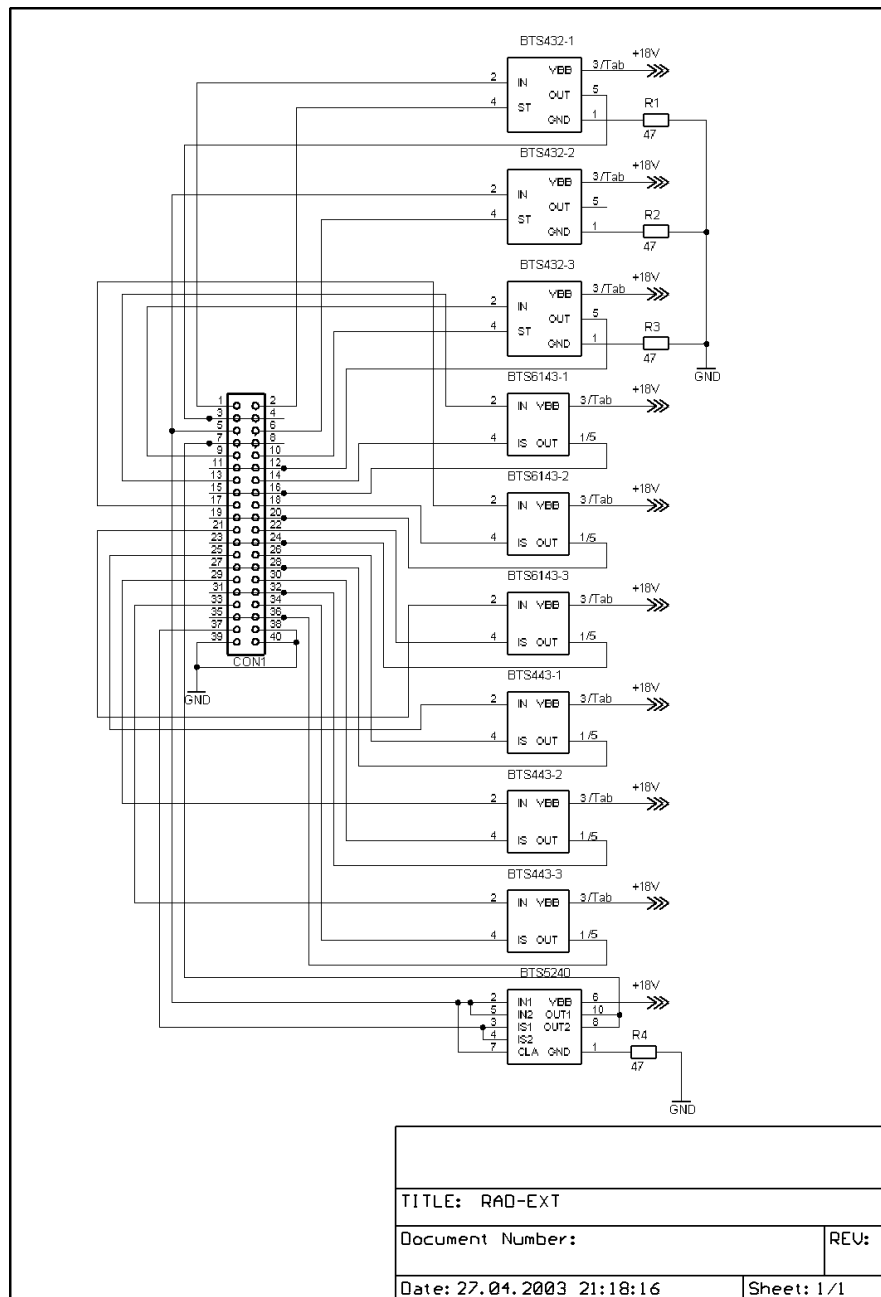


Figure 4.29: Radiated circuit (extern) for the room with CO₆₀ source. Radiated with 2k Rad/h; connected to the Interface and protection - circuit with 5m ribbon cable (CON1) and 5m wire to the power supply (+18V).

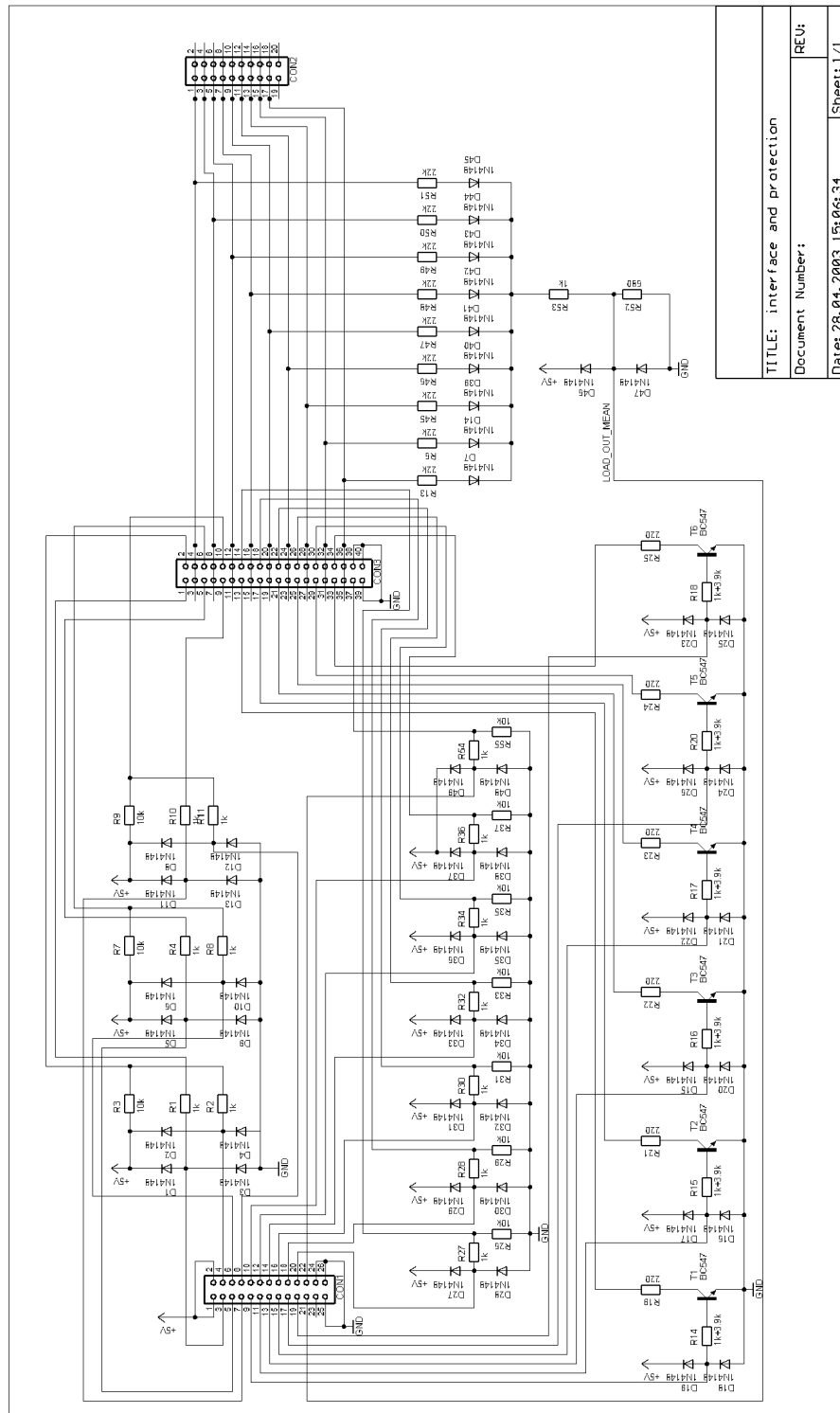


Figure 4.30: Interface and protection - circuit.

Where U_{LOM} is the LOAD_OUT_MEAN - voltage and U_{OUTx} is the output voltage of any MOSFET.

4.9.1.3 Radiation Test Description

Test sequence for the radiation test:

1. Serialisation of the devices (device allocated to the data through the test-electronic, see section 4.9.1.2 on page 104)
2. Verification of the electrical parameters of the device, which are not measured during the test.
3. Start the test-electronics (signals described in section 4.9.1.1 on page 104) in unexposed conditions.
4. Start test-electronics at radiation facility without exposure (min 10 min).
5. Start radiating the test-electronics with 2k Rad for at least 6 h.
6. Stop radiation (test-electronics should work for at least 30 min longer)

4.9.1.4 The Results for PROFET®

Test results are unfortunately not available because the test could not be done as the data logging didn't work correctly and another test could not be done during this diploma project. The test will be done in Vienna at a later stage. The test results will be published in a separate document via the Internet. The filename will be `rtsp_profet.pdf` for "Radiation Test for Satellite Power Systems on Infineon PROFET's".

4.9.1.5 Note To Test Results

The devices should only be used for missions with less than half of the discovered total dose - value. Different voltages can influence the results (this effect was not evaluated). Different dose rates can also influence the results (this effect was also not evaluated). No Single Event Effects (SEE) were analyzed. It is recommended that the total dose - value should reach a point where most devices show a malfunction, or three times the expected total dose for the space mission.

5 Conclusion

For the first part, namely the sizing and selecting of a power source, different possibilities were shown. It is impossible to select the energy storage or size the solar array without knowing the orbit or the power requirements. The method with which to do the sizing was shown and tools were developed to make that process easier.

For missions with continuous sun (twilight orbit) and high power requirements at a low duty cycle, capacitors could be a good approach. No Supercapacitors were physically available and, therefore, no tests could be done. For Supercapacitors, MPP regulators are strongly recommended. Single cell management (over and under voltage-protection) is absolutely necessary. Future work can focus on well matched capacitors to examine if there is a small self-balancing effect due to different efficiencies at different voltages.

Commercial LiIon cells show high energy density. This research has shown that nearly all analysed commercial cells show a small *leakage of electrolyte*, which is not acceptable for use in space. Unfortunately, only Panasonic cells and some cells from an unknown manufacturer could be analysed, maybe other manufacturers use tighter gaskets. However, the leakage problem has to be analysed precisely before using LiIon cells in space applications.

Cell matching and measurement electronics were built and the function was demonstrated using cells from old battery packs. For space applications, it is highly recommended to use cells from one batch so as to minimize the divergences.

Smart FETs for switching on and off of modules, could be a good and new approach. Unfortunately, the total dose test (radiation) could not be done so far because of a problem with the datalogger. However, these products are very robust since they are designed for use in the automobile industry. Load dump (higher voltage with low internal resistance), ESD and other serious interferences are common in automobile power systems.

In general it can be said that commercial products can make satellites much cheaper but comprehensive testing is required, which is expensive. For university projects low costs are important and a higher risk is acceptable. Hence smaller and less expensive tests are acceptable.

Bibliography

Advice: Books and online information has been considered

- [1] BaSyTec - Homepage. URL: <http://www.basytec.de/>; access-date: 2003-05-05
- [2] Comparing performance. Removed from the internet. URL: http://www.saft.fr/space_industry/c/c3/c3d.htm; access-date: 2002-10-22
- [3] Edan Technology Inc. URL: http://www.edancell.com/supplier_branch.html; access-date: 2003-05-04
- [4] Holograms brighten up the environment. URL: http://www.spie.org/web/oer/february/oer_feb96_1.html; access-date: 2003-05-03
- [5] How to prolong lithium-based batteries. URL: <http://www.batteryuniversity.com/parttwo-34.htm>; access-date: 2003-05-06
- [6] Imaging Sensor Description RADARSAT - 1. URL: <http://imaging.geocomm.com/features/sensor/radarsat1/>; access-date: 2003-05-04
- [7] *Multifunctional Bifacial Photovoltaic Elements*, Institut für Solarenergieforschung Hameln/Emmerthal(ISFH); D-31860 Emmerthal. URL: [http://wire0.ises.org/wire/doclibs/EuroSun96.nsf/id/A048769707FBE911C12565E60037357F/\\$File/paper.pdf](http://wire0.ises.org/wire/doclibs/EuroSun96.nsf/id/A048769707FBE911C12565E60037357F/$File/paper.pdf); access-date: 2003-04-24
- [8] Non-Correctable Battery Problems. URL: <http://www.batteryuniversity.com/parttwo-32.htm>; access-date: 2003-05-06
- [9] PC/104 Embedded-PC Modules. URL: <http://www.pc104.org>; access-date: 2003-05-03
- [10] Photovoltaic Detectors: Properties and Characterization. 470PVDETLEC.pdf. URL: <http://www.optics.arizona.edu/Palmer/opti470a/470lectures/470PVDETLEC.pdf>; access-date: 2003-04-24
- [11] Ultracapacitors: Managing Power and Energy. URL: http://www.powerpulse.net/powerpulse/archive/aa_061200b1.stm; access-date: 2003-05-04

- [12] What is PC/104-Plus. URL: http://www.pc104.org/technology/plus_info.html; access-date: 2003-05-03
- [13] *Satellite Cell Development: Lithium-Ion Profile*, Eagle-Picher Technologies, LLC; Advanced Electrochemical Systems Operation; P.O. Box 47; Joplin, Missouri 64802, 1998.
- [14] *Performance Characteristics of Lithium-Ion Cells for NASA's Mars 2001 Lander Application*, 1999.
- [15] *Dose Rate and Bias Dependency of Total Dose Sensitivity of Low Dropout Voltage Regulators*, Jet Propulsion Laboratory, 4800 Oak Grove Drive, Pasadena, California USA 91109, 2000. URL: <http://nepp.nasa.gov/docuploads/BFFE2875-CE21-4696-A95D39570DE879BF/LowDrop-00.pdf>; access-date: 2003-04-07
- [16] *Proton Damage in Linear and Digital Optocouplers*, Jet Propulsion Laboratory, 4800 Oak Grove Drive, Pasadena, California USA 91109, 2000. URL: http://nepp.nasa.gov/docuploads/67F6DAF8-A724-4A4B-8AE07F09EDCD161F/RAD_LinOpt-00.pdf; access-date: 2003-04-24
- [17] *Radiation Damage of Electronic and Optoelectronic Devices in Space*, Jet Propulsion Laboratory, 4800 Oak Grove Drive, Pasadena, California USA 91109, October 2000. URL: http://nepp.nasa.gov/DocUploads/D41D389D-04D4-4710-BBCFF24F4529B3B3/Dmg_Space-00.pdf; access-date: 2003-04-07
- [18] *Lithium-Ion Batteries for Space*, AEA Technology Space, Culham Science Centre, Abingdon, Oxfordshire, UK, OX14 3ED, 2002.
- [19] C. Belk, J. Robinson, M. Alexander, W. Cooke, and S. Pavelitz, "Meteorites and Orbital Debris: Effects on Spacecraft," National Telecommunications and Information Administration (NTIA), U.S. Dept. of Commerce, Reference Publication NASA RP-1408, Aug. 1997. URL: <http://trs.nis.nasa.gov/archive/00000356/01/rp1396.pdf>; access-date: 2003-4-18
- [20] I. Buchmann. Will Lithium-Ion Batteries Power the New Millennium? URL: http://www.powerpulse.net/powerpulse/archive/pdf/aa_103000c.pdf; access-date: 2003-05-05
- [21] "www.celestrak.com." URL: <http://www.celestrak.com>; access-date: 2003-01-29
- [22] V. A. Chobotov, Ed., *Orbital Mechanics*, 2nd ed., ser. AIAA Education Series. American Institute of Aeronautics and Astronautics, Inc., 1991.

- [23] RØMER Mission Technical Description. Danish Space Research Institute. URL: http://www.dsri.dk/roemer/pub/Documents/ROEMER_Mis_Tech_Descr_2_Dr_6.pdf; access-date: 2003-05-05
- [24] RØMER Webpage. Danish Space Research Institute. URL: <http://www.dsri.dk/roemer/pub/>; access-date: 2002-05-05
- [25] *Lithium-Ion Cell Performance under Environmental Extremes*. Eagle-Picher Technologies, LLC, 1999.
- [26] Sixth European Space Power Conference. ESA. URL: <http://www.estec.esa.nl/conferences/espc-2002/fp.html>; access-date: 2002-11-28
- [27] *Total Dose Steady-State Irradiation Test Methode*, ESA/SCC Std. 22 900, 1995.
- [28] *Space engineering - Space environment*, European Cooperation For Space Standardization Std. ECSS-E-10-04A, 01 2000.
- [29] J. Forest, Ed., *Investigation of Plasma Induced Charging of Satellite Systems*. ESA / ESTEC, October 2000. URL: <http://www.spis.org/spine/picup3d/docs/URD1.4.pdf>; access-date: 2003-04-08
- [30] C. D. Gregory, "Win Orbit 3.6." URL: <http://www.amsat.org/amsat/ftpsoft.html>; access-date: 2003-04-26
- [31] J. Hill. Circuit Board Effects on Lithium-Ion Protection Circuits. URL: http://www.powerpulse.net/powerpulse/archive/pdf/aa_031201b.pdf; access-date: 2003-05-05
- [32] S. Honda, M. Toriyama, H. Suzuki, and Y. Nakazawa, "Battery charging apparatus," European Patent Application Patent 0 498 679 A2, Aug. 12, 1992.
- [33] K. A. LaBel, M. M. Gates, and A. K. Moran. Commercial Microelectronics Technologies for Applications in the Satellite Radiation Environment. URL: <http://radhome.gsfc.nasa.gov/radhome/papers/aspen.htm>; access-date: 2003-04-07
- [34] W. J. Larson and J. R. Wertz, Eds., *Space Mission Analysis and Design*, 2nd ed., ser. Space Technology Series. Microcosm, Inc. and Kluwer Academics Publishers, 1995.
- [35] (2000, jan) LG Li-ion. LG Chem. URL: <http://www.bktsi.com/documents/LG-Li-ion.pdf>; access-date: 2003-05-05
- [36] D. Linden and T. B. Reddy, Eds., *Handbook of Batteries*, 3rd ed. McGraw-Hill, 2002.
- [37] J. Ludman. Photovoltaic Systems Based on Spectrally Selective Concentrators. URL: http://www.winbmdo.com/scripts/sbir/abstract.asp?log=0152&Phase=1&Ph1Yr=91&firm_id=1545&int=91; access-date: 2003-05-03

- [38] H. Machado. Evaluation of Maxwell Technology PowerCache Ultracapacitor. NASA Johnson Space Center. URL: http://nepp.nasa.gov/index_nasa.cfm/619/CAA0270B-9C86-4829-8D7054B3AFC3ACB1/; access-date: 2002-10-22
- [39] B. Maher. Ultracapacitors, Gateway to a New Thinking in Power Quality. URL: <http://www.maxwell.com/ultracapacitors/support/presentations.html>; access-date: 2003-05-04
- [40] G. Maral and M. Bousquet, Eds., *Satellite Communications Systems*, 3rd ed. John Wiley and Sons, Ltd, 1999.
- [41] M. A. Masoum and H. Dehbonei, "Design, Construction and Testing of a Voltage-based Maximum Power Point Tracker (VMPPPT) for Small Satellite Power Supply," 13th Annual AIAA/USU Conference on Small Satellites, Iran University of Science & Technology and Advanved Electronic Research Center, Tech. Rep. SSC99-XII-7, 1999. URL: <http://www.sdl.usu.edu/conferences/smallsat/proceedings/13/tech-xii/ts-xii-7.pdf>; access-date: 2003-5-3
- [42] S. W. Moore and P. J. Schneider. (2001, 03) A Review of Cell Equalization Methods for Lithium Ion and Lithium Polymer Battery Systems. SAE 2001 World Congress Detroit, Michigan. Delphi Automotive Systems. URL: <http://www.delphi.com/pdf/techpapers/2001-01-0959.pdf>; access-date: 2002-5-5
- [43] J. H. Mulkern and G. T. Lommasson. Out Of This World Products—Designing For Space. URL: http://www.powerpulse.net/powerpulse/archive/aa_080999b1.stm; access-date: 2003-04-01
- [44] S. F. Palmore and A. D. H. Stephenson, "Lithium cell recharging," European Patent Application Patent EP 0 797 283 A2, Sept. 24, 1997.
- [45] Applications of battery power supply devices and battery drive circuit design. Seiko Instruments Inc. Application Note No.104. URL: <http://www.siielctroniccomponents.com/intcir/products/power/pdf/generalapp.pdf>; access-date: 2003-04-26
- [46] J. J. Sellers, W. J. Astore, R. B. Giffen, and W. J. Larson, *Understanding Space*, 2nd ed., ser. Space Technology Series, D. Kirkpatrick, Ed. McGraw-Hill Companies, Inc., 2000.
- [47] 26.8% Improved Triple Junction (ITJ) Solar Cell. SPECTROLAB. URL: <http://www.spectrolab.com/DataSheets/TNJCell/tnj.pdf>; access-date: 2003-04-24
- [48] H. Steyn, "Matlab Model for Spacecraft Simulation," PO Box 3183; Matieland 7602; SOUTH AFRICA. URL: <http://www.sunspace.co.za>; access-date: 2003-01-01

-
- [49] D. D. J. Summhammer, "Solar Cell Physics," Atomic Institute, email (date) or lecture/script SS2002 (ls). URL: <http://www.ati.ac.at>; access-date: 2003-04-24
- [50] I. Technical Marketing Stuff of Gates Energy Products, Ed., *Rechargeable Batteries Applications Handbook*, 1st ed. Butterworth-Heinemann, 1992.
- [51] A. C. Tribble, Ed., *The Space Environment*. Princeton University Press, 1995.
- [52] J. F. Uys, "Charge Control and Power Management of SUNSAT1 Microsatellite," Master's thesis, University of Stellenbosch, feb 1999.
- [53] W. A. van Schalkwijk and B. Scrosati, Eds., *Advances in Lithium-Ion Batteries*. Kluwer Academic/Plenum Publisher, 2002.
- [54] A. Wagner. Peak-Leistung- und Serien-Innenwiderstand-Messung unter Natürlichen Umgebungsbedingungen. Fachhochschule Dortmund; Postfach 10 50 18; 44047 Dortmund; GERMANY. URL: http://www.pv-engineering.de/_docs/PpkundRS.pdf; access-date: 2003-04-24

A Appendix

A.1 Appendix to Satellite Orbits

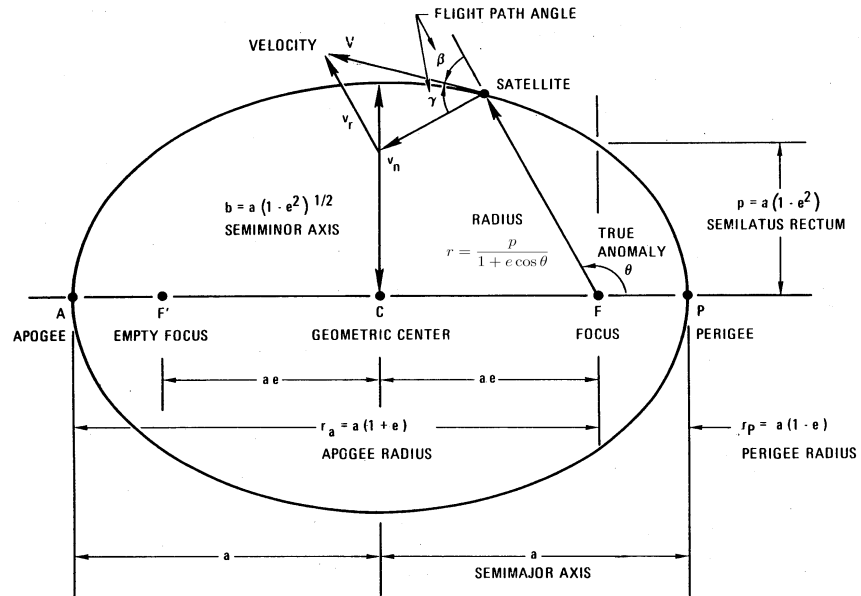


Figure A.1: Ellipse Geometry. (e is the eccentricity) [22, p.36]

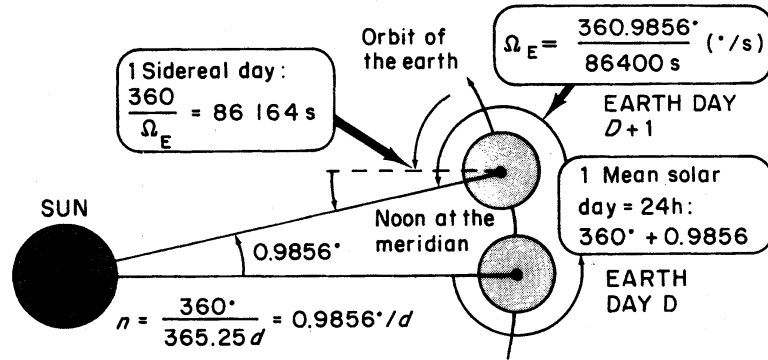


Figure A.2: Sidereal and Mean Solar Day [40, p.263]

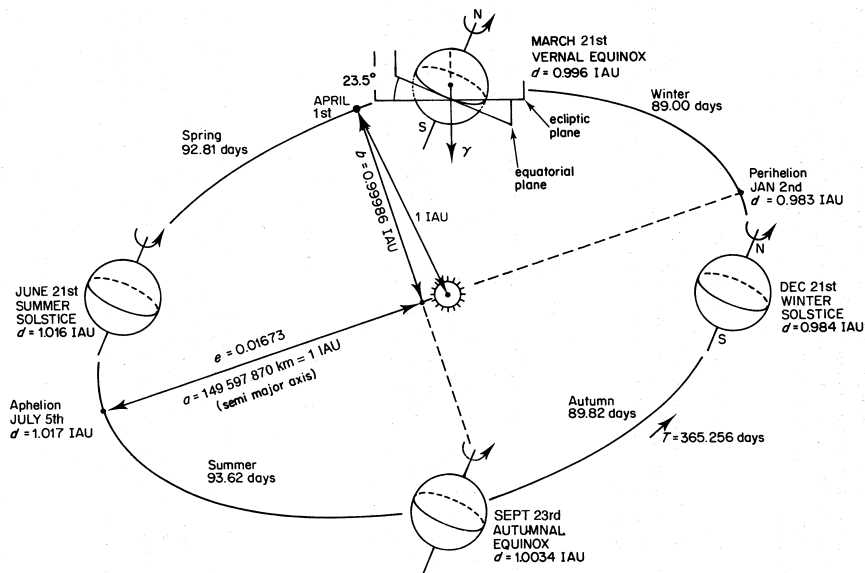


Figure A.3: Orbit of the Earth Around the Sun [40, p.258]

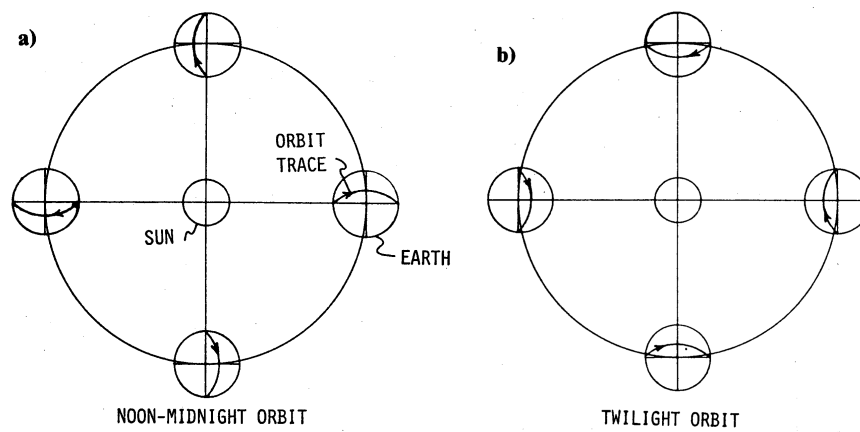


Figure A.4: Sun-Synchronous Orbits [22, p.285]: a) noon-midnight orbit b) twilight orbit (dawn-dusk)

A.2 MATLAB Simulation Outputs

These are the screenshots produced by the MATLAB simulation described in section 4.2 on page 49. The names Azimuth1, Elevation1, Power factor and Solar power refer to figure 4.5 on page 52. The NORAD 2 line element for SUNSAT—from which the orbit parameters were taken—is:

SUNSAT

```
1 25636U 99008C 01128.97266161 +.00000715 +00000-0 +19965-3 0 05158
2 25636 096.4723 260.1847 0149953 231.6439 127.1180 14.41855678116021
```

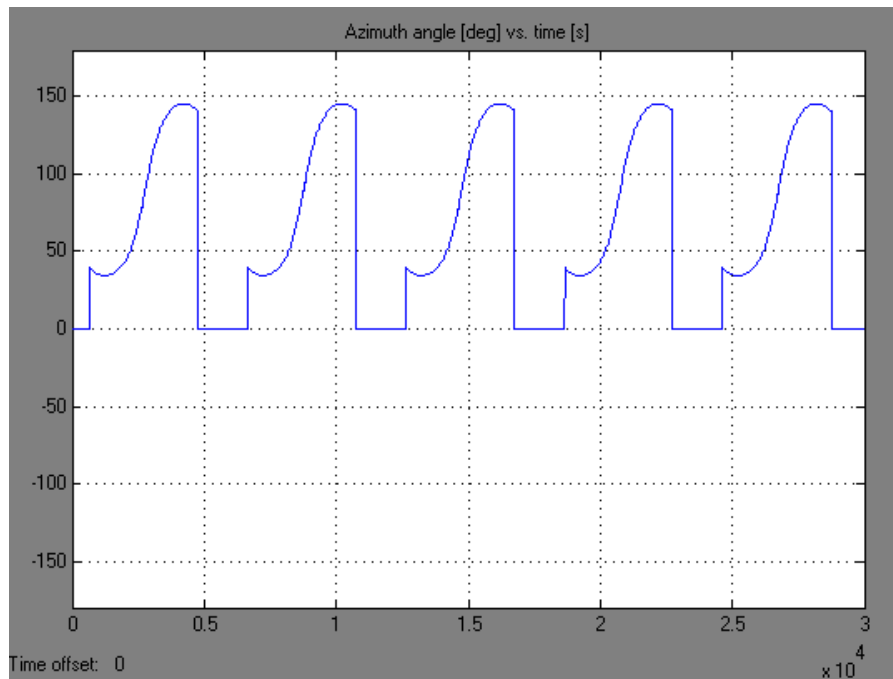


Figure A.5: Azimuth angle over time (Module Azimuth1)

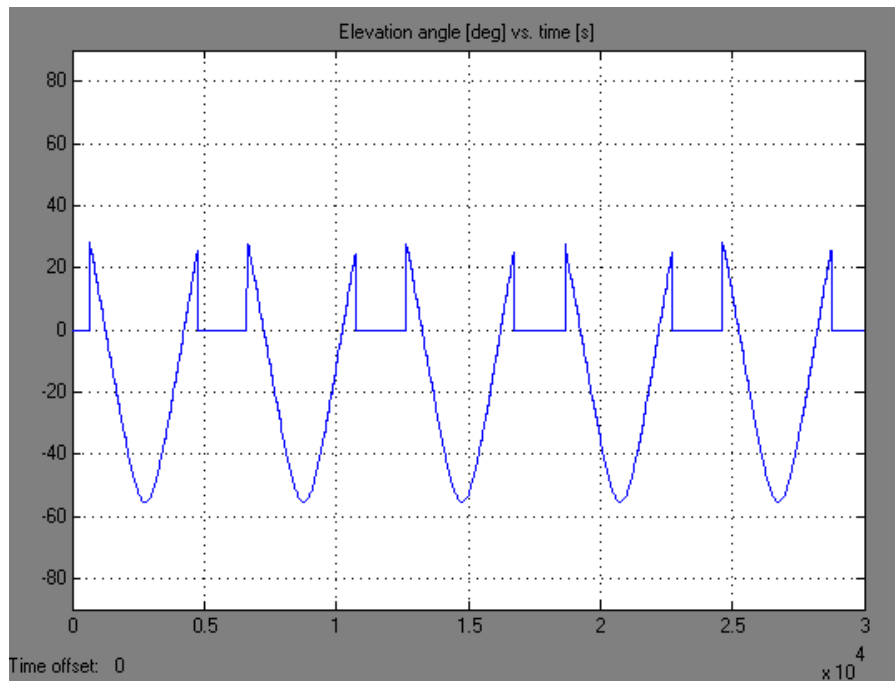


Figure A.6: Elevation angle over time (Module Elevation1)

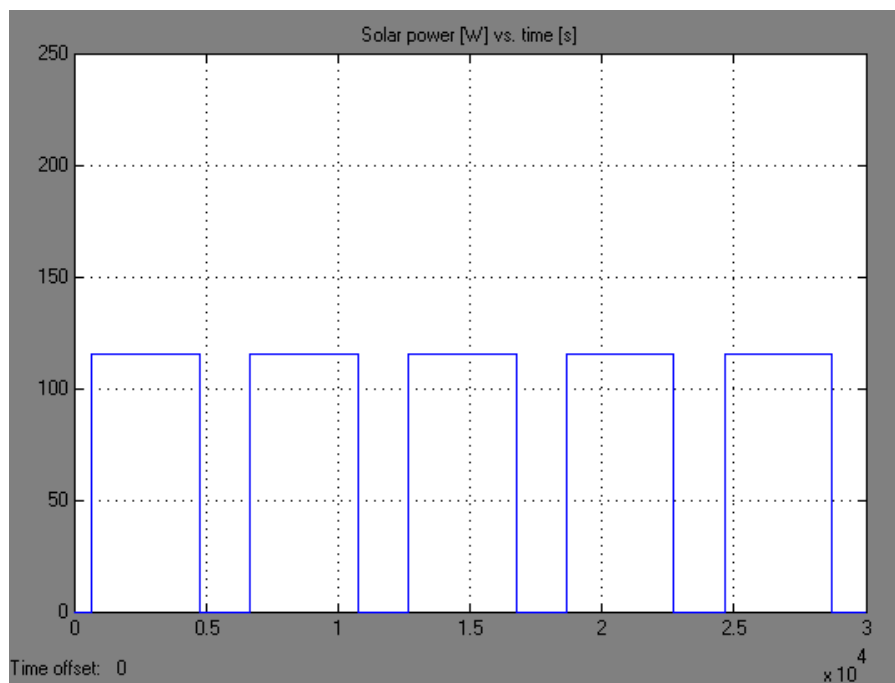


Figure A.7: Solar power over time (Module Solar power)

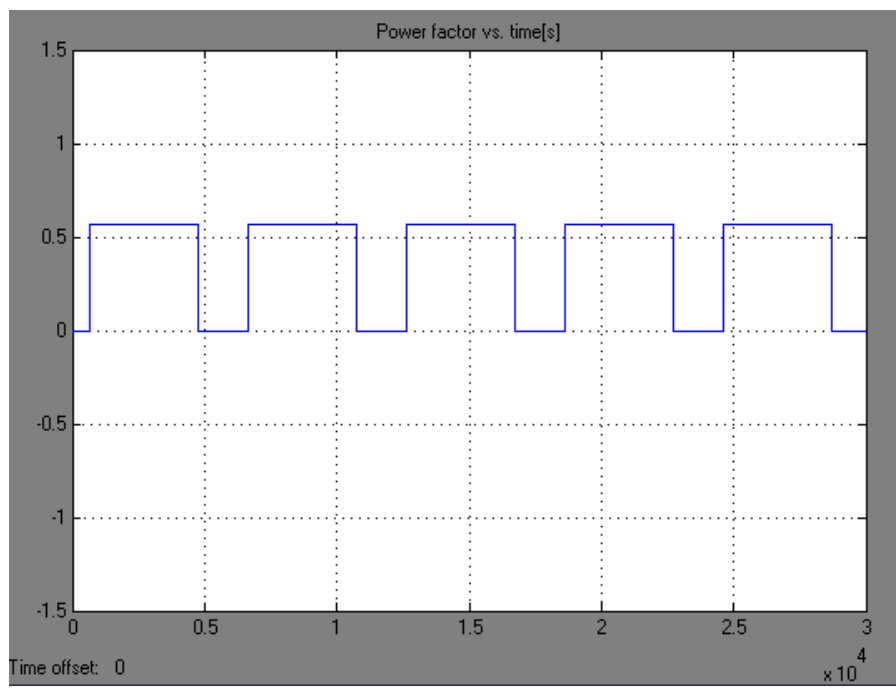


Figure A.8: Solar power factor over time (Module Power factor)

A.3 Analysis of Commercial Lilon Cells

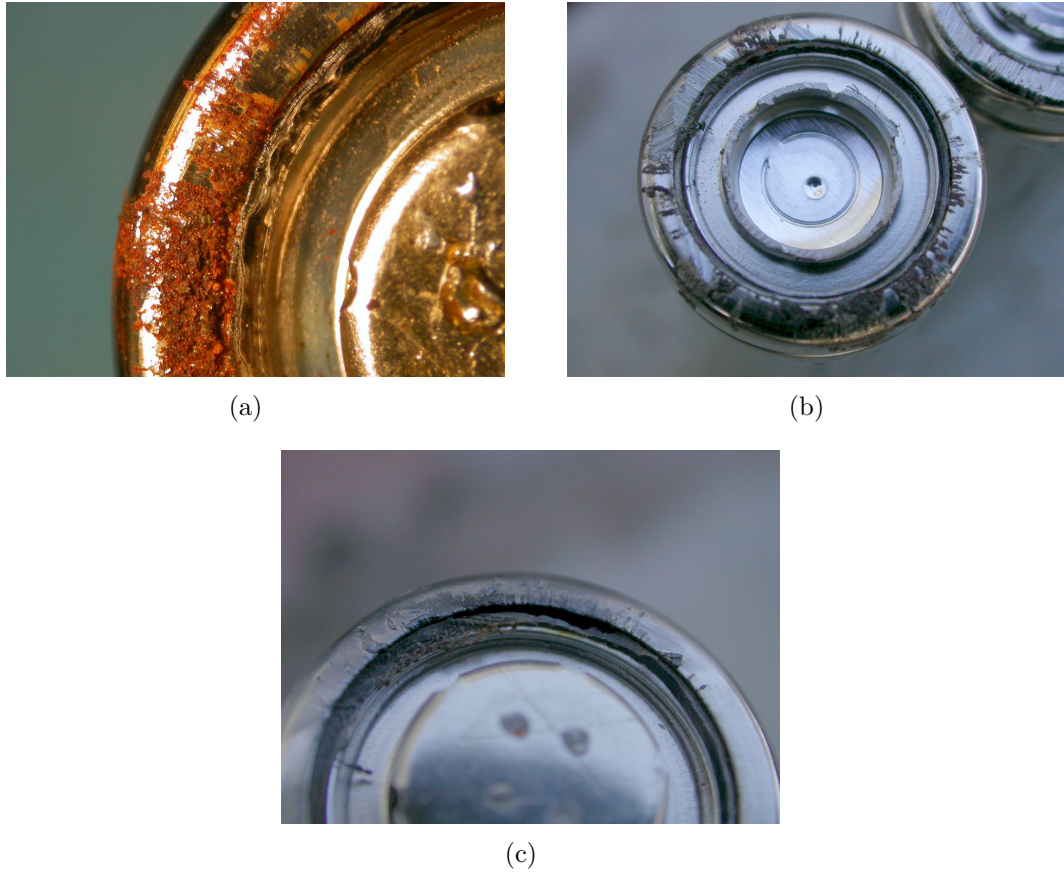


Figure A.9: Examples of Corrosion Near the Gasket. (a) CGR18650HM; (b) and (c) CGR18650H. (c) Leakage of electrolyte after polishing the rust away

A.4 AEA Battery Measurement

Cell No.	Received	Nearly charged	charged 14V	charged 15V	charged 16.5V	charged 16.7V	charged 16.85V	discharge 16.85V to 16.7V	discharge 16.85V to 16.5V	discharge 16.5V to 16.7V	discharge 16.5V to 16.85V	discharge 16.85V to 11.5V	discharge 16.85V to 11.4V	charge to 16.5V	discharged to 12.3V				
1	11.505	15.753	14.033	15.010	15.953	16.447	16.725	16.815	16.858	16.511	16.052	15.048	13.029	11.492	10.849	14.994	11.377	16.816	12.312
2	2.876	3.943	3.506	3.751	3.988	4.111	4.181	4.204	4.164	4.127	4.012	3.758	3.252	2.869	2.719	3.746	2.841	4.204	3.077
3	2.880	3.941	3.510	3.753	3.989	4.112	4.181	4.204	4.165	4.128	4.013	3.764	3.260	2.878	2.719	3.749	2.849	4.204	3.081
4	2.873	3.941	3.511	3.755	3.989	4.112	4.181	4.204	4.164	4.128	4.013	3.765	3.258	2.871	2.708	3.752	2.841	4.205	3.077
5	2.876	3.939	3.507	3.751	3.988	4.111	4.182	4.204	4.165	4.128	4.013	3.761	3.257	2.874	2.714	3.747	2.845	4.204	3.078
6	2.879	3.940	3.509	3.753	3.988	4.111	4.181	4.204	4.165	4.128	4.013	3.763	3.259	2.875	2.716	3.748	2.844	4.204	3.078
7	2.864	3.938	3.503	3.750	3.987	4.111	4.181	4.204	4.164	4.127	4.012	3.758	3.249	2.862	2.697	3.749	2.847	4.204	3.080
8	2.866	3.940	3.512	3.755	3.989	4.112	4.182	4.204	4.165	4.129	4.014	3.766	3.266	2.862	2.724	3.751	2.854	4.204	3.085
9	2.879	3.939	3.510	3.753	3.988	4.112	4.181	4.204	4.164	4.127	4.013	3.762	3.257	2.873	2.713	3.748	2.845	4.204	3.079
10	2.876	3.938	3.508	3.753	3.988	4.112	4.181	4.204	4.165	4.128	4.013	3.762	3.258	2.874	2.714	3.749	2.845	4.204	3.078
11	2.874	3.938	3.507	3.752	3.988	4.112	4.181	4.204	4.164	4.127	4.013	3.761	3.255	2.871	2.710	3.748	2.842	4.204	3.077
12	2.876	3.938	3.508	3.753	3.988	4.112	4.181	4.204	4.164	4.128	4.013	3.763	3.258	2.874	2.713	3.749	2.845	4.204	3.078
13	2.881	3.936	3.510	3.753	3.988	4.111	4.181	4.204	4.164	4.127	4.013	3.763	3.260	2.876	2.718	3.748	2.848	4.204	3.083
14	2.876	3.937	3.509	3.752	3.988	4.112	4.181	4.204	4.165	4.128	4.013	3.763	3.258	2.874	2.714	3.748	2.846	4.204	3.078
15	2.870	3.936	3.508	3.753	3.988	4.111	4.181	4.204	4.165	4.127	4.012	3.762	3.255	2.868	2.704	3.749	2.838	4.204	3.075
16	2.876	3.936	3.507	3.751	3.988	4.112	4.182	4.204	4.165	4.129	4.013	3.761	3.256	2.874	2.712	3.747	2.845	4.204	3.077
17	2.884	3.937	3.513	3.756	3.988	4.111	4.180	4.204	4.164	4.127	4.012	3.765	3.262	2.877	2.719	3.752	2.849	4.204	3.083
18	2.879	3.937	3.509	3.753	3.988	4.112	4.182	4.204	4.165	4.128	4.013	3.763	3.260	2.876	2.717	3.749	2.847	4.204	3.079
19	2.880	3.937	3.509	3.752	3.988	4.112	4.181	4.204	4.164	4.127	4.013	3.762	3.259	2.876	2.716	3.748	2.848	4.204	3.080
20	2.882	3.936	3.502	3.748	3.988	4.112	4.182	4.204	4.165	4.128	4.013	3.757	3.249	2.863	2.697	3.745	2.833	4.204	3.069
21	2.874	3.936	3.506	3.750	3.988	4.111	4.181	4.204	4.164	4.127	4.013	3.760	3.252	2.869	2.708	3.746	2.841	4.204	3.075
22	2.872	3.936	3.505	3.750	3.988	4.111	4.181	4.204	4.164	4.128	4.013	3.760	3.253	2.870	2.709	3.747	2.842	4.204	3.075
23	2.878	3.936	3.512	3.755	3.988	4.112	4.181	4.204	4.164	4.127	4.013	3.766	3.262	2.876	2.716	3.751	2.847	4.204	3.082
24	2.879	3.937	3.510	3.754	3.988	4.112	4.182	4.204	4.165	4.128	4.013	3.764	3.261	2.876	2.717	3.750	2.847	4.204	3.080
sum of cell 1 - 4	11.505	15.766	14.034	15.010	15.954	16.447	16.725	16.815	16.858	16.511	16.051	15.048	13.027	11.492	10.849	14.994	11.376	16.817	12.313
sum of cell 5 - 8	11.507	15.757	14.032	15.010	15.953	16.446	16.726	16.816	16.858	16.511	16.052	15.048	13.030	11.491	10.848	14.994	11.377	16.816	12.313
sum of cell 9 - 12	11.505	15.753	14.033	15.011	15.952	16.446	16.725	16.815	16.857	16.510	16.051	15.049	13.028	11.492	10.850	14.994	11.377	16.816	12.312
sum of cell 13 - 16	11.505	15.751	14.033	15.009	15.953	16.446	16.726	16.814	16.858	16.511	16.051	15.049	13.029	11.492	10.848	14.992	11.377	16.816	12.312
sum of cell 17 - 20	11.505	15.747	14.033	15.009	15.953	16.447	16.725	16.815	16.858	16.510	16.051	15.047	13.030	11.492	10.849	14.994	11.377	16.815	12.311
sum of cell 21 - 24	11.503	15.745	14.033	15.008	15.953	16.446	16.725	16.816	16.857	16.510	16.052	15.048	13.028	11.491	10.850	14.994	11.377	16.816	12.312
15 max	14	2	6	4	1	1	1	1	0	1	1	5	8	11	15	3	12	1	9
-12 min	-10	-5	-5	-4	-1	0	-1	-1	-1	-1	-1	-4	-9	-9	-12	-4	-10	-1	-7

Figure A.10: The measured cell voltages on the AEA Battery (electric equivalent with 4S-6P - structure)

A.5 Cell Measurement

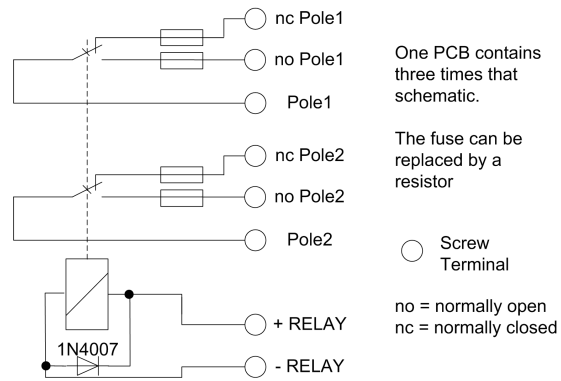


Figure A.11: Circuit for the relay with options like fuses or resistor and screw terminals.

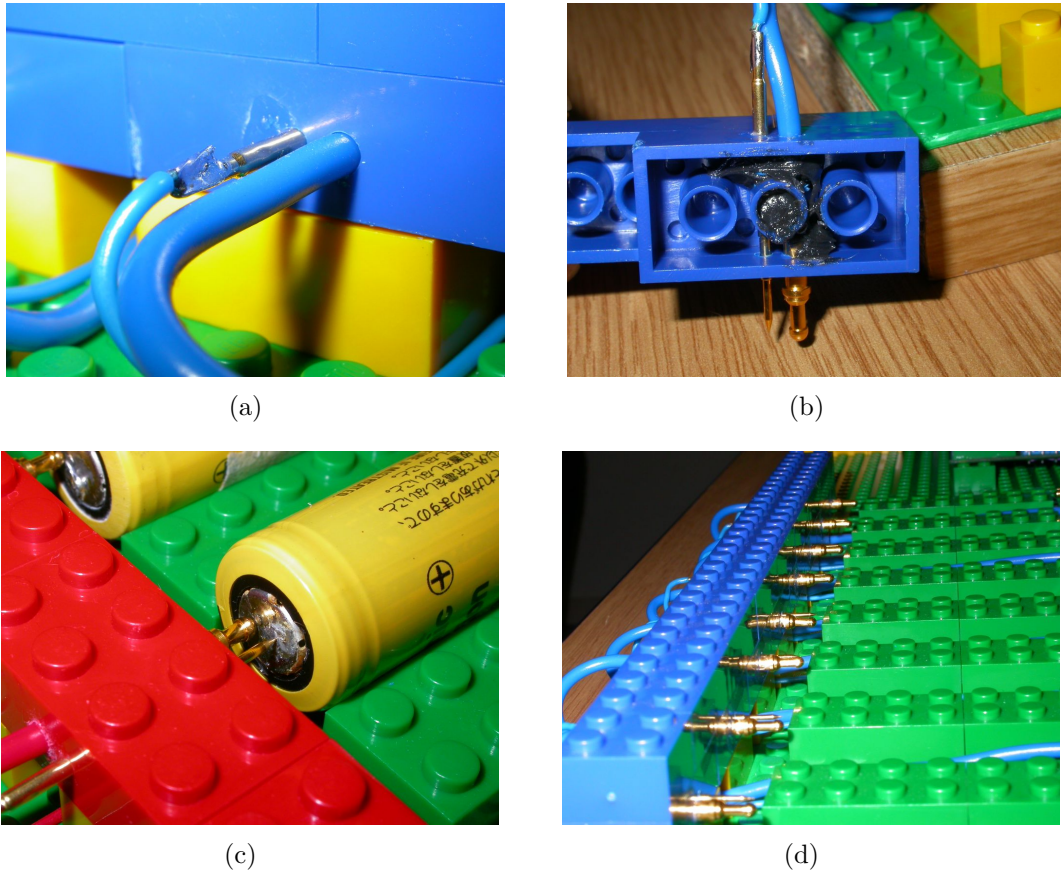
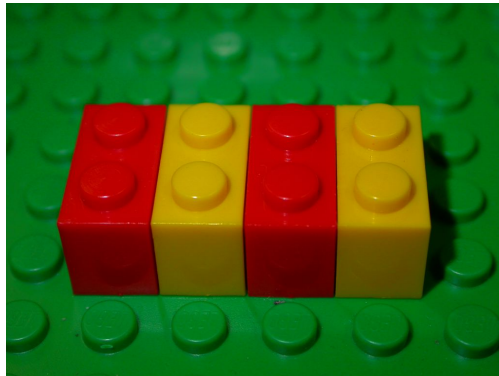
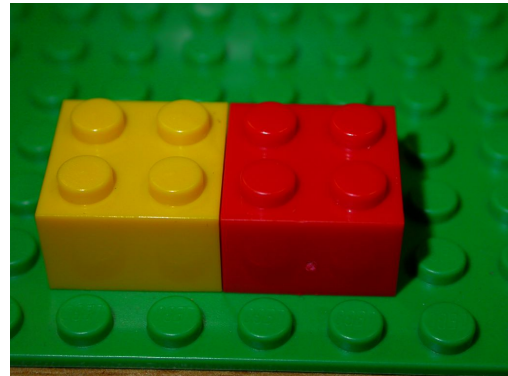


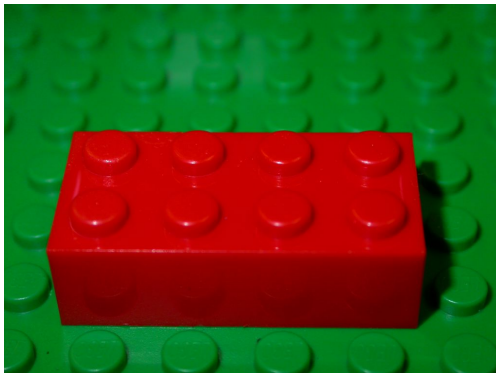
Figure A.12: The LEGO block with the spring forced probe. (a) blue block for negative pole; (b) epoxy glue used to fix the probe in the LEGO block; (c) red lego block used to connect the positive pole of the cell; (d) the negative poles of the setup.



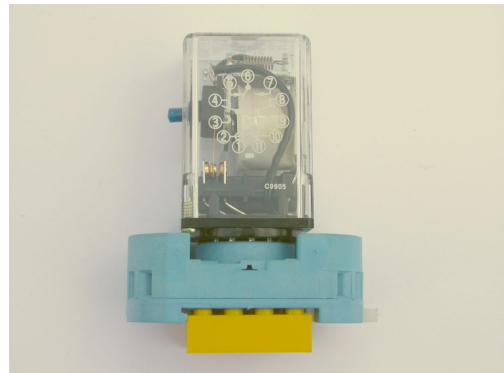
(a)



(b)



(c)



(d)

Figure A.13: LEGO Building Blocks; higher sticking with more small blocks. (a) best stability, (b) less stability, (c) easy to remove, (d) the power relay mounted on two big blocks, many small blocks would have given a better stability, but not enough small blocks were available.

A.6 Radiation Test

Table A.1: 20-pin 2-way Connector (To Load; 24V/21W - bulbs)

Pin no.	Function	Device
1	OUT	BTS 432E2 - 1
2	OUT	BTS 432E2 - 1
3	OUT	BTS 5240L
4	OUT	BTS 5240L
5	OUT	BTS 432E2 - 3
6	OUT	BTS 432E2 - 3
7	OUT	BTS 6143D - 1
8	OUT	BTS 6143D - 1
9	OUT	BTS 6143D - 2
10	OUT	BTS 6143D - 2
11	OUT	BTS 6143D - 3
12	OUT	BTS 6143D - 3
13	OUT	BTS 443P - 1
14	OUT	BTS 443P - 1
15	OUT	BTS 443P - 2
16	OUT	BTS 443P - 2
17	OUT	BTS 443P - 3
18	OUT	BTS 443P - 3
19	N.C.	
20	N.C.	

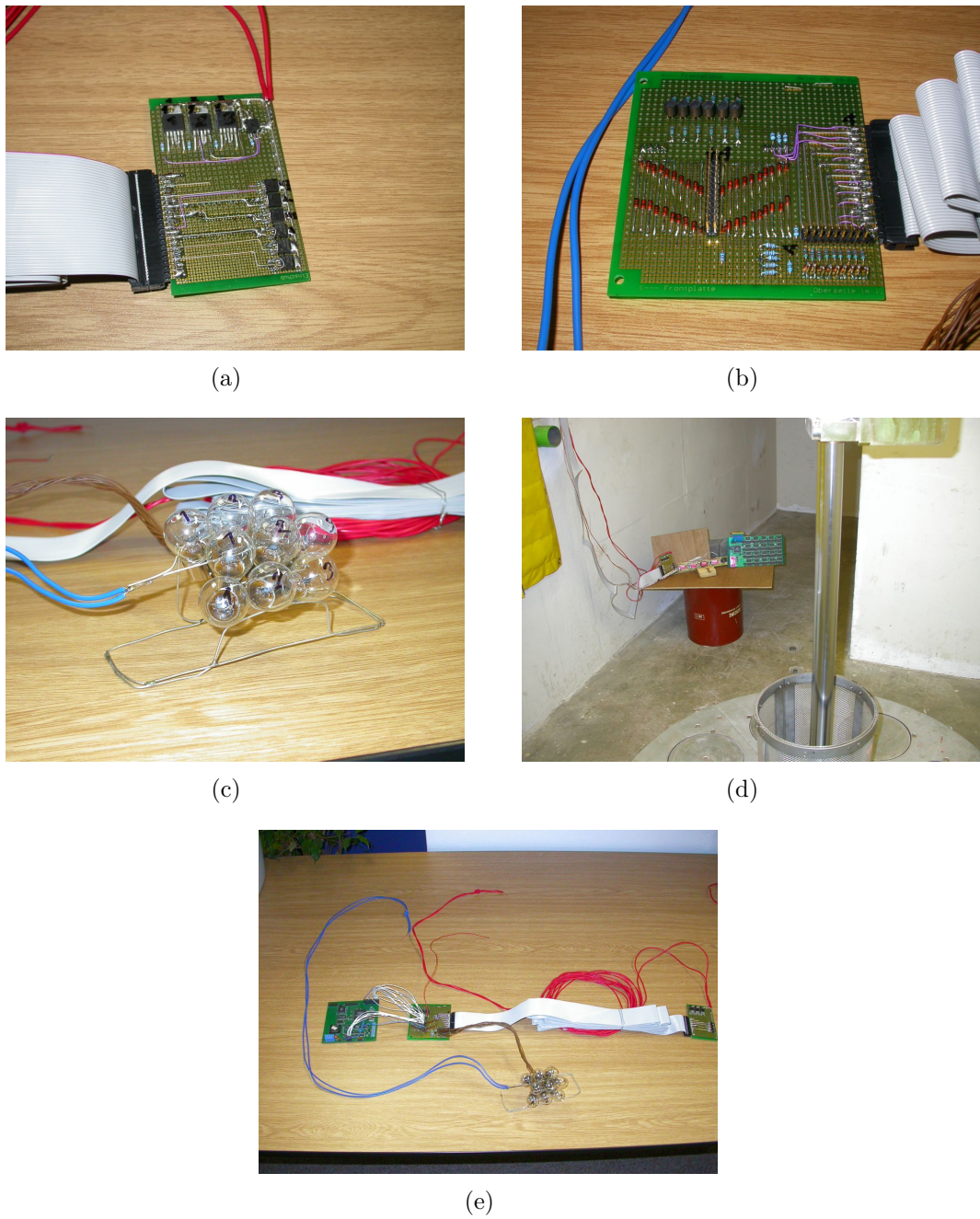


Figure A.14: Radiation Test: (a) radiated electronics; (b) interface and protection electronics; (c) the load (24V/21W bulbs); (d) prepared for the radiation in Stellenbosch; (e) the complete electronics

Table A.2: 26-pin 2-way Connector (Data - Logger & Control)

Pin no.	Function	Type (Data-logger)	Device
1	+5V	SUPPLY	
2	+5V	SUPPLY	
3	IN	DIG-OUT	BTS 432E2 - 1
4	ST	DIG-IN	BTS 432E2 - 1
5	IN	DIG-OUT	BTS 432E2 - 2 & BTS 5240L
6	ST	DIG-IN	BTS 432E2 - 2
7	IN	DIG-OUT	BTS 432E2 - 3
8	ST	DIG-IN	BTS 432E2 - 3
9	IN	DIG-OUT	BTS 6143D - 1
10	IS	ADC	BTS 6143D - 1
11	IN	DIG-OUT	BTS 6143D - 2
12	IS	ADC	BTS 6143D - 2
13	IN	DIG-OUT	BTS 6143D - 3
14	IS	ADC	BTS 6143D - 3
15	IN	DIG-OUT	BTS 443P - 1
16	IS	ADC	BTS 443P - 1
17	IN	DIG-OUT	BTS 443P - 2
18	IS	ADC	BTS 443P - 2
19	IN	DIG-OUT	BTS 443P - 3
20	IS	ADC	BTS 443P - 3
21	LOAD_OUT_MEAN	ADC	BTS 5240L
22	IS	ADC	BTS 5240L
23	N.C.		
24	GND	SUPPLY	
25	GND	SUPPLY	
26	GND	SUPPLY	

Table A.3: 40-pin 2-way Connector (Circuit Interconnection)

Pin no.	Function	Device
1	IN	BTS 432E2 - 1
2	ST	BTS 432E2 - 1
3	OUT	BTS 432E2 - 1
4	OUT	BTS 432E2 - 1
5	IN	BTS 432E2 - 2 & BTS 5240L
6	ST	BTS 432E2 - 2
7	OUT	BTS 5240L
8	OUT	BTS 5240L
9	IN	BTS 432E2 - 3
10	ST	BTS 432E2 - 3
11	OUT	BTS 432E2 - 3
12	OUT	BTS 432E2 - 3
13	IN	BTS 6143D - 1
14	IS	BTS 6143D - 1
15	OUT	BTS 6143D - 1
16	OUT	BTS 6143D - 1
17	IN	BTS 6143D - 2
18	IS	BTS 6143D - 2
19	OUT	BTS 6143D - 2
20	OUT	BTS 6143D - 2
21	IN	BTS 6143D - 3
22	IS	BTS 6143D - 3
23	OUT	BTS 6143D - 3
24	OUT	BTS 6143D - 3
25	IN	BTS 443P - 1
26	IS	BTS 443P - 1
27	OUT	BTS 443P - 1
28	OUT	BTS 443P - 1
29	IN	BTS 443P - 2
30	IS	BTS 443P - 2
31	OUT	BTS 443P - 2
32	OUT	BTS 443P - 2
33	IN	BTS 443P - 3
34	IS	BTS 443P - 3
35	OUT	BTS 443P - 3
36	OUT	BTS 443P - 3
37	IS	BTS 5240L
38	GND	
39	GND	
40	GND	

A.7 Some Ideas for Satellite Systems

Some ideas, which were not followed during this research, should be noted.

A.7.1 PC/104-plus

Electronics circuits on satellite systems are expensive and the housing made of solid aluminium blocks by milling most of the material away is not a low cost approach. I've not done extensive research on that, but industry standard PC/104 and the new standard PC/104-plus is made to work reliable in harsh environments. The form factor is defined and if one uses this form factor for more modules on the satellite, maybe costs can be reduced. For more information on the specs, look on the homepage of PC/104 [9] or the specifications on PC/104-plus [12].

The use of standardized modules in satellite systems can save the development time, costs and increases the reliability because of the use of known components.

A.7.2 Spectrally Sensitive Concentrators for Solar Energy

Concentration of solar energy improves the power output of the solar cell area and reduces the required number of cells. A holographic filter is used to select the right spectrum of the solar light and focus it on a string of cells, which increases the efficiency of the solar cell. Different cell types for different wavelength of light can be used. [37, 4]

A.7.3 Pressurized Module Battery

LiIon cells for the automobile industry are available with big capacities (12Ah, 20Ah or 100Ah) [3]. These cells have a case made of plastic, and according to the manufacturer, they cannot work in a vacuum environment. The specific energy density is 100W/kg. The advantage is, that these cells can be obtained easily, that the cells are less expensive than normal LiIon cells and that they are rated for >800 cycles lifetime. The maximum current for short periods (less than twelve seconds) of time is 5C to 10C. The idea of building a pressurized box for one or more parallel-connected cells so that these cells can be used could not be followed because of a lack of time.

Maybe this module and a DC/DC converter with voltage mode maximum power point tracking for the solar module can save costs. This can be the focus of future work.

A.8 Interesting Sources

There are some interesting articles and other documents, which might be interesting.

A.8.1 RØMER Mission Technical Description

It seems, that this satellite also uses AEA batteries, at least the same cell type that AEA uses (SONY US18650) in a 7S3P - structure. In this document information about the power structure and other subsystems are also described. The specific document [23] can be found on the RØMER-website [24]. Also documentation and information to other subjects (e.g. thermal, meachanical, the space environment or orbital mechanics) could be found there.

A.8.2 BaSyTec - Battery Testing Equipment

On the homepage of BaSyTec under “Literature”, one can find information about different battery systems. Also codes for rechargeable Li-systems. [1]

A.8.3 Sixth European Space Power Conference

Unfortunately the proceedings from that conference were not available, but the planned program schedule from [26] showed some interesting conference contributions.

B Acknowledgements

I want to thank my parents for all their help as well as all my friends, relatives and colleagues at all the companies I've worked. Thanks also to Richard Auer who provided the opportunity for an excellent apprenticeship; Klaus Haber, who was my first trainer during my apprenticeship and Gerhard Rimpler, who made it possible to work during my study; Dr. Sias Mostert from Stellenbosch University who made it possible to do practice-and-diploma semesters in South Africa.

Special thanks to Martin Jacobs who supplied me with feedback on this thesis, supported my work and was always a good discussion partner. And also thanks to Johan Czanik for support of my work.

Also thanks to my lecturers and the Technikum Wien; especially Dr. Ernst Soudek as well as Dr. Felix Himmelstoss for reading the thesis and their feedback; Klaus Desl and Andrea Krann my friends and colleagues from the Technikum Wien, who were a special link during my diploma semester to Austria (support team for my homepage).

And last but not least I also want to thank all the people in Austria who made it possible for all the students to study by paying taxes which finance the universities and the "Studienbeihilfenstelle".